

AN ABSTRACT OF THE THESIS OF

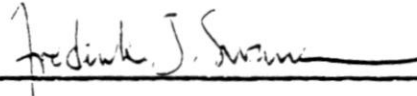
Bryan A. Hicks for the degree of Master of Science

in Geology presented on February 9, 1982

Title: Geology, Geomorphology, and Dynamics of Mass Movement in

Parts of the Middle Santiam River Drainage, Western Cascades, Oregon

Abstract approved:



Frederick J. Swanson

ABSTRACT

Landforms sculpted by mass movements comprise much of the landscape in the Middle Santiam study area. Bedrock in the area is mostly basalt and andesite flows and varied volcanoclastic rocks of the Little Butte Volcanic Series of Oligocene and early Miocene age, unconformably overlain by andesite flows and tuffs of the Sardine Formation of middle and late Miocene age. Some mass movements in the study area may have originally occurred during glacial or interglacial periods of the late Pleistocene, although this is largely speculative. Active slump-earthflows, debris avalanches, and debris torrents impact streams, timber resources and man-made structures.

Earthflows are associated with intercalated lava flows and volcaniclastics, especially stratified volcaniclastics which have low strength, high plasticity, and contain montmorillonite, an expandable clay mineral. Debris avalanches are associated with non-cohesive soils on steep slopes.

Slump-earthflows show distinctive morphological and vegetative characteristics which reflect recency and rates of movement. Areas with different levels of activity can be mapped and the data used for certain land-planning applications.

Surface movement rates can be measured on active earthflows by conventional surveying and the use of stake arrays. Results indicate that rapid surface movement exceeding 20 ft/yr is occurring on at least two earthflows, and that intraannual and annual periods of accelerated movement coincide with periods of greater water input from precipitation and snowmelt. Movement of the Jude Creek earthflow also appears to be related to erosion of the toe by Jude Creek. Movement on the Middle Santiam earthflow has greatly accelerated in the last three years (since 1978), compared with average rates for the previous 13 years. Road construction in 1965 preceded the most recent pulse of movement at this site.

Inventory of debris avalanches in the study area indicate a link between road construction, storm history and debris avalanche occurrence. Rates of soil transfer for road-related events is much greater than those for either forested or clearcut events.

Geology, Geomorphology, and Dynamics of Mass Movement
in Parts of the Middle Santiam River Drainage Basin,
Western Cascades, Oregon

by

Bryan A. Hicks

A THESIS

submitted to

Oregon State University

in partial fulfillment of
the requirements for the
degree of

Master of Science

Completed February 9, 1982

Commencement June 1982

APPROVED:

Frederick J. Swanson

Assistant Professor of Geology in charge of major

Head of Department of Geology

Dean of Graduate School

Date thesis is presented February 9, 1982

Typed by Patty Wickliff for Bryan A. Hicks

ACKNOWLEDGMENTS

As I concluded this project, I realized that without a supporting cast of some enthusiastic and capable people, the task would have been far more difficult.

To those who helped me in the field, a toast to you and the outdoors we share and love. Thanks to Douglas Shank, Paul McCarter, Bill Siebold, Tim Heironimus, Fred Swanson, Kathy Miller, Jim Graham, Dennis Harr, George Lienkaemper, and Oz.

Doug Shank, Mark Truebe and Bob Deane of the Santiam Zone, Willamette National Forest opened my eyes to the Middle Santiam and provided laboratory and field support.

To Fred Swanson, special thanks for assuming the onus of guiding an aspiring scientist through times of mental befuddlement. Your professionalism and patience are very much appreciated.

My gratitude to Dr. Swanson's colleagues: all the denizens of RWU 1653, Forestry Sciences Lab, who kept the spark alive through their interest, personal support and friendship. This research was supported in part through supplement no. 245 to the master memorandum of understanding between the Forest Service and Oregon State University, thanks to Dr. Fred Swanson and Dr. Logan Norris. I owe thanks also to the word processing team of Gwen White, Patty Wickliff, and Tawny Blimm for their good work and grace under pressure.

My gratitude to Bob Ziemer of Redwood Sciences Laboratory, Arcata, California for his help with the slope indicator data, to

Rich Mahood for showing me how to process clay samples for x-ray diffraction, to Dr. Edward Taylor for help with petrography, and to Dr. Lee Schroeder and Dr. Rick Thrall for soil testing laboratory support.

Finally, thanks to all my friends and family for being there and being patient.

TABLE OF CONTENTS

	<u>Page</u>
INTRODUCTION	1
Purpose	1
Previous Work	2
GEOGRAPHY	8
Location	8
Climate	8
Vegetation	10
Geomorphology	11
Land Use	12
GEOLOGY	13
Regional Geology	13
Geology in the Study Area	15
Mapping Methods	15
Laboratory Methods	15
Stratigraphy	15
Little Butte Volcanic Series	18
General Statement	18
Rock Types and Distribution	20
Petrography	22
Sardine Formation	23
General Statement	23
Rock Types and Distribution	23
Petrography	24
Pliocene Rocks	25
Petrography	25
Intrusives	25
Petrography	26
Surficial Deposits	27
General Statement	27
Talus	27
Glacial Deposits	27
Soils	28
Alluvium	29
Mass Movement Debris	30
Structure	30
Bedding and Folds	30
Faults	30
Joints	31
MASS MOVEMENT IN THE MIDDLE SANTIAM BASIN	33
Classification	33
Creep	33

Rockfall-Rockslide	34
Debris Avalanches	35
Debris Torrents	36
Slump-Earthflows	36
Mass Movement and Material Properties	37
Weathering and Alteration	37
Soils	40
General Statement	40
Soil Strength	43
Classification of Soils	47
Atterberg Limits and Clay Contents	48
Clay Mineralogy	52
Permeability and Groundwater Flow	53
Mass Movement and Geologic Structure	54
General Statement	54
Structure and Slip Surfaces	54
Structure and Groundwater	55
Mass Movement and Pleistocene Glaciation	58
General Statement	58
Dating of Mass Movement Sites	58
Glaciation	59
Effects of Glacial Climates and Glaciation	60
 MASS MOVEMENT SITE CASE STUDIES	 62
General Statement	62
Movement Rate Monitoring Methods	62
Mapping Methods	63
Geomorphic Units	63
 Case Study I: Donaca Mass Movement Complex	 67
General Statement	67
Mass Movement Sites of the Donaca Complex	67
Geomorphic Units of Mass Movement Site A	71
Crown Scarp	71
Boulder Fields	71
Slump Benches	75
Bench A'	76
Swamp Creek Watershed - Hydrology and Mass Movement	77
Slump Earthflow Hydrology and Impacts	79
Case Study II: Jude Creek Mass Movement Site	81
Jude Creek Watershed - Hydrology and Mass Movement	81
Jude Creek Earthflow	83
Geomorphic Units of the Jude Creek Earthflow	83
Boundary Scarps	83
Boulder Fields	84
Upper Interior Scarp	85
Slump Benches	86
Lower Interior Scarp	88
Lower Jude Creek Earthflow	89
Earthflow-Jude Creek Interactions	90
Movement Rates of the Jude Creek Earthflow	93
Earthflow Movement, 1979-1980	93

Precipitation and Movement Rates	94
Sediment Input Rate	97
Case Study III: Middle Santiam Mass Movement Site	99
Introduction	99
Geomorphic Setting and Site Geomorphology	101
Scope of Investigation	102
Stratigraphy, Lithology, and Stability	103
General Statement	103
Roadcut Lithologies	103
Stability Relationships	104
Geomorphic Units	105
Crown Scarp	109
Boundary Sidescarps	111
Boulder Fields	113
Slump Benches	114
Flow Front	114
Debris Avalanche-Debris Flow Complex	115
Debris Avalanche-Debris Flow Deposits	116
Earthflow Movement Rates	119
Surface Movement, 1979-1981	119
Subsurface Movement, 1979-1980	129
Correlation of Subsurface Movement Data with the	133
Drilling Record	
Correlation with Precipitation	134
Recent Movement History	134
MASS MOVEMENT INVENTORIES	136
Earthflow Inventory	136
Debris Avalanche Inventory	136
Mass Movement and Recent Storm History	144
Mass Movement Impacts on the Middle Santiam River	148
SUMMARY	151
BIBLIOGRAPHY	156

LIST OF FIGURES

<u>Figure</u>		<u>Page</u>
1	Location map of the Middle Santiam study area	9
2	Regional geologic map of the western Cascade Range, showing the physiographic provinces of western Oregon and the location of Figure 1	14
3	Geologic map of the Middle Santiam study area	16
4	Stratigraphic chart for geologic units exposed in the Middle Santiam study area	19
5	Location and classification of soil samples	42
6	Sample logs and plots of %H ₂ O vs undrained shear strength for Shelby tube samples from the Middle Santiam mass movement site	44
7	Sample log and plot of %H ₂ O vs undrained shear strength for Shelby tube sample from roadcut in Jude Creek drainage	45
8	Atterberg limits for 24 soil samples	49
9	View looking north into basin formed by Donaca mass movement complex (photo)	68
10	Mass movement site map (1) and geomorphic unit map (2) of the Donaca mass movement complex	69
11	Rock types exposed on crown scarp of site A, Donaca mass movement complex	72
12	Series of lava flows and flow breccias exposed on southwestern portion of crown scarp of site A, Donaca mass movement complex (photo)	73
13	Ashflow units and bedded tuffs exposed on crown scarp of site A, Donaca mass movement complex (photo)	74
14	Swamp Creek watershed	78
15	Jude Creek watershed	82
16	Leaning, twisted and curved trunks of Douglas Fir trees on Jude Creek earthflow (photo)	87
17	Southern lobe of Jude Creek earthflow flow front (photo)	91

	<u>Page</u>
18	Northern lobe of Jude Creek earthflow flow front (photo) 91
19	Cumulative movement along northern shear boundary, Jude Creek earthflow, at SA-3 95
20	Aerial photograph of Middle Santiam mass movement site 100
21	Rock types exposed on roadcut west of Middle Santiam earthflow 107
22	Excavation of flow front materials, Middle Santiam earthflow (photo) 108
23	View of crown scarp, Middle Santiam earthflow, looking east (photo) 112
24	Deposit of "slide breccia" adhering to crown scarp of the Middle Santiam earthflow (photo) 112
25	Shear movement along western shear boundary, Middle Santiam earthflow 121
26	Crackmeter and stake array movement data for the Middle Santiam earthflow 122
27	Surface movement vectors on the Middle Santiam earthflow, 7/30/79 and 10/28/79 to 9/18/80 127
28	Principles of inclinometer operation 130
29	Profiles of borehole casing, assuming casing bottom was founded in stable materials, modified from computer-plotted profiles by Redwood Sciences Lab, Arcata, California. 132

LIST OF TABLES

<u>Table</u>		<u>Page</u>
1	Surface movement data from recent studies of earthflows	6
2	Key to Figures 6 and 7	46
3	Soil groups and index properties of 28 soil samples	50
4	Geomorphic units for mass movement sites--terrain types and activity classes	65,66
5	Ground extension across tension cracks, Jude Creek earthflow	96
6	Borehole log and drilling record, Middle Santiam earthflow	106
7	Ground extension across tension cracks, Middle Santiam earthflow, from 11/30/79 to 5/8/81	125
8	Movement of surveyed surface points on the Middle Santiam earthflow	128
9	Mass movement inventory	137,138,139
10	Frequency, average volume, and soil transfer rates of debris avalanches under forested, clearcut and road right-of-way conditions in several study areas in the Willamette Forest and the Bull Run watershed	142
11	Ranking of highest peak flows, watershed 2, H.J. Andrews Experimental Forest, 1955-1980. Modified from Harr, 1981	145
12	Distribution of debris avalanches and combined debris avalanche--debris torrent events in different land types, 1955-1981	146
13	Mass movement impacts on the Middle Santiam River	150

LIST OF PLATES

<u>Plate</u>		<u>Page</u>
1	Jude Creek earthflow	in pocket
2	Middle Santiam mass movement site	in pocket
3	Mass movements in the Middle Santiam study area	in pocket

Geology, Geomorphology, and Dynamics of Mass Movement
in Parts of the Middle Santiam River Drainage Basin,
Western Cascades, Oregon

INTRODUCTION

Purpose

The extensive lava flows, volcanoclastic deposits, breccias, and intrusive bodies of the western Cascade Range were emplaced by volcanic events which have long since ceased. Deep weathering and high natural erosion rates in a humid climate with high annual precipitation have combined to transform the landscape.

In the western Cascades, mass wasting of volcanic bedrock and deep regolith is a dominant process of erosion and landform development. In the Middle Santiam basin, mass movement in the form of complex slump-earthflows affects large areas of land and directly impacts drainageways. Abundant streambank failures and small debris avalanches and torrents also contribute to basin-wide erosion. All types of active mass movements can be damaging to timber resources and to roads, bridges, and culverts.

This study determines the overall extent and distribution of different types of mass-movement features in parts of the Middle Santiam watershed. In a qualitative sense, major geologic, hydrologic, and vegetative factors controlling distribution, occurrence, and type of mass movement are generally understood (Swanston and Swanson, 1976; Swanson and Swanston, 1977). In the

study area, these factors interact in a complex fashion to bring about and perpetuate mass movement. The extent and distribution of unstable and stable areas may be generally correlated with these factors. However, local or site-specific conditions related to geologic structure and stratigraphy and to topography, road building, and timber-harvest activities may cause local variations in influence by these controlling factors. Three mass-movement sites are discussed in greater detail than other mapped unstable areas, to show specific geomorphic features and site-specific conditions which may have helped to initiate and perpetuate instability. Rates of downslope movement on two of these sites were monitored to estimate impact on adjacent streams and to measure the response of movement to precipitation.

The engineering characteristics of soils in the study area indicate the influences of grain-size distribution, plasticity, strength of soils, and clay mineralogy on the distribution and behavior of unstable areas.

The ultimate goal of this study is to better understand the behavior, form, and materials of mass movement sites, to examine controlling geologic and climatic factors, and to assess influences of certain forest-management practices. Other goals are to provide an inventory data base for planning land use and for predicting stability of areas with similar climate and soil-bedrock conditions.

Previous Work

Studies of terrain containing abundant mass-movement features

indicate that a large proportion of mass movement occurs in areas underlain by certain bedrock types. Volcaniclastic rocks initially rich in glass weather rapidly to thick, cohesive clay-rich soils. Generally, a high percentage of these clays are expandable clays such as smectites (Paeth, 1971; Borchardt, 1977; Taskey, 1977). The presence of these materials is a major factor in the occurrence and distribution of deep-seated mass movements (Taskey, 1977).

In the H. J. Andrews Experimental Forest in the western Cascades, earthflow landforms mantle 25% of the area underlain by volcaniclastics, in contrast to disturbance by earthflow of only one percent of the area underlain by lava flow rock (Swanson and James, 1975). Dyrness (1967) found that 94% of the mass-movement events mapped in the Andrews Forest occurred in areas underlain by volcaniclastic rocks. Schulz (1980) noted that the highest number of slump-earthflows per unit area in the Bull Run watershed occur on the Rhododendron Formation (comprised mainly of volcaniclastic rocks) and Quaternary landslide debris.

This lithology and clay mineralogy-influenced distribution of mass movement applies to other regions as well. An abundance of expandible montmorillonite in sheared argillites and carbonaceous mudstones of the Waipaoa River catchment of New Zealand leads to intensive mass movement and aggradation of river valleys (Claridge, 1960; Gage and Black, 1979). Similar extensive slump-earthflow contributing to extremely high sediment yield occurs in the drainage basins of several California north coast rivers. Underlying this earthflow terrain is the complex Franciscan assemblage which includes

sandstones and sheared metasediments, or melange (Janda, 1975; Kelsey, 1977).

The processes of mass movement alter topography, creating distinctive landforms, drainage patterns, and microtopography. Varnes (1978) offers a graphic compilation of landforms characteristic of various types of mass movement. Slump-earthflow topography is characterized by scarps, blocks, and bulging toes. On a microtopographic scale, undrained depressions, ground cracks, and springs may be present. These features can be found on slump-earthflows everywhere, but scale, distribution, density, and definition of the features vary.

Keefer (1977) illustrates several mapped earthflow complexes in the coast ranges of central California, showing scarps, lateral ridges, and open tension cracks among other features. Extensive, detailed mapping of active and older (fossil) slump-earthflows and other landslide types has been accomplished in Czechoslovakia (Nemcok and Rybar, 1968). Swanson and Swanston (1977) mapped geomorphic and hydrologic features on two complex mass-movement sites in the western Cascades.

Maps illustrating surficial features help define the types of subsurface movements taking place; profiles depicting the projection of slip surfaces are useful for engineering studies and mass-movement control (Sowers and Royster, 1978). Rybar (1965) states that the landslide maps of Czechoslovakia have demonstrated their usefulness in city and regional planning.

The current relative activity of a slump-earthflow may be quantified by measuring surface and subsurface downslope movement

rates. Stake lines and stake arrays have been widely used to track surficial movement. Movement vectors are disclosed by surveying the distortion of initial stake arrangements over a period of time (Keefer, 1977; Kelsey, 1977; Swanson et al., 1980). Relative movement of slump blocks separated by shear or tension cracks may be measured continuously with a crackmeter, consisting of a metal tape or cable anchored to a deadman on a one block and wound on a pulley on an adjacent block; slope movements pull the tape or cable and drive the pulley. The pulley is mechanically linked to a revolving chart system on which cumulative movement data are conveniently recorded. Crackmeters have been used on earthflows in the H. J. Andrews Experimental Forest (Swanson et al., 1980), in Redwood Creek, north coastal California (Janda, 1975), and in Ireland (Prior, 1973).

Subsurface displacement can be monitored by using flexible plastic inclinometer tubes or electronic inclinometer devices. Swanston and Swanson (1976) used inclinometer tubes at several western Cascade and coast range localities in Oregon. An inclinometer device can accurately locate slip planes in the borehole profile, and has been used to monitor movement of landslides, dams, bulkheads, and other earth-related structures (Merriam, 1960; Durr, 1974; Wilson, 1974; Broms, 1975).

Table 1 presents surface-movement data from several completed studies.

A historical record of movement can be provided by dendrochronology. Mass movement stresses trees, causing structural and growth-ring changes. Shroder (1980) examined these changes in conifers growing on mass-movement sites on Table Cliffs Plateau,

Location	Measurement method	Parent material	Average Surface ^a movement (in/yr)	Cumulative ^a Precipitation (in/yr)	Period of record
H. J. Andrews Experimental Forest					
Oregon ^{1/}					
Lookout Creek earthflow	Crackmeter	Little Butte Volcanic Series: lava flows and deeply weathered volcaniclastic rocks.	5.2	76.4	1978-1979
Lookout Creek earthflow	Stake array		3.8	87.6	1974-1975
			5.6	93.0	1975-1976
			.08	41.3	1976-1977
			2.4	83.7	1977-1978
			5.2	74.9	1978-1979
Redwood Creek Basin					
northern California ^{2/}					
River Creek earthflow	Stakelines	Franciscan Assemblage: sheared sediments and metasediments	5.0	51.3	1975-1976
Poison Oak Prairie earthflow	Stakelines		60.5	63.4	1975-1976
Van Duzen River Basin, northern California^{3/}					
Donaker earthflow	Stakelines & aerial photo-graphs	Franciscan Assemblage		ppt. record (winter)	Movement record
Cashpounda Cr. earthflow			96.0	65.4	1974-1975
west tongue			180.0	77.5	1974-1975
east tongue			180.0	77.5	1974-1975
Chimney Rock earthflow			108.0	77.5	1974-1975
Falling Tree earthflow			72.0	77.5	1974-1975
Broken Road earthflow					1974-1975
west tongue			84.0	77.5	1974-1975
east tongue			72.0	77.5	1974-1975
Halloween earthflow			264.0	64.8	1974-1975

^{1/}Data Source: Swanson, Hart, and Fredriksen, 1980.
^{2/}Data Source: Harden, Janda, and Nolan, 1978.
^{3/}Data Source: Kelsey, 1978.

^aSome figures for yearly surface movement and yearly precipitation are projections from part-year data.

Table 1. Surface movement data from recent studies of earthflows in California and Oregon, U.S.A.

Utah. Agard (1979) used similar methods on recent mass movements near Telluride, Colorado. These studies noted correlations between periods of high precipitation and greater relative movement.

Effects of forest-management activities on erosion and mass movement have been investigated by a number of workers. Swanston and Swanson (1976) summarize the conclusions of several studies. : Deforestation and roading alter the factors influencing mass movement in a variety of ways. Clearcutting impacts slope stability by reducing rooting strength and the binding influence of roots on soils, and also by modifying the movement and detention of water in soils. Road construction alters subsurface and surface-water movement, leading to disturbance of the natural stability of some slopes by decreasing the resistance of soil to failure and increasing downslope gravitational stresses.

GEOGRAPHY

Location

The study area lies within the boundaries of Willamette National Forest in the north-central part of the western Cascade Range of Oregon (Figure 1). The study area encompasses approximately 23 square miles in the Middle Santiam River watershed and occupies parts of the Quartzville, Detroit, Echo Mountain, and Cascadia 15-minute quadrangles. Access to the south part of the area is provided by Forest Service and private logging road systems linked to U.S. Highway 20 to the south. That part of the study area north of the Middle Santiam River is directly accessible chiefly by trails and cross-country hiking.

Climate

The Middle Santiam watershed owes its climate of wet winters to its position on the western flank of the Cascade Range. Cyclonic storms from the Pacific Ocean move eastward and intensify over the range due to orographic effects. Generally, summers are quite dry.

Average annual precipitation varies from about 100 to 120 inches, with most of the precipitation falling between October and March. Yearly snowpack amounts fluctuate with elevation from a few inches per year near the river to several feet at elevations above 4,000 feet. Mean annual air temperatures range from near 60° F. at lower elevations to less than 45° F. at the highest elevations.

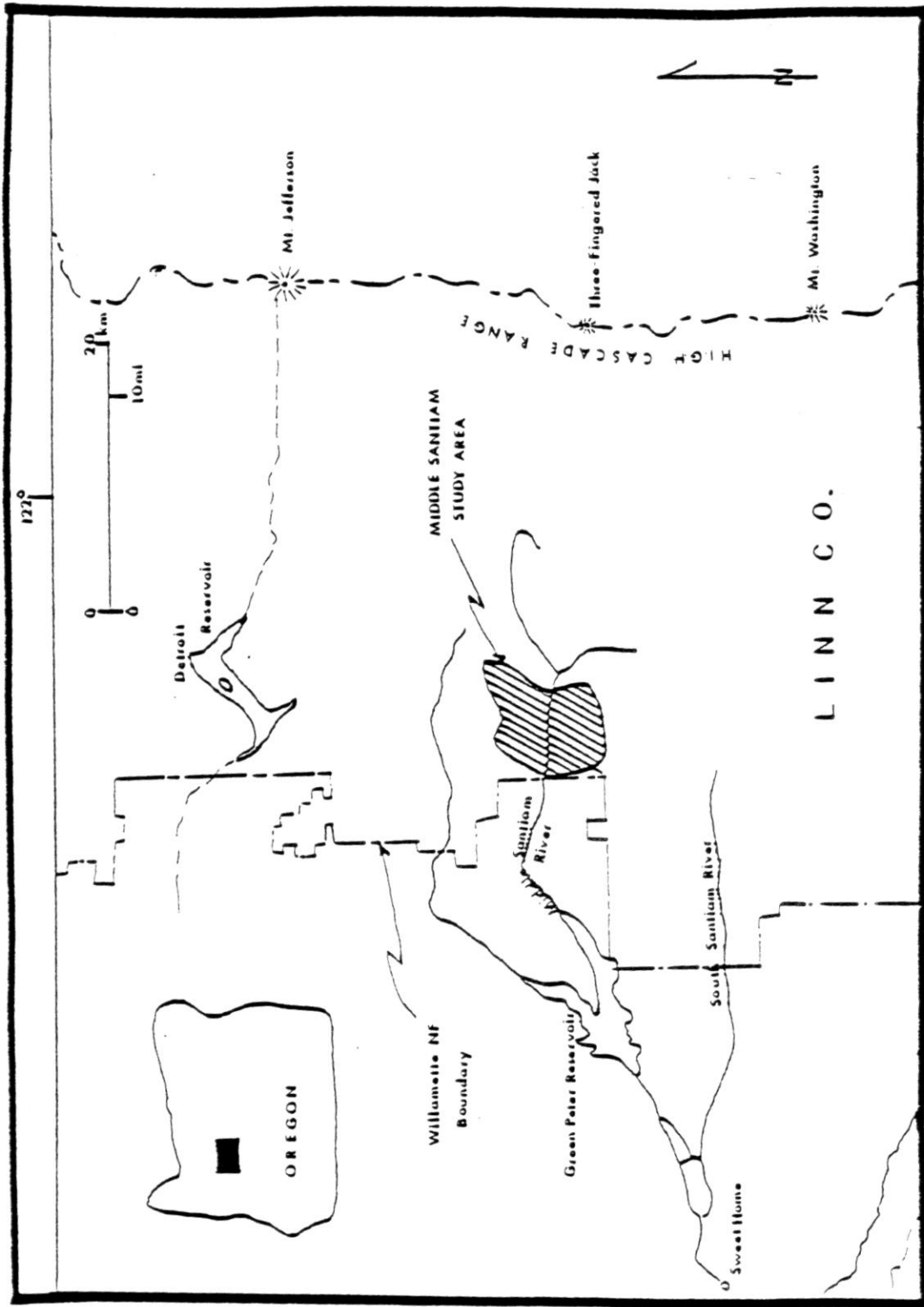


Figure 1. Location map of the Middle Santiam study area.

Vegetation

The Middle Santiam study area is inhabited by a range of tree, shrub, and forb species. Variations in elevation, topography, soil depth, and moisture control the distribution of these species. Generally, the higher ridges (above 4,000 feet), peaks, and the rocky, steep slopes south of Chimney Peak support stands of subalpine fir (Abies lasiocarpa), Pacific silver fir (Abies procera), and mountain hemlock (Tsuga mertensiana). Some madrone (Arbutus menziesii), Douglas-fir (Pseudotsuga menziesii), and white fir (Abies concolor) inhabit drier areas. Dominant shrub species include vine maple (Acer circinatum), ocean spray (Holodiscus discolor), manzanita (Arctostaphylos columbiano), and rhododendron (Rhododendron macrophyllum). Devil's club (Oplapanax horridum), tag alder (Alnus sinuata), and vine maple grow near springs and seeps and on talus slopes. Slopes at lower elevations with deeper soils support dense Douglas-fir forests, with minor western hemlock (Tsuga heterophylla) and western red cedar (Thuja plicata), and an understory of swordfern (Polystichum munitum), vine maple, rhododendron, ceanothus, and hazel (Corylus cornuta).

Red alder (Alnus rubra) and western red cedar are dominant overstory trees in and around undrained depressions or boggy areas, and skunk cabbage (Lysichitum americanum), water lilies (Nymphaeaceae), and bog orchid (Habernaria) grow on the wet bog surfaces.

Geomorphology

The study area is characterized by varied landforms. The highest ridges and peaks are capped by lava flows of probable Pliocene age. Broad, flat or gently dipping plains or benches at lower elevations are underlain by lava flows of Oligocene to Miocene age. Mass-movement landforms are abundant; most of the active mass-movement sites indicate wasting of the erodible volcanoclastic rocks of the Little Butte Formation, and have gentle to moderate slopes below very steep scarps. Old, inactive slump topography covers much of sections 21 and 22 south of the Middle Santiam River. These older mass-movement areas are primarily concave, benched basins with gentle to moderate (10 to 45%) slopes and deep soils. Small valley glaciers left isolated deposits of till near the heads of Jude Creek and Bachelor Creek drainages.

The Middle Santiam River roughly bisects the study area, providing primary drainage. The river flows into Green Peter reservoir, approximately eight miles southwest of the western study area boundary. Near the eastern boundary of the study area, the Middle Santiam flows north towards its confluence with Pyramid Creek, then bends sharply to flow in a westerly direction. The main channel between Pyramid and Jude Creeks is aggraded, flowing between wide gravel and sand bars. Several major creeks flow into the Middle Santiam: Jude Creek, flowing northward, and Donaca Creek, Egg Creek, Fitt Creek, and Chimney Creek, flowing southward. The overall drainage pattern is dendritic.

Elevations in the study area range from a maximum atop Chimney Peak (4,965 feet) in the northwest corner to 1,600 feet on the Middle Santiam River at the western boundary. Knob Rock (4,715 feet) is another prominent peak located 2.7 miles east of Chimney Peak.

Land Use

The study area lies within the boundaries of the Willamette National Forest; most of the area is publicly owned, with roughly 2.5 square miles south of the Middle Santiam River managed by private landowners.

The Middle Santiam River divides the study area into two parcels of land which presently show a sharp contrast in land use. South of the river, the land has been extensively roaded and harvested for timber; north of the river, the study area contains one road and two major clearcut areas. Parts of the northern parcel had been considered for inclusion into the proposed Middle Santiam Wilderness area, but is now classified as unroaded. Several timber sales have been planned in the area and are proposed for harvest within the next few years. Parts of the study area, notably north of the river, provide camping, hiking, and other recreational activities. A fairly well-maintained trail system links the river with the major peaks in the area.




GEOLOGY

Regional Geology

The Cascade Range in Oregon consists of two physiographic provinces, the western Cascades and the High Cascades (Callaghan, 1934) (Figure 2). The study area lies entirely within the western Cascades province, which consists of early to late Tertiary volcanic flows, volcanoclastic rocks, and small intrusive bodies. These rocks were folded and faulted in the mid-Miocene.

Peck et al. (1964) helped to define the petrology of mapped rock types and to determine the gross aspects of volcanic stratigraphy and structure of the central and northern parts of the western Cascades. Thayer (1936, 1937, 1939) analyzed the petrology of some western Cascade rocks and discussed the geologic structure of the North Santiam basin. Callaghan and Buddington (1938) studied mineralization related to intrusive bodies in the western Cascades.

The High Cascades Range is a volcanic platform of overlapping basalt and basaltic andesite lava flows which occupies a north-south trending graben (Taylor, 1980). Taylor postulates that this graben formed during the Pliocene by subsidence of a Pliocene volcanic range along a system of north-south trending fractures; these fractures may have served as channelways for ascending magma which later built up the High Cascades.

-  Pliocene to Recent volcanic rocks of the High Cascade Range
 _____ unconformity _____
-  Miocene to Pliocene volcanic rocks of the Sardine Fm. including basalts of the Columbia River Basalt Group
 _____ unconformity _____
-  Oligocene to Miocene volcanic rocks of the Little Butte Volcanic Series

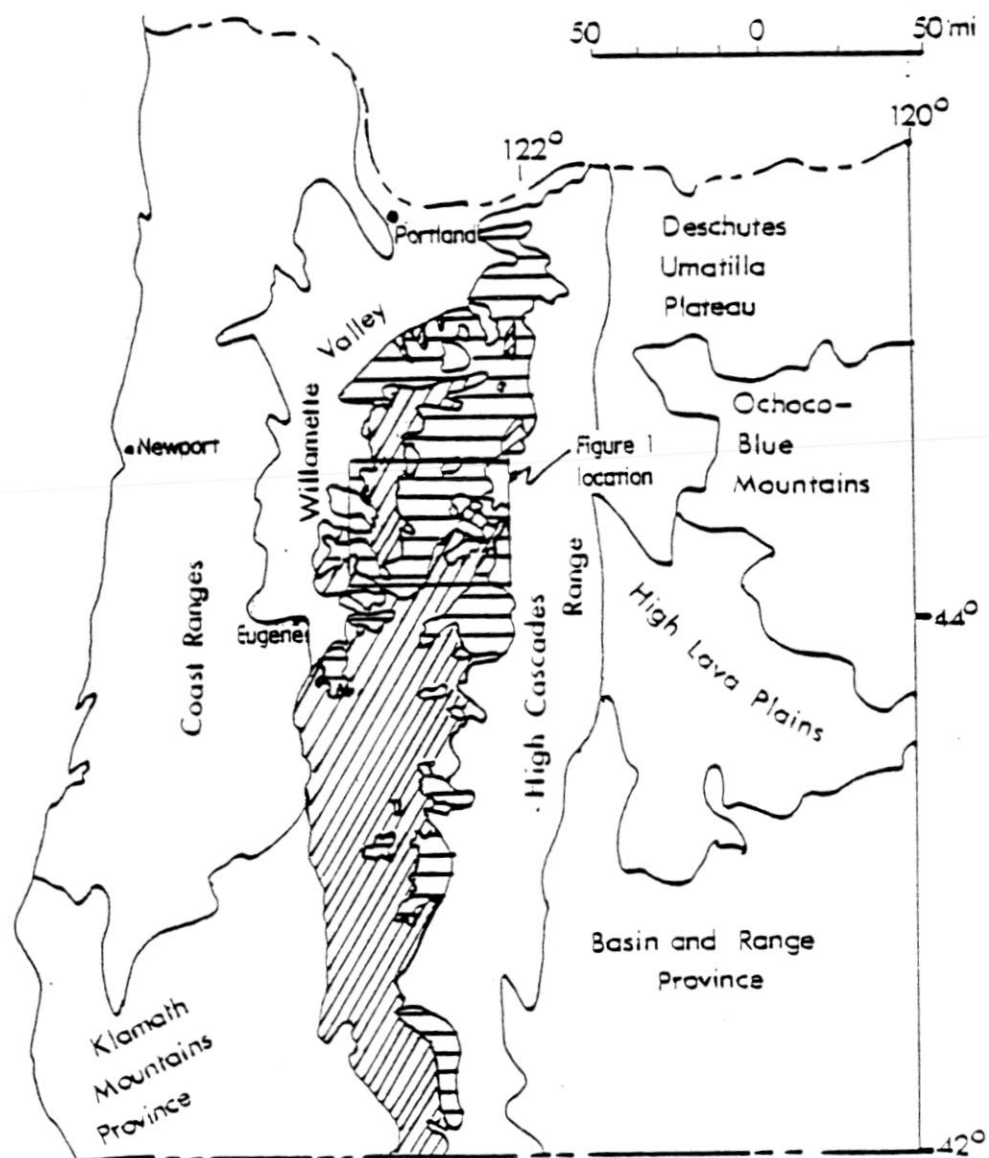


Figure 2. Regional geologic map of the western Cascade Range, showing physiographic provinces of western Oregon and the location of Figure 1.

Geology in the Study Area

Mapping Methods

Geologic mapping done in the study area is mainly reconnaissance in nature, due to limited outcrop exposure, dense vegetation cover, and difficult access (Figure 3). The most detailed mapping was done in and around certain mass movement sites.

Most geologic mapping was conducted from April 14, 1980 to June 6, 1980. Geology and mass movement features were plotted on 1:15480 Forest Service maps (USGS 15-minute quadrangle topographic base). Sets of color and black-and-white aerial photos from the Forest Service and Army Mapping Service at 1:63360 (1955 and 1974), 1:12000 (1959), 1:10000 (1977) and 1:15480 (1967, 1972, 1973) scales were used in mapping.

Laboratory Methods

Eight thin sections were prepared from rock samples representative of several rock types from the Little Butte Volcanic Series, Pliocene rocks, and a few intrusives. Thin sections were examined with a standard petrographic microscope.

Stratigraphy

The Little Butte Volcanic Series of Oligocene and early Miocene age and the Sardine Formation of middle and late Miocene age underlie

GEOLOGIC MAP LEGEND

Bedrock Symbols

- Pliocene **Pv** - Pliocene Volcanics: Flows and less abundant volcaniclastic rocks of basaltic andesite and olivine basalt
- Miocene **I_{sa}** - Sardinia Formation: Platy pyroxene andesite flows with tuff breccia and lapilli tuff

- Upper Oligocene **III** - Little Bute Volcanic Series: Basalt and andesite flows and flow breccias, lapilli tuffs, vitric tuffs, interbeds of tuffaceous sandstones and siltstones
- Miocene **I_a** - Basalt or basaltic andesite plug
- I_g** - Diorite or monzonite stock

- Dikes - dotted where inferred
- Area of argillically altered rocks

Map Symbols

- Strike and dip
- Contact (observed, inferred, obscured by mass movement)
- Fault with relative up (U) and down (D) displacement
- Unsatton identified in air photo
- 400-foot contour lines
- Anticline (approximately located)

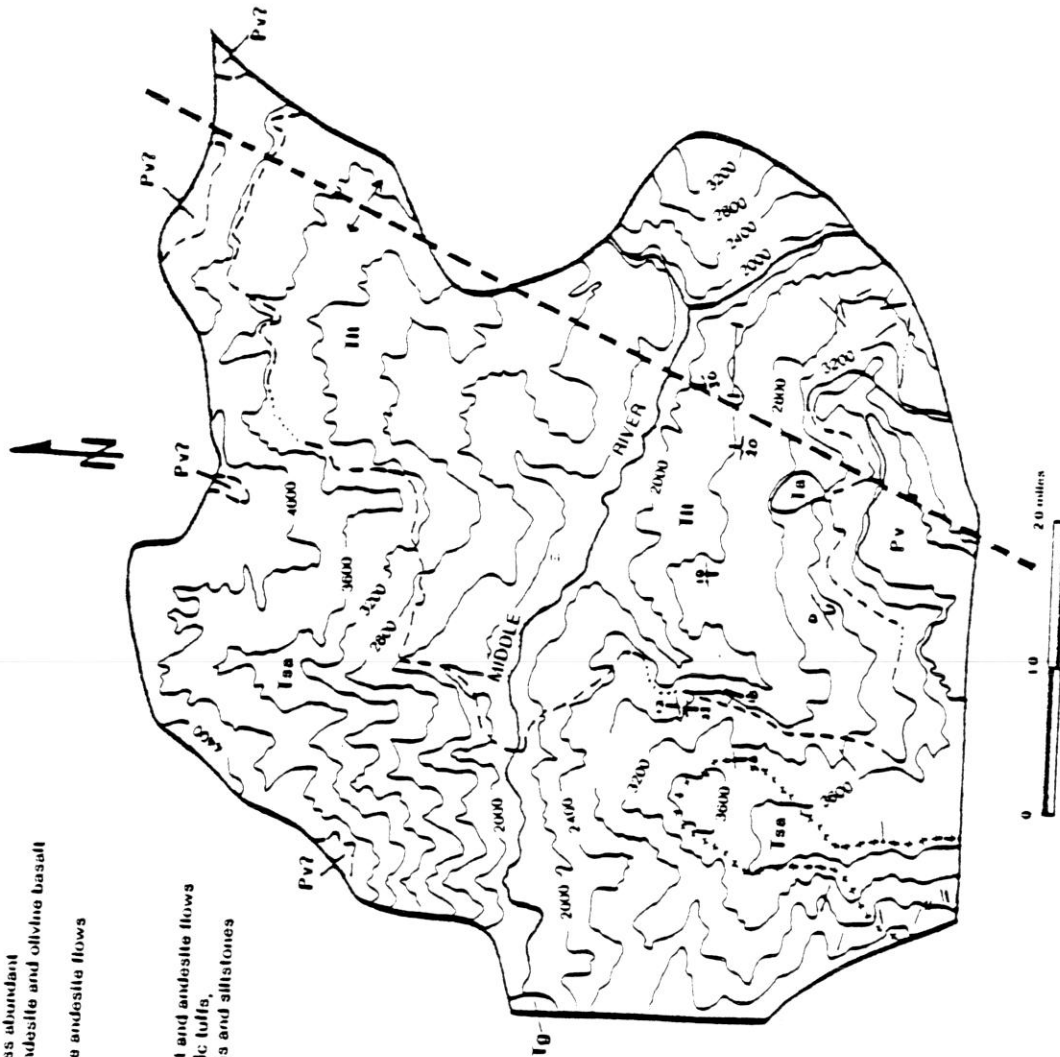


Figure 3. Geologic map of the study area.

most of the study area. Peck et al. (1964) distinguished the Little Butte Volcanic Series and the Sardine Formation on the basis of broad lithologic differences without close petrographic control, so that the contact is uncertain in many places. The Little Butte Volcanic Series averages 5,000 to 10,000 feet in thickness and contains massively bedded vitric andesitic and dacitic lapilli tuff, basalt and andesite lava flows and breccia, welded tuffs, lahars, domes and flows of dacite and rhyodacite, a basal unit of welded rhyodacitic tuff, and water-laid tuffs (Peck et al., 1964). The Little Butte Volcanic Series as mapped by Peck et al. includes the Mehama Volcanics and Breitenbush Series of Thayer (1939). The Sardine Formation (Thayer, 1936) overlies the Little Butte Volcanic Series with angular unconformity in the central and southern portion of the western Cascade Range. The Sardine Formation averages 3,000 feet in thickness and consists of lapilli tuff, hypersthene andesite tuff, tuff-breccias, lahars, and less abundant basaltic andesite, augite andesite, aphyric silicic andesite, dacite and olivine basalt. The Sardine Formation includes the Rhododendron Formation (Hodge, 1933), the Boring Agglomerate (Treasher, 1942), and the Fern Ridge Tuffs and parts of the Breitenbush Series (Thayer, 1936).

Absolute age determinations made by McBirney and coworkers (1974) on rocks of the Sardine Formation and Little Butte Series indicate that some rocks mapped as part of the Little Butte Series actually should be included in the Sardine Formation. Peck et al. (1964) mention that the contact between the Little Butte and the Sardine is uncertain at many places along the Breitenbush anticline. These uncertainties may be attributed to lithologic similarities of rocks

in both formations, and to poor exposure in much of the western Cascades.

As mapped by Peck et al. (1964), some 3,000 feet of undivided Pliocene and Quaternary flows, minor pyroclastic rocks, and less abundant pyroxene andesite and dacite of the High Cascade province unconformably overlie rocks of the Sardine Formation and Little Butte Volcanic Series in some localities.

Intrusive rocks ranging in composition from rhyodacite to basalt and in age from late Eocene to late Miocene are represented in the western Cascade Range by abundant scattered stocks, plugs, dikes, sills, and domes. These intrusives are surrounded by zones of propylitic alteration (Callaghan and Buddington, 1938). It is commonly difficult to distinguish the finer grained intrusives from their extrusive equivalents in the field.

Figure 4 charts the stratigraphic units in the study area. Peck et al (1964) show rocks younger than Pliocene age in the study area, but according to E. M. Taylor (personal communication, 1982) and work done by McBirney et al (1974), these rocks are probably Pliocene.

Structural deformation occurred during the middle Miocene in the western Cascades, resulting in sets of broad, northeast trending en echelon faults and northwestern trending faults (Peck et al., 1964).

Little Butte Volcanic Series

General Statement

Rocks of the Little Butte Volcanic Series are the oldest in the

PERIOD	EPOCH	AGE (my)	UNIT	DESCRIPTION
QUATERNARY	Holocene		Surficial Deposits	<u>Surficial Deposits</u> : Landslide debris, terrace gravels, soils and glacial deposits.
	Pleistocene			
TERTIARY	Pliocene	1.8	Pliocene Rocks (undifferentiated)	<u>Pliocene Volcanics</u> : Flows and less abundant volcanoclastic rocks of basaltic andesite and olivine basalts.
	Miocene	7-9	Sardine Formation	<u>Sardine Formation</u> : Platy pyroxene andesite flows with tuff breccia and lapilli tuff.
	Oligocene	26	Little Butte Volcanic Series	<u>Little Butte Volcanic Series</u> : Basalt and andesite flows and flow breccias, lapilli tuffs, vitric tuffs, interbeds of tuffaceous sandstones and siltstones.
		Middle-Late		

Figure 4. Stratigraphic chart for geologic units exposed in the Middle Santiam study area.

study area, ranging from early or middle Oligocene to early Miocene (Peck et al., 1964). Approximately 53% of the study area is underlain by Little Butte rocks. The base of the Series is not exposed in this area.

Jude Creek exposes interbedded massive lapilli tuffs, tuff breccias, and lava flows where it has cut through deep colluvium and landslide debris. Little Butte andesitic and basaltic flows are exposed along the Middle Santiam River. Scattered outcrops of lava flows and indurated lapilli tuffs occur throughout the area. In the study area, the Little Butte Series attains a maximum thickness of about 2,400 feet along the Middle Santiam River.

Over most of the western Cascades the Series is between 5,000 and 10,000 feet thick, and attains a maximum thickness of 15,000 feet along the North Umpqua and Little Rivers between Glide and Ilahee Rock.

Rock Types and Distribution

The section of Little Butte Series underlying the study area is composed of an assortment of rock types: andesite and basalt flows and flow breccias, laharic breccias, lapilli tuffs, pyroclastic breccias, welded tuffs, and bedded tuffs.

Laharic breccias are exposed on cuts along a logging road on the west side of Jude Creek drainage. These are massive deposits of subangular to rounded cobbles and boulders of andesite in a gray, gray-green or brown, indurated fine-grained matrix.

Some 700 feet of lapilli tuffs and pyroclastic breccias are exposed on cliffs and roadcuts north of the Bachelor Creek drainage. These rocks consist of an assortment of poorly sorted lithic andesite fragments, rounded, cream, pink, or green pumice fragments (5-10 mm across), and red cinder fragments (10 mm) in a gray to gray-green matrix. The andesite fragments (up to .5 m) are multitextured, multicolored, and subrounded to subangular. These breccias and tuffs are poorly to moderately well lithified; breakage occurs through grains as well as matrix. Generally, lapilli tuff units are massive, and represent ashflow events.

Sections of bedded airfall and waterlaid tuffs were observed throughout the study area. It is likely that a combination of airfall, fluvial transport, and deposition in quiet water formed these stratified tuffs. A roadcut just west of the Middle Santiam mass movement site provides a good exposure of these materials. The section is about 30 feet thick and lies between two andesite flows; it consists of interbedded epiclastic volcanic breccias and tuffaceous sandstones and mudstones. The breccias form the basal layer of a depositional unit and grade upward to silt- and clay-size materials. Clasts in the volcanic breccias and sandstones are densely packed, angular to subangular, and moderately well sorted. Many of the clasts appear altered, and zeolites fill interstices. The mudstones are closely fractured.

Andesite and basalt flows in the Little Butte Series average about 50 feet in thickness, and are commonly interbedded with tuffaceous units. Stacked flows are usually separated by several feet of poorly to moderately indurated, oxidized red flow breccias.

The predominantly olivine basalt and basaltic andesite flows show blocky to columnar jointing. Flows are well exposed along the Middle Santiam River and on the scarps of several recent mass movement sites.

Petrography

Three thin sections of andesites and one of epiclastic volcanic breccia were examined petrographically. A medium-gray porphyritic pyroxene andesite from a flow exposed in the Bachelor Creek drainage contains approximately 20% phenocrysts of labradorite, 5% clinopyroxene, and 5% olivine phenocrysts in a pilotaxitic groundmass of feldspar microlites, intergranular pyroxene and magnetite, and interstitial material. Rims of olivine phenocrysts are altered to iddingsite and magnetite, and cores appear to be replaced by antigorite and cryptocrystalline quartz. In the hand sample, pyroxenes are black to dark green, olivine appears rust-brown or orange due to alteration, and feldspars are yellowish.

Blocks of mafic rock exposed in the Jude Creek slump-earthflow are composed of a dark gray porphyritic basaltic andesite containing phenocrysts of bytownite and glomerocrysts of clinopyroxene in a felty groundmass of plagioclase and magnetite. Scattered microvesicles are filled with brown clay, hematite, and cryptocrystalline quartz.

The epiclastic volcanic breccia contained subangular, densely packed, moderately well-cemented, 2-mm to 1-cm clasts of porphyritic andesite lithic fragments. Some of these clasts were replaced by

calcite and cryptocrystalline quartz. The matrix is devitrified glass and clay.

Sardine Formation

General Statement

The Sardine Formation of middle and late Miocene age overlies the Little Butte Volcanic Series in the northern, western, and southern parts of the study area. The contact is not clearly exposed in the study area; however, Peck et al. (1964) have determined that the Sardine overlies the Little Butte Volcanic Series with an angular unconformity over much of the western Cascade Range.

The Sardine Formation is less than 3,000 feet thick in most places. In the study area it attains a maximum thickness of approximately 2800 feet. Peck reports that the centers of maximum volcanism, as indicated by the greater thickness of the formation there, form a belt which extends from the Middle Santiam River to the headwaters of the Collawash River.

Rock Types and Distribution

Most of the Sardine Formation consists of lava flows, primarily platy hypersthene andesite. Other rock types include massive lapilli tuff, tuff-breccia, and water-laid tuff.

About 250 feet of platy hypersthene andesite flows cap the ridges in the southwestern part of the study area. Below these flows lie

intercalated flows, flow breccias, massive lapilli tuffs, and bedded tuffs. These tuffs are similar to those found in the Little Butte Volcanic Series, but Peck et al. (1964) note that Sardine tuffs generally contain more abundant hypersthene crystals.

Some of the Sardine rocks in the southwestern portion of the study area are quite altered, and contain some disseminated pyrite. Original textures of the rocks have been masked by this alteration, and predominant colors are chalky white, ochre, and pale green. Abundant small dikes and shear zones were noted in this area. This is an area of argillic and possibly some propylitic alteration related to intrusive activity.

Petrography

An unusual rock type, a light gray biotite-bearing porphyritic dacite, was examined in thin section. The biotite phenocrysts are euhedral and are up to 5 mm across. The rock contains 5% feldspar phenocrysts. Groundmass consists of feldspars and magnetite. Some biotite phenocrysts have rims which are altered to magnetite, and other phenocrysts have been completely replaced by magnetite.

According to Peck et al (1964), hypersthene andesite, the most abundant flow rock type, contains phenocrysts of labradorite and hypersthene, less abundant augite and magnetite, and occasional olivine set in a hyalopilitic to pilotaxitic groundmass containing andesine microlites, pyroxene, and magnetite in finely crystalline alkali feldspar, cristobalite, and clay.

Pliocene Rocks

Andesite flows of probable Pliocene age cap ridges in the south-central part of the study area. A small quarry .75 miles east of Cool Camp exposes a dark gray porphyritic pyroxene andesite flow. Another ridge-capping flow a mile northeast of the headwaters of Jude Creek has a vesicular top; the vesicles are unfilled by secondary products, which is characteristic of younger flows.

Petrography

A thin section of a dark gray porphyritic pyroxene andesite from a ridge-capping flow displays 40% plagioclase and clinopyroxene glomerocrysts in a felty groundmass of feldspar, orthopyroxene, clinopyroxene microlites, and magnetite. The rock also contains sparse, unfilled microvesicles.

Intrusives

Intrusives in the western Cascade Range vary greatly in type and composition, and generally play a strong role in the alteration of surrounding country rock. Peck et al. (1964) distinguish between medium-grained intrusive rocks and fine-grained intrusive rocks. The medium-grained rocks are pipes, dikes, and small stocks, ranging in composition from augite diorite to biotite-quartz monzonite. They probably range in age from late Eocene to late Miocene. The fine-grained intrusive rocks occur as dikes, sills, pipes, plugs, and

domes and are similar lithologically and in age to related extrusive rocks of the Little Butte Volcanic Series and Sardine Formation. They include porphyritic and aphyric types of basalt, andesite, dacite, and rhyodacite. Some intrusives may also be feeders for Pliocene rocks in the area.

The study area contains numerous dikes of varied composition ranging from 10 to 30 feet wide. Abundant narrow dikes were noted in the argillically altered zone in the southwest portion of the study area. A system of dikes was also found in the southeast corner of the study area, near Bachelor Creek. One andesite dike cutting massive tuffs of the Little Butte could be clearly traced for about 2,000 feet. Most of the mapped dikes in both the southwest and southeast portions of the study area trend in an east-west direction.

An intrusive body located in the south-central part of the study area is possibly a plug. It covers approximately 36 acres, and is roughly elliptical in plan. A high quarry cut made on its north face exposes dense aphanitic basalt.

Petrography

Examination of a thin section from a distinctive, well-exposed andesite dike in the Bachelor Creek drainage revealed a porphyritic texture, with phenocrysts of plagioclase (up to 3 mm long), olivine and clinopyroxene in a felty groundmass of plagioclase, pyroxenes, and magnetite. The feldspars are zoned and extensively sericitized, and the olivine is altered to iddingsite and antigorite. Numerous amygdules are filled with zeolites.

Surficial Deposits

General Statement

Surficial deposits of Quaternary and Recent age overly bedrock throughout the study area. They include mass movement debris deposits, talus, scattered glacial deposits, alluvium, and a variety of soils.

Talus

Large piles of rock and boulder debris lie at the base of steep rock bluffs and peaks in the study area. The size of the rock blocks is controlled mainly by the geometry of fracturing in the parent rock mass. Wind, rain, freeze-thaw processes, and vegetation pry blocks from these steep faces. Talus deposits stand at an angle of repose of 30-40°, but may experience downslope movement from undercutting by stream erosion and road construction.

Most of the talus deposits in the study area were probably formed within the cooler, wetter climatic regime which prevailed during the Pleistocene epoch.

Glacial Deposits

Glacial deposits occur in the study area as isolated, small and discontinuous patches overlying bedrock or colluvium. These deposits consist of unsorted, heterolithologic, rounded to subangular cobbles

and boulders in a compacted matrix of light brown, gravelly sandy silt and clay. Glacial deposits mixed with colluvium and landslide debris occur in the upper drainage areas of Jude and Bachelor Creeks. Glacial deposits are commonly hard to distinguish from slide debris and some colluvial soils.

Soils

Soils in the study area vary greatly in terms of origin, types, and thickness. Residual soils are developed in situ from the weathering of bedrock. Soils derived from lava flows and intrusives are sandy to gravelly in texture and generally are shallow (10 feet or less). Residual soils derived from pyroclastic bedrock may be thicker and contain more clay. The distribution of residual soils directly reflects the distribution of rock types. Residual soils are thickest on stable sites such as ridgetops and level plateaus, where they are not subject to transportation by hillslope processes.

Colluvial soils, soils which have been transported, may be a mixture of residual soil types. Colluvial soils are transported by hillslope processes such as mass movement, creep, and sheet wash. Transport of colluvium alters the distribution and textures of residual soils. Colluvial soils mantle hillslopes, exist as thick mass movement deposits, or as deposits in topographic depressions.

Organic soils form primarily from the decomposition of vegetation. In forested portions of the study area, a surface organic layer averaging 2-3 inches thick overlies mineral soil.

Organic materials accumulate along with sediments in lakes, ponds, and boggy areas.

Alluvium

Alluvial deposits in the study area are primarily gravels and boulders lining segments of the Middle Santiam River and other streams. These deposits form channel islands or bars, and older terraces which rise a few feet above the unvegetated channel bars. The bars are formed from bedload materials which are too coarse for the stream to move except during a large flood, and finer sediments in temporary storage. Numerous alluvial islands are part of the braided pattern of the Middle Santiam River between Pyramid Creek and Fitt Creek, about 2.8 miles. Channel bars subject to seasonal flooding characteristically lack vegetation; older terraces or terraces subjected only rarely to flooding support shrubs and small trees. Only one level of terraces just above the river could be easily recognized; higher terrace levels, if they exist, are discontinuous, obscured by vegetation, or can be mistaken for old slump-bench type topography.

Sediment wedges are materials deposited behind dams of large organic debris and inorganic sediment which accumulate in stream channels after periods of high flow, or from hillslope mass movement processes. Sediment wedges may be stable for a number of years, but failure of the confining debris dams may rapidly release tons of sediment to downstream areas (Swanson, Lienkaemper, Sedell, 1976; Swanson and Lienkaemper, 1978).

Mass Movement Debris

Mass movement debris includes any material, organic and inorganic, moved downslope by mass movement processes. The inorganic materials show a full range of particle sizes, are largely unconsolidated, saturated in some cases, and may be located below headwall scarps, on the body or the toe of a mass movement site. Extensive mass movement deposits are located throughout the study area; some deposits directly impact stream drainages.

Structure

Bedding and Folds

Bedding attitudes of thinly bedded tuffs and epiclastic breccias were measured. Dips of up to 35° on these strata suggest localized folding. Peck et al. (1964) map a northeast-trending anticline axis through the eastern portion of the study area; this axis is an extension of the Breitenbush anticline as mapped by Thayer (1936).

Faults

Faults in the western Cascade Range have a regional northwesterly trend. Peck et al. (1964) mapped a number of faults in the drainage basins of the Middle Fork of the Willamette River and the North Umpqua River, but none in the study area. Callaghan and Buddington (1938) mapped mineralized veins probably deposited along fault planes trending N50-60W in the Quartzville and other mining districts.

The age of faulting is not completely known, but Quaternary rocks at Bull Run Lake have been cut by a northwest-trending high-angle fault, suggesting some faulting as young as Quaternary (Shannon and Wilson, 1961; Schulz, 1980).

A high-angle fault was noted at a south-central location in the study area, just above a large earthflow. The fault cuts an eight-foot thick andesite flow and an underlying gray to pink ashflow unit of the Little Butte Volcanic Series. About ten feet of brecciated and sheared rock marks the fault trace. A drag fold in the andesite flow unit indicates apparent downward displacement to the north of about 30 feet.

Joins

Rocks in the study area display two types of jointing, formed either by the cooling of a rock mass or by tectonic stresses.

Cooling joints form in patterns characteristic of cooling gradients and the chemical composition of a solidifying flow. Andesites show columnar jointing, but more commonly platy and blocky jointing. Basalt flows primarily show columnar and blocky jointing. Cooling joints in volcaniclastic units are poorly developed or badly weathered.

Tectonic joints tend to be open, planar fissures, often crosscutting cooling joint sets. Schulz (1980) finds that tectonic joints in the Columbia River basalt and Pliocene-Quaternary volcanic rocks dominantly trend N10-20W and N40-50W. Beeson et al. (1979) postulate the existence of a N45W dextral wrench zone cutting across

the Cascade Range; N40-50W fractures are an echelon, and the N10-20W fractures are extensional.

MASS MOVEMENT IN THE MIDDLE SANTIAM BASIN

Classification

Mass movement is a complex phenomenon involving many factors, and can be viewed as a system of earth materials and disturbing agents combining to bring about instability. Because of this complexity and number of variables, there are many approaches for categorizing types and behavior of mass movements (Savarenski, 1935; Sharpe, 1938; Skempton, 1953; Zaruba and Mencl, 1969; Varnes, 1978). The classification of Varnes will be used in the following discussions. Varnes' approach is widely used, and is based on these four parameters: (1) type of movement, (2) rapidity of movement, (3) character of material, and (4) water content. Each of these parameters varies widely among unstable terranes in separate areas, and may even vary within a single complex mass movement area. Within the Middle Santiam study area, creep, rockfall-rockslides, debris avalanches, debris torrents, and slump-earthflows occur.

Creep

Creep in the western Cascades occurs within deep soils as a very slow, quasi-viscous movement downslope in response to continuous gravitational stress. Intergranular rotational and translational movements and deformation of clay minerals occur in a creeping soil zone. Creep zones may extend several feet below ground surface in some deep forest soils. Unlike other types of mass movement, creep

zones are not bounded by discrete shear planes, but merely decrease in influence with depth. Incipient shear planes may be indicated by inclinometer monitoring (Swanston and Swanson, 1976). Creep in deep, poorly consolidated materials may grade into other types of mass movement, such as slump-earthflow. Indications that a soil-rock mass is undergoing failure of a shear plane include the development of shear cracks, tension cracks, and pressure ridges. A shear plane develops when shear resistance in a soil at a specific depth is exceeded by shear stress.

Creep occurs in the study area wherever soils mantle a sloping surface, and is a continuous process of sediment input to streams. Creeping soils are often indicated by leaning or bowed conifers growing on sideslopes and above streambanks.

Rockfall-Rockslide

As defined by Varnes (1978), rockfall movement is by freefalling, leaping and bounding, toppling, and rolling of bedrock fragments. The size of rock fragments is initially controlled by the spacing of joint fracture and bedding plane sets.

The likelihood of rockfall is controlled primarily by the orientation of discontinuities relative to that of the slope face, and secondarily by the movement of water and the formation of clayey filling material in between fractures, both of which decrease shear resistance. As the strike of discontinuities in the rock mass approaches that of the slope face, instability increases and the

effects of the other properties are generally unimportant (Piteau and Peckover, 1978).

Rockfall occurs in the Middle Santiam basin from rock outcrops, artificial rock faces such as road cuts and quarry cuts, and fresh slump-earthflow scarps. Impacts of rockfall include damage or destruction of timber, and road or quarry safety and maintenance.

Debris Avalanches

Blong (1973) is critical of groupings used by Varnes (1958, 1978) to classify certain rapid mass movements as a gradational series of debris slides, avalanches, and flows. Varnes bases his classification on increase in moisture content (a flow having the most moisture), but Blong points out that such a criterion is difficult to use in the field, and suggests using compound names such as debris slide-debris avalanche. For clarity, the term debris avalanche is herein to be used to include debris flows and debris slides.

Debris avalanches are shallow, very rapid translational mass movements of soil, rock, and organic debris. Generally, they occur in cohesionless materials and fail on a firm substratum such as bedrock or joint and bedding planes. In the study area, debris avalanches occur in glacial till, colluvial soils, mass movement debris, and road sidecast materials.

A debris avalanche has a shallow, spoon-shaped depression at the head, a V-shaped chute below, and a mass of debris at the toe, if not

removed by erosion. Erosion by streams may be a major agent in triggering streamside debris avalanches.

Debris Torrents

Debris torrents are rapid mass movements initially confined to channels with high gradients. They involve the entrainment and movement of organic debris, soil, and rock as a water-charged mass. Slump-earthflows, debris avalanches, and unstable artificial fills may suddenly supply large quantities of material to a narrow channel whose stream lacks the energy to remove it, often creating dams of sediment and organic debris. These dams may fail during or after intense storms, releasing a torrent of debris which can scour stream channels down to bedrock. Most debris torrents in mountainous areas of western Oregon appear to be triggered by debris avalanches entering channels (Swanson, Lienkaemper, and Sedell, 1976). These events can be highly destructive to streamside vegetation, soil cover, and manmade structures (Swanston and Swanson, 1976).

Slump-Earthflows

In the western Cascades, large slump-earthflows form distinctive topography and may cover several square miles of terrain. Varnes distinguishes between a slump type of mass movement and an earthflow type, but in the study area, as in the H. J. Andrews Experimental Forest to the south (Swanson and Swanston, 1977), both types of

movement and the geomorphological features they create are evident within a single mass movement complex.

In the study area, high, near-vertical crown scarps mark the upper boundaries of active slump-earthflows. Large boulders and talus litter the scarp bases. Downslope, the terrain can be very disturbed, scored with deep tension and shear cracks, and broken into slump blocks and grabens. A rotational component is indicated by upslope-leaning trees and backtilted blocks. Wide, continuous benches or grabens may contain undrained depressions. As slump-earthflow basins narrow toward the toe, as is often the case, moisture is concentrated in the lower portions of the earthflow. These portions may have high soil moisture all year long, showing signs of relatively rapid movement.

Slump-earthflows in the study area have definite, mappable boundaries and distinctive drainage systems. Very large, complex sites have a combination of different mass movement processes in different parts.

Mass Movement and Material Properties

Weathering and Alteration

A number of workers correlate the type, occurrence, and distribution of mass movement sites in the western Cascades with prevalent bedrock types (Pope and Anderson, 1960; Dyrness, 1967; Paeth et al., 1971; Swanson and James, 1975; Burroughs et al.,

1976). Due to their original mineralogy, texture, and alteration history, these rock types are extremely susceptible to mechanical and chemical weathering. Bedrock in the study area has been subjected to a wide range of mechanical, chemical, and tectonic processes (folding and faulting).

Volcaniclastic rocks generally contain a large proportion of glass, which is unstable at the chemical and thermal conditions present at the surface of the earth. This glass, in reaction with H_2O (meteoric or hydrothermal), CO_2 , and O_2 , rapidly alters to hydrated halloysite and the expandible smectites, including montmorillonite (Loughnan, 1969; Taskey, 1978). These minerals comprise the clay fraction of soils. Montmorillonite can also be an end product of weathering of plagioclase and ferromagnesian minerals (Paeth, 1971).

The most widespread type of alteration in the western Cascades, affecting mainly volcaniclastic rocks, results in mineral assemblages which are characteristic of the zeolitic metamorphic facies (Peck et al., 1964). Glass in volcaniclastic rocks is replaced by zeolites and green clay, also accompanied by chalcedony, cristobalite, and a carbonate mineral (Peck et al., 1964). The green clay is identified as montmorillonite.

Propylitic alteration occurs in more restricted areas around intrusive bodies; the characteristic suite of alteration minerals includes albite, epidote-clinozoisite, chlorite, quartz, carbonate minerals, sericite, celadonite, magnetite, and pyrite, but no montmorillonite. In the study area, rocks of the Little Butte

Volcanic Series and Sardine Formation are extensively altered, while younger rocks are fairly unaltered.

Paeth et al. (1971) suggest a relationship between greenish, altered volcanoclastic rocks in the western Cascades and mass movement, based on high amounts of smectite clays (montmorillonite and beidellite) and moderate amounts of free iron oxide in these rocks. Reddish volcanoclastic rocks seem to be more stable and contain kaolin, chlorite, chloritic intergrades, less smectite, and higher amounts of free iron oxide. They found that soils containing a greater proportion of smectite could be expected to show less resistance to shear failure due to the tendency of smectites to swell when wetted.

Basalt and andesite weather to soils containing smectites, kaolin minerals, amorphous aluminosilicates, and amorphous hydrous oxides. The competence of these cooled lava flow units increases their resistance to weathering. Using a chi-square test, Schulz (1980) found that the distribution of mass movements, especially slump-earthflow, is strongly controlled by bedrock geology. The highest number of slump-earthflows per unit area occur on Quaternary landslide debris of the Rhododendron Formation, which largely consists of volcanoclastic bedrock.

The ultimate products of rock weathering are soils, and the most critical materials in mass movement processes are soils or extremely weathered bedrock with the strength properties of soils. The strength of a soil determines its resistance to shear failure, and a slope failure will always occur, or slip will be initiated, within the weakest material.

Soils

General Statement

Slope failures discussed herein develop in soil, very weathered bedrock, or at a soil-bedrock interface. Terzaghi and Peck (1967) indicate that soils are earth materials with an unconfined compressive strength of less than 4.0 kg/cm^2 . Slope stability is directly influenced by soil strength, and indirectly by permeability. Moisture content of a soil significantly affects strength; permeability is related to soil texture and clay mineralogy.

Clay content of a soil determines whether it is cohesive or noncohesive. Most slope failures occur in soils with textures intermediate between cohesive and noncohesive (Borchardt, 1977).

Slope failures generally occur in cohesive clayey materials after thorough wetting by precipitation and groundwater, often over long periods of time. Slow decreases in shear strength are concomitant with large increases in water content and very slow drainage. Creep and slump-earthflow are associated with cohesive materials; slump-earthflow failures are generally rotational and occur along circular failure planes.

Mass movement also occurs in noncohesive coarse, sandy materials. Shear strength decreases rapidly with only slight increases in water content, even though drainage is relatively rapid. Debris avalanches and debris torrents are associated with noncohesive materials, and failure generally occurs on planar surfaces.

Smectites are primarily responsible for high plasticity, adsorption of much water, slow drainage, and subsequent loss of shear strength in soils containing these clay minerals (Borchardt, 1977; Taskey, 1978).

In order to demonstrate some of these soil-stability relationships, a total of 58 soil samples were taken at different locations throughout the study area (Fig. 5). Most of these samples were from unstable or mass movement sites underlain by the Little Butte Volcanic Series. Samples were collected by hand excavation from roadcuts, stream banks, scarp exposures, and earthflow flow front areas. Others were collected in Shelby tubes (thin-walled steel tubes about two feet in length and three inches in diameter) by driving the tubes into the soil (Thrall, 1981). The Middle Santiam mass movement site near the junction of the Middle Santiam River and Pyramid Creek was cored using a truck-mounted Forest Service drill rig, but no intact soil samples were collected during drilling.

All soil samples were stored in plastic bags to prevent drying; drying of clays causes irreversible structural changes and changes in the index properties of some soils (Thrall, 1981). Samples were analyzed in the laboratory for undrained shear strength, plasticity, texture, and clay mineralogy.

From a stability-lithologic standpoint, the samples are assigned to four main groups: (1) residual soils overlying nonvolcaniclastic bedrock; (2) nonvolcaniclastic soils from slump scarps and debris avalanches; (3) soils derived from volcaniclastic materials: (a) from unstable sites, and (b) from stable sites; and (4) lava flow

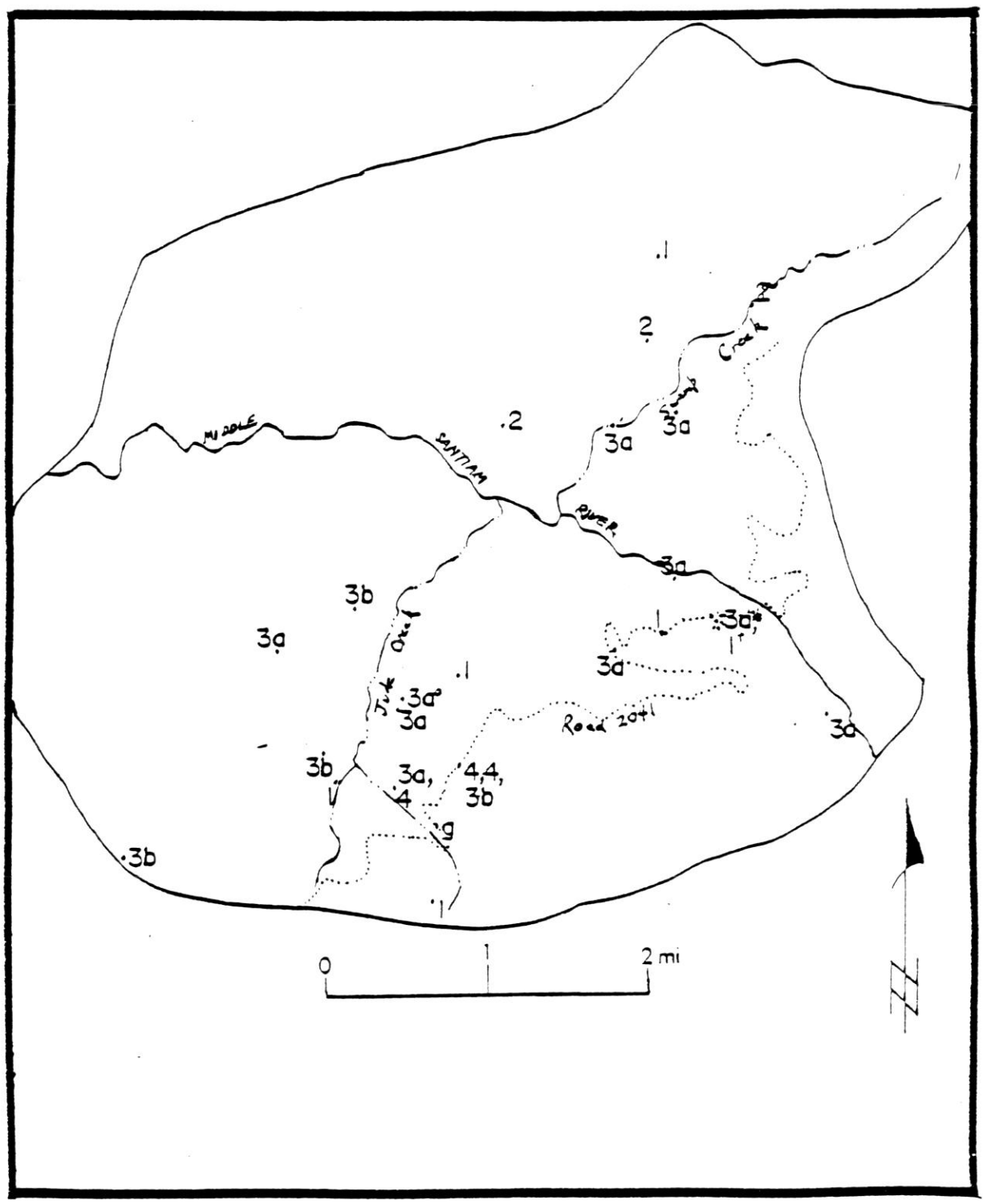


Figure 5. Location and classification of 45 soil samples; see Table 3 for collection methods and explanation of soil group symbols.

breccia soils. In addition, one sample of glacial soils was collected.

Soil Strength

Undrained shear strength values were derived for selected soils from the study area, using a shear vane device (Cadling and Odenstad, 1950). The shear vane device was used on samples encased in Shelby tubes; readings were taken at different depths within the soil as it was extruded from the tube.

The amount of sample disturbance is unknown; some of the sampled materials are very soft, but are interbedded with coarser, denser materials so that the Shelby tube had to be hammered rather than pushed into the soil. The effect of sample disturbance by this method is most severe in soft, sensitive soils (Wu and Sangrey, 1978). Disturbance generally lowers the strength of a soil, so that some of the shear strength values obtained may be low. Additionally, Shelby tube samples SS-34MS and SS-40MS were extracted from blocks of material which appeared to have undergone downslope transportation by mass movement, and repeated wetting and drying because they were exposed on an actively sloughing, bare soil slope. However, internal stratification of volcanoclastic materials could still be recognized. Results of these simple strength tests should be applied with caution to slope stability problems (Bjerrum, 1973).

Figures 6 and 7 plot undrained shear strength values vs. natural moisture contents of three Shelby tube samples (SS-34MS, SS-40MS, and SS-45). Table 2 is a key to Figures 6 and 7. These data indicate

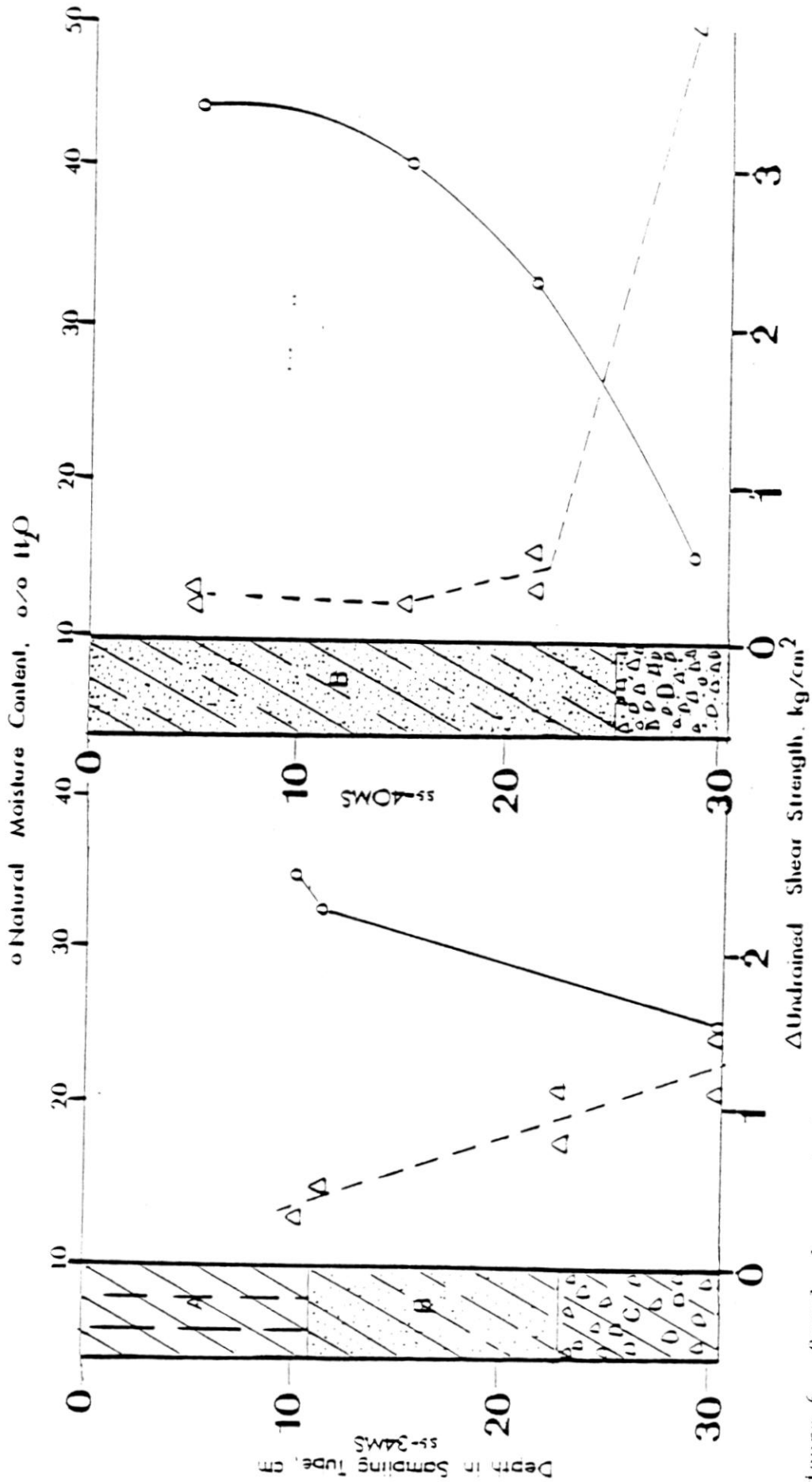


Figure 6. Sample logs and plots of %H,0 vs. undrained shear strength for Shelby tube samples SS-34MS and SS-40MS from the Middle Santiam mass movement site (see Table 2 for key to soil types A, B, C, D).

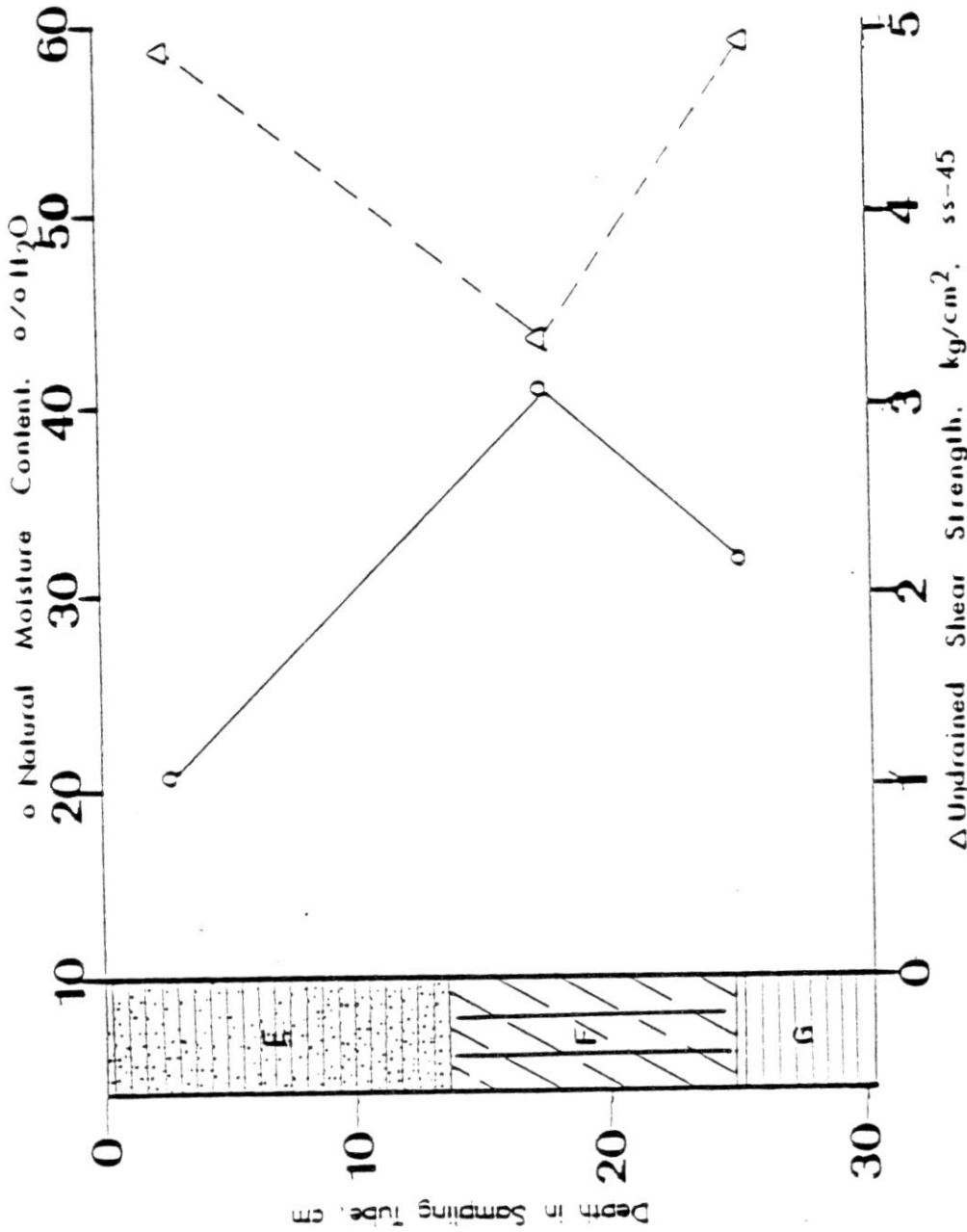


Figure 7. Sample log and plot of %H₂O vs. undrained shear strength for Shelby tube sample SS-45 from roadcut in Jude Creek drainage. See Table 2 for key to soil types E,F,G.

Soil Units A through G

- A. purple, soft and plastic silty clay interlaminated with green and red silt and clayey silt.
- B. purple to yellow soft and plastic sandy clay and clayey sand.
- C. purple, stiff sandy clay with slickensided pebbles.
- D. weathered epiclastic volcanic breccia—sandy, firm, non-cohesive; interbedded with clayey laminae approximately 1 cm thick.
- E. gray, siltstone, firm, with polished bedding planes.
- F. brick-red clayey silt; low plasticity.
- G. Purple buffaceous siltstone

Curve Symbols



moisture content curve



undrained shear strength curve

Table 2. Key to figures 6 and 7.

that soils with higher moisture content have lower strength. Other studies demonstrate this correlation (Borchardt, 1977; Mitchell, 1976; Thrall, 1981). The shear strength values in Figures 6 and 7 probably reflect the residual strength of these soils, which have undergone mass movement. Sample SS-45 was taken from a roadcut with seepage and minor soil slumping; however, only intact materials were sampled.

The moisture content profiles in Figures 6 and 7 indicate that the more clayey, plastic materials naturally adsorb more water. Their natural water contents are fairly close to their liquid limit, or the water content below which the material assumes plastic properties. These soils are primarily derived from thinly bedded tuffaceous mudstones, possibly interbedded with airfall ash layers.

Classification of Soils

The Unified Soil Classification System (USCS), used here, is widely applied in the United States. The USCS was originally designed by A. Casagrande in 1948 and modified and adopted by the U.S. Armed Forces and the U.S. Bureau of Reclamation. The system allows soils to be classified under standards based on index properties which can be easily and rapidly determined. To classify a soil using the USCS, the gradation characteristics of its coarse-grained fraction (not passing a No. 200 sieve) are determined by sieving and obtaining a gradation curve. The physical (plasticity) characteristics of the fine-grained fraction (not passing a No. 40 sieve) are determined by finding its Atterberg

limits. Both grain-size distribution and the determination of Atterberg limits are test procedures standardized by the American Society for Testing and Materials (test procedures ASTM-D422 and D423, respectively). Any soil identified by the USCS can be represented by a combination of two or more letter symbols.

Most soils in the study area, regardless of parent bedrock, are SM soils in USCS classification (silty sands or poorly graded sand-silt mixtures)(Table 3). The fine-grained fraction of these soils is nonplastic or has a low plasticity index. The average plasticity index for the SM soils sampled in this study is 12.7. All the soils sampled contain a range of grain sizes; even soils which appeared clayey and plastic in the field contain appreciable amounts of sand and silt.

Figure 8 presents the Atterberg limits of 24 soil samples, and the distribution of these limits with respect to the four soil groups. Seventy-nine percent of the samples are below the A-line, indicating the predominantly silty nature of the fines. Sixty-two percent of the samples have low to moderate plasticity.

Atterberg Limits and Clay Contents

Atterberg limits, clay content, and activity (plasticity index/% clay) were determined for 28 soil samples (Table 3). High plasticity indices indicate high compressibility, low permeability, and high shrink-swell potential. Borchardt (1977) notes a direct correlation (0.77) between the plasticity index and smectite content. The activity of a soil relates the plasticity index to the proportion of

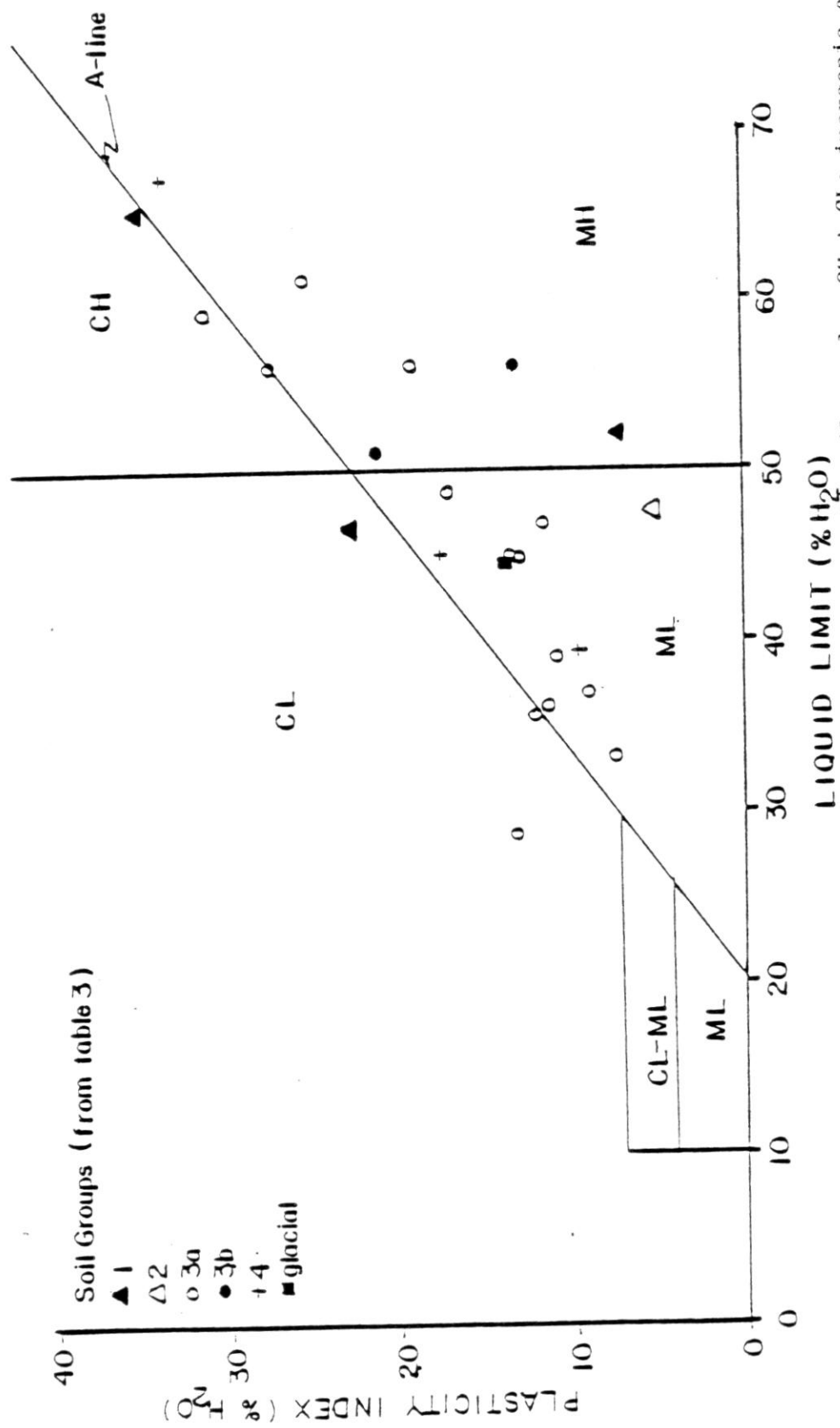


Figure 8. Atterberg limits of fine fraction (-40 sieve) for 24 soil samples CH + CL: inorganic clays; MIH + ML: inorganic silts, very fine sands, silty or clayey fine sands, elastic silts.

Soil group	Liquid Limit		Plasticity Index		Band/width/decay	Activity Index	URCS symbol
	Limit W_L	Index W_p	W_L	W_p			
1. Residual soils, non-volcaniclastic or mixed (3 samples)	50.6	6.9					SH
Average values	46.5	22.5					SH ^F SC ^F
	40.6	14.7					
2. Soils from stump escape (3 samples)	65.0	31.5					SH ^F
Average values	47.6	5.1				.51	SH
	56.3	19.0					
3a. Volcaniclastic soils, unstable silicea (14 samples)	46.1	16.6					SH ^F SH ^F SH ^F
	19.2	10.4					SH ^F SH ^F
	61.2	25.0			50/15/27	.90	SH ^F
	35.0	12.0			72/14/14	.66	SC
	56.2	27.0					SC ^F
	16.0	0.9			76/12/10	.09	SH
	44.7	12.6			16/10/14	.90	SH
	33.2	7.5					SH
	16.1	11.5			13/15/12	.94	SH ^F
	56.0	10.7			69/20/11	1.7	SH
	44.7	12.4					SH ^F
	46.7	11.6			59/28/13	.93	SH ^F
	59.2	10.6			62/31/5	5.7	CH ^F
	28.4	13.4			66/23/11	1.2	SC ^F
Average values	44.0	15.6			60/19/13	1.6	
3b. Volcaniclastic soils, stable silicea (14 samples)	51.0	21.0					SH ^F
Average values	56.0	13.0					SH ^F
	53.5	17.0			05/0/7 92/4/4 09/6/5		
4. Lava flow breccia soils (3 samples)	44.9	17.7					SH ^F
Average values	67.3	33.3			70/25/5	3.2	SH ^F
	39.6	9.0			49/39/12	2.7	SH ^F
	50.6	20.3			60/32/0	1.0	SH ^F
Glacial soil (1 sample)	44.2	13.5					SH
					--/--/16.7	.80	

1r. Non plastic soils, Atterberg limits could not be determined

2r. Sample SS 1489 from Middle Santiam mass movement site

3r. Sample SS 4049 from Middle Santiam mass movement site

* Classification based on Atterberg limits of minus 40 sieve material

F: Samples processed by technicians at Santiam Engineering zone or supervisor's office, Willamette National Forest

Table 3. Soil groups and Index properties of 23 soil samples.

clay particles in a soil, and is also a function of the activity of the clay species present. Materials with high activity indices generally have lower strength.

Liquid limits for all soils tested average 50.6%, with a high of 67.3% in a soil derived from a flow breccia horizon. This soil also has the highest measured plasticity index of 33.3%, while the average plasticity index for all samples is only 16.6%. At the sampling site, this breccia soil was saturated, moldable, and clayey. Flow breccias weather rapidly to clay because of their vesicular and fragmental texture and large amounts of interstitial glass.

Other high Atterberg limits were obtained from samples from slump scarps and volcanoclastic soils on unstable sites underlain by the Little Butte Volcanic Series. The highest liquid limit among these soils is 65%, and the highest plasticity index is 34.5%. One sample of material taken from the earthflow toe of the Middle Santiam mass movement site has a liquid limit of 61.2% and a plasticity index of 25%.

The particle-size distribution and amount of clay fraction (2 um and less) was determined by the Bouyoucos hydrometer method (Bouyoucos, 1962). Determination of the clay content of a soil is difficult and results vary with the method of soil preparation (drying, dispersal time, dispersing agent). Terzaghi (1958) reports the clay content of an Indonesian soil varying from 6 to 33% depending on the dispersing agent used. Thrall (1981) reports that upon drying, poorly crystalline soils (allophane soils) derived from volcanic ash undergo an irreversible increase in average grain size. Some of the samples in this study were air-dried, but the same dispersal agent was used throughout.

The average clay content of volcanoclastic soils on unstable sites is higher than the average clay content in other groups; however, the number of determinations in this group is greater than the number of determinations in all other groups. The average clay content of all soils in the study area is 11.2%.

The activity indices of flow breccia samples are very high, suggesting that flow breccias weather into very weak soils and may be responsible for numerous slope failures. Activity indices of volcanoclastic soils from unstable sites are also high; the value 5.7 for one sample may be based on inaccurate clay content data.

Clay Mineralogy

Schulz (1980) used X-ray diffraction techniques developed by Theisen and Harward (1962) to determine the clay mineralogy of 40 soil samples from the Bull Run watershed. These samples were taken from different types of mass movements and from soil overlying various geologic units; many of the rock types are similar to those found in the study area. The clay mineralogy of two soil samples from the Middle Santiam mass movement site was determined in this study using the same techniques.

Schulz (1980) found that mass movement occurrence in the Bull Run watershed is favored by high smectite and possibly hydrated halloysite contents, whereas stable sites contain abundant chloritic intergrade and kaolinite. The latter clay minerals are primarily found in soils weathered from andesite and basalt flows; smectites and hydrated halloysites are found in volcanoclastics of the

Rhododendron Formation, Quaternary landslide debris, and flow breccias.

The samples from the Middle Santiam site contain only montmorillonite (smectite) and kaolinite, with montmorillonite dominating. Sample SS-57MS contains almost pure montmorillonite, while SS-58MS contains minor kaolinite. Montmorillonite diffraction peaks for both samples are well resolved and quite intense.

Permeability and Groundwater Flow

Permeability defines the ability of a rock or soil to transmit fluids, and therefore controls the movement of groundwater. The permeability of a rock or soil mass is in part dependent on the size, shape, and continuity of pore spaces. Different rock types have differing permeabilities based on their texture. Also, the fracture pattern of rock units influences permeability. Soils texture may vary greatly from point to point; thus, permeability may vary more than any other soil property. Furthermore, the order of magnitude of the variation of permeability in most soils, ranging from gravels to clays, is greater than the variation of other properties relevant to mass movement analysis. Gravels are most permeable, while clays can be relatively impermeable.

Mass Movement and Geologic Structure

General Statement

Geologic structure is a major factor in the occurrence and distribution of mass movement. Regional structure such as large-scale fault trends and fold axes are significant, but smaller structural discontinuities (joints, small faults and shear zones, lithologic contacts and bedding planes) are strong local factors. Structural discontinuities influence mass movement by acting as slip surfaces and by serving as avenues for or barriers to groundwater flow. Schulz (1980) tested the validity of correlations between mass movement occurrence and geologic contacts, springs, seeps, and joints in the Bull Run watershed, using chi-square tests. In each case the correlations were positive, although he found that the influence of jointing attitudes on mass movement was minor compared to that of geologic contacts.

Structure and Slip Surfaces

The role of bedrock joints in rockfall and rockslide events has been previously discussed. Deposits of fallen bedrock joint blocks of boulder size and smaller exist throughout the study area. Such a deposit, covering approximately 3,600 acres, lies beneath Chimney Peak, an eroded, possibly glaciated, remnant of a basaltic flow, of Pliocene (?) age. Chimney Peak's faces are densely scored by some

combination of cooling joints, tectonic fractures, and superficial fractures produced by frost wedging.

Besides joint spacing and orientation, the strength of soil filling joints is also a factor; some of this soil may contain montmorillonite clays from rock alteration, and the pressures of montmorillonite swelling against joint walls leads to instability of joint blocks. An example of the significance of joint filling can be observed on the crown scarp of the Middle Santiam mass movement site, where thin coatings of slickensided clayey soil were noted adhering to joint faces on fallen joint blocks.

Slump-earthflow and other types of slope failures may be initiated as failure of a weak soil or rock stratum. The attitude of this stratum may or may not control the likelihood of mass movement.

Faulting or shearing produces zones of crushed and brecciated rock on either side of a fault plane. Materials in a fault zone are weakened and susceptible to mass movement.

Structure and Groundwater

Structural discontinuities, groundwater, and the permeability of soil and rock work in combination to produce conditions favorable for mass movement.

Joints conduct water through a bedrock unit. The freezing of water within joints exerts great pressure on the walls and promotes rockfall and rockslide. If bedrock underlying a fractured rock unit is relatively impermeable, a perched water table may develop, saturating materials above this permeability discontinuity. Slope

failure occurs through a buildup of positive pore pressures, which decrease the effective weight and internal friction of soil and weathered rock. In some cases, pore pressure may be relieved by seepage from a free slope face.

In the study area, the stratigraphic juxtaposition of rock types with differing permeabilities greatly influences mass movement. Permeability discontinuities exist where, for example, lava flows are interbedded with less permeable volcanoclastic bedrock.

Interbedded lava flows and volcanoclastic rocks occur throughout the study area, notably in the Little Butte Volcanic Series. Mass movements commonly occur where sequences of thinly bedded epiclastic and ash layers are intercalated with andesitic or basaltic flows. Where these lithologies are exposed on a free slope face, springs occur at the lava flow-volcanoclastic contacts, and slow seepage occurs between tuffaceous sandstones and underlying tuffaceous siltstones or fine ash. Any dip in bedding attitudes aids the mobility of groundwater, but it appears that slope failures may develop in strata dipping at angles as low as $10-15^{\circ}$. The Middle Santiam mass movement site is capped by an andesite flow which overlies bedded volcanoclastics. The Jude Creek mass movement site is underlain by a very weathered vitric lapilli tuff-breccia and capped by a massively jointed volcanic breccia.

Fault zones containing gouge are usually impermeable because of high clay content, and the fault plane may act as a barrier to groundwater flow, affecting the stability of overlying materials by increasing pore pressure.

Only a few fault and shear zones could be recognized in the study area. It is possible that structural disruption and bedrock alteration from faulting and subsequent effects on groundwater flow contribute to more mass movement than can be recognized with the poor exposure prevalent in the study area. Minor slumping and debris avalanching occurs in the gouge material along a minor fault in the south-central portion of the study area.

Mass Movement and Pleistocene Glaciation

General Statement

The occurrence of large, complex slump-earthflows and other mass movement types in the study area and elsewhere in the western Cascades may have been related in part to climatic, hydrologic, vegetative and terrain conditions which prevailed during late Pleistocene time.

Dating of Mass Movement Sites

Ages of slump-earthflows and other mass movements may be determined by dating litter and woody materials entrained in their deposits, using C-14 techniques. The radiocarbon ages of these materials can be assumed to correspond with the time of the original mass movement event or subsequent activity. Swanson (unpublished data) dated a piece of wood contained within a large, mostly inactive, slump-earthflow in the Lookout Creek drainage of the H. J. Andrews Experimental Forest. This location is approximately 20 miles south of the study area in terrain underlain by the same general rock types. The wood had a C-14 age of $> 40,000$ years B.P.

Gottesfeld, et al. (1981) dated a fossil wood, needle, and pollen assemblage contained in a deposit interpreted as of possible debris torrent origin in the Lookout Creek drainage in the H. J. Andrews Experimental Forest at $> 35,500$ radiocarbon years in age. The fossil assemblage probably represents a flora of late Pleistocene age, and

may have formed during early Wisconsin or a previous glaciation. In the Northwest, glaciation during early Wisconsin time is represented in part by the Hayden Creek, Jack Creek (Scott, 1977) and other drifts.

Slump-earthflows in the study area may have been active thousands of years ago, and active slump-earthflows may have a history of activity spanning millenia. The fact that there are old-growth trees on both active and inactive earthflows establishes a minimum age of several hundred years. No other age data were collected. On the strength of age determinations on slump-earthflows in similar terrain underlain by similar rock types elsewhere (Swanson, unpubl. data; Gottesfeld, et al., 1981), earthflows in the study area may date back as far as the Pleistocene. Stout (1977) determined the age of several landslides in southern California as late Wisconsin. Assuming that some mass movements in the study area may be as old as Pleistocene in age, the next step in this discussion is to establish the extent of glaciation in the study area.

Glaciation

Crandell (1965) shows no glacial activity in the study area on his map of Pleistocene glaciation in the Cascade Range. Geologic mapping of the study area disclosed small patches of possible glacial drift at scattered locations, but other evidence of the existence of glacial ice such as U-shaped valleys, moraines and cirques is lacking. However, definite glaciated landforms exist just outside the study area; the horns and cirques of the three Pyramids four

miles to the east, and the large cirque of Crescent Mountain four miles to the southeast are examples. Gregg Creek flows northward from Chimney Peak along a somewhat U-shaped valley.

Scott (1977) studied glacial features in the Central Oregon Cascades, and determined the equilibrium line altitudes (ELA's) for glaciers which existed during early and late Wisconsin glaciations. An ELA is the elevation at which the net balance on a glacier equals zero, and accumulation equals ablation.

Scott determined that the ELA was 3100 to 3300 feet below its present elevation of 8000 feet in the Mt. Jefferson area during the late Wisconsin glaciation and 3600 to 3800 feet lower during the more intense early Wisconsin glaciations. ELA's were even lower in the western Cascades during these glacial periods, because they received heavier precipitation than the High Cascades. The elevations of cirque floors at the Pyramids and Crescent Mountain (about 4500 feet) indicate that glaciers may have existed there during the Wisconsin. If so, the study area was in a periglacial environment.

Effects of Glacial Climates and Glaciation

Climatic changes and associated glaciation has massive, fairly rapid impacts on geomorphology, hydrology, and vegetation. Timberline is suppressed or lowered in elevation by direct advances of glacial ice or by cold temperatures (Heusser, 1956). This results in the denudation of landscapes above suppressed timberline. During the Wisconsin glaciations, timberline suppression undoubtedly had some effects on the hydrologic regime in terms of reduced

evapotranspiration and infiltration, with concomitant increases in runoff potential. If the ground was frozen, infiltration would have been further inhibited.

Reduced evapotranspiration and reduced root strength on landscapes above timberline are favorable conditions for shallow mass movement (Swanston and Swanson, 1976). Increases in runoff and peak flows would have led to increased bank cutting.

Although terrain was impacted by glaciation and large mass movements during glacial stages, it may be just as valid to associate mass movement activity with warm interglacial periods. Snowmelt from warmer temperatures and rain-on-snow events (Harr, 1981) may have caused erosion in headwater areas and downstream flooding. Increased water input to soil and higher pore water pressures are favorable conditions for slope failures. Perhaps the large amounts of water quickly released by melting of glacial ice and snow on sparsely vegetated terrain led to many mass movements ranging from shallow debris avalanches to deep slump-earthflows.

This discussion is largely speculative, and is included to propose possible associations between Pleistocene climatic changes and the occurrence of mass movement. The primary question may be whether conditions were more favorable to mass movement during glacial periods or interglacial periods. Other unknowns exist, such as the rates of water delivery to the soil from melting of snow and ice and the seasonal availability of this water.

MASS MOVEMENT SITE CASE STUDIES

General Statement

In the following section, three complex slump-earthflow sites are discussed in detail. Geomorphic features of all three and rates of current movement on the Jude Creek site and current and historic movement on the Middle Santiam sites are described.

The complexity of each site is indicated by the variety of distinctive mappable geomorphic units within each. Landforms and vegetation on these units reflect the type of mass movement, relative movement rates, and recency of mass movement. Geomorphic units consist of a terrain type, based on landforms, and a relative activity class, based on various terrain and vegetation indicators (Table 4).

The three sites are informally named Donaca, Jude Creek, and Middle Santiam. The size, rates and histories of movement, relative influence of man's activities, and impacts on natural systems of each differ considerably; however, there also are features common to all three.

Movement Rate Monitoring Methods

Methods used by previous workers to measure surface and subsurface movement of active slump-earthflows are discussed in a previous section. Methods used in this study on Jude Creek and Middle Santiam mass movement sites are: surveying, stake arrays, crackmeter, and an inclinometer.

Surface and subsurface mass movement rates were determined for several reasons: (1) to compare surface movement vectors at different locations within the same mass movement site, (2) to determine how rates are related to amounts and timing of precipitation, and (3) to provide data for estimating sediment yield by earthflow movement into impacted drainageways.

Mapping Methods

Mass movement sites and major geomorphic features such as scarps, drainage ways, and undrained depressions could be identified on aerial photographs. Other mass movement sites, geomorphic units, and microtopography were identified and mapped in the field.

Detailed maps of mass movement sites were produced by surveying baselines and using tape, compass, and rangefinder to map geomorphic features and indicators of activity level. Geomorphic mapping data were used to classify mass movement types and to delineate geomorphic units.

Geomorphic Units

Each mass movement site is divided into mappable geomorphic units. Each unit consists of one terrain type paired with a relative activity class. In this study, seven terrain types and three relative activity classes are identified (Table 4). This classification system is based on features observable on mass movement sites within the study area. Its usefulness is limited in

other areas, where vegetation characteristics and styles of mass movement differ. Within the study area, the system has broad area-wide planning applications and limited site-specific planning applications.

Terrain types are identified primarily on the basis of surface morphology. Secondary features useful in distinguishing terrain types are patterns of vegetation, drainage patterns and location on the mass movement site. Secondary characteristics of the same terrain type are similar on different mass movement sites in the study area but there are variations due to scale, age, and level of mass movement activity. Also, terrain types tend to occupy the same relative locations on different mass movement sites.

Relative activity for each geomorphic unit in this study can be identified by indications of stress imposed by mass movement on vegetation and landforms. An inactive geomorphic unit may have undergone mass movement in the past, but shows no discernible indications of current activity. Vegetation and landforms on active (both moderately and very active) units are stressed. Both mechanical and moisture stress influence vegetation growth. The difference between the two classes of current activity is based on internal deformation, movements relative to stable ground, or a combination of both. The higher the relative movement rates, the more dramatic and obvious are the signs of stress.

This activity classification system is qualitative rather than quantitative. Movement rates were determined on only two mass movement sites, so that activity classification on other sites is essentially an extrapolation of characteristics from a small sample.

MORPHIC TYPES

	Background	Vegetation	Drainage Patterns	Location
I. Boundary Scarps	Steep walls of exposed rock and/or soil	Spars to heavy moss and brush growth in rock fractures, talus and soil pockets, or understorey and overstorey	Spillage from rock fractures, soil cracks or lithologic contacts, waterfalls from top of scarp	Crevasse and parts of lateral boundaries of slide
II. Boulder Fields	Fills of rockfall debris; upper size limit of boulders depends on fracture pattern in bedrock	Variable, dependent on rockfalls, shifting of boulders and substrate mass movement activity	Low surface drainage density; water percolation through voids and soil pockets	Below scarps
III. Scarp Benches	Gently sloping bench-like landform bounded by scarps or ground cracks. Scale may vary from vegetation to dense stands of timber	Variable, ranging from moss shifting of boulders and substrate mass movement activity	May support surface streams, ponds, or poorly drained depressions	Throughout interior of slide
IV. Interior Scarps	Steep walls of exposed rock and/or talus	Spars to heavy as in boundary scarps	as in boundary scarps	Interior of mass movement site, spreading particularly in sense of movement below scarp
V. Flow Fronts	Bulging or rounded steep faces consisting of soilflow debris	Spars to heavy, depending on soilflow activity and stream or other impacts	Mills and gullies through soil, exposed soilflow debris; ponds, seeps, and springs	Terrestrial end of mass movement site
VI. Stream Erosion Impact Zones	Bank and stream channel areas	Riparian	Streamflow and subsurface soil moisture (bank water tables) affected by seasonal storm activity	Above, below or around flow fronts along stream reaches
VII. Debris Avalanches - Debris Flows	Defined as active, or recently active, slope failures with hollows in the source area and depositional mass domeslope	Hydrophytes on depositional masses	Springs at the source area, till erosion on track and depositional areas	Steep slopes, streambanks, interior scarps

Table 4. Geomorphic units for mass movement sites - terrain types.

RELATIVE ACTIVITY CLASSES

A. Inactive

Past activity is indicated by:

1. Vegetated scarps
2. Ponds and poorly drained depressions
3. Vegetated boulder fields
4. Vegetated bare upstream from old flow fronts, suggest channel aggradation in the past

B. Moderately Active

Indicated by:

Stressed terrain

1. Unvegetated or sparsely vegetated scarps
2. Sparsely vegetated boulder fields
3. Shear and tension ground cracks and grabens
4. Poorly drained depressions
5. Discontinuous surface streams
6. Abraded and constricted boundary stream reaches
7. Streambank failures
8. Horst-graben microtopography

Stressed vegetation

1. Conifers with bent, curved or bowed trunks
2. Leaning conifers with straight trunks
3. Down live trees
4. Scarred, partially buried, abraded trunks
5. Split trees, stretched aligned roots
6. Holes in canopy
7. Hydrophytes, bog plants on poorly drained areas

C. Very active

The same stress indicators found on moderately active terrain, but faster movement rates result in an overall more disturbed appearance. Most trees are leaning or jackstrawed. Ground cracks are wider. Changes are more apparent over periods of observation.

Table 4. (continued) Geomorphic units for mass movement sites - relative activity classes.

There is a continuum of movement rates, and any quantitative cut-off point is quite arbitrary and based on limited data. Seasonal variations in movement are an additional complication.

This geomorphic unit classification system is used on maps of Donaca, Jude Creek and Middle Santiam mass movement sites (Figure 9, Plates 1 and 2) and at a smaller scale on a map of the entire study area (Plate 3).

Case Study I: Donaca Mass Movement Complex

General Statement

The Donaca mass movement complex lies in a forested basin north of the Middle Santiam River (Figure 9). The complex consists of four topographically discrete mass movement sites dominated by deep slump-earthflow processes (Figure 9). Interactions of stream cutting, massive slump-earthflow failure, and impact on stream reaches resulted in the present geomorphology of the complex.

Swamp and Donaca Creeks are the major streams draining the basin, and numerous smaller streams form an internal dendritic drainage system. The entire drainage system empties southward into the Middle Santiam River (Figure 14).

Mass Movement Sites of the Donaca Complex

The four mass movement sites of the complex are designated as A, B, C, and D in Figure 10.

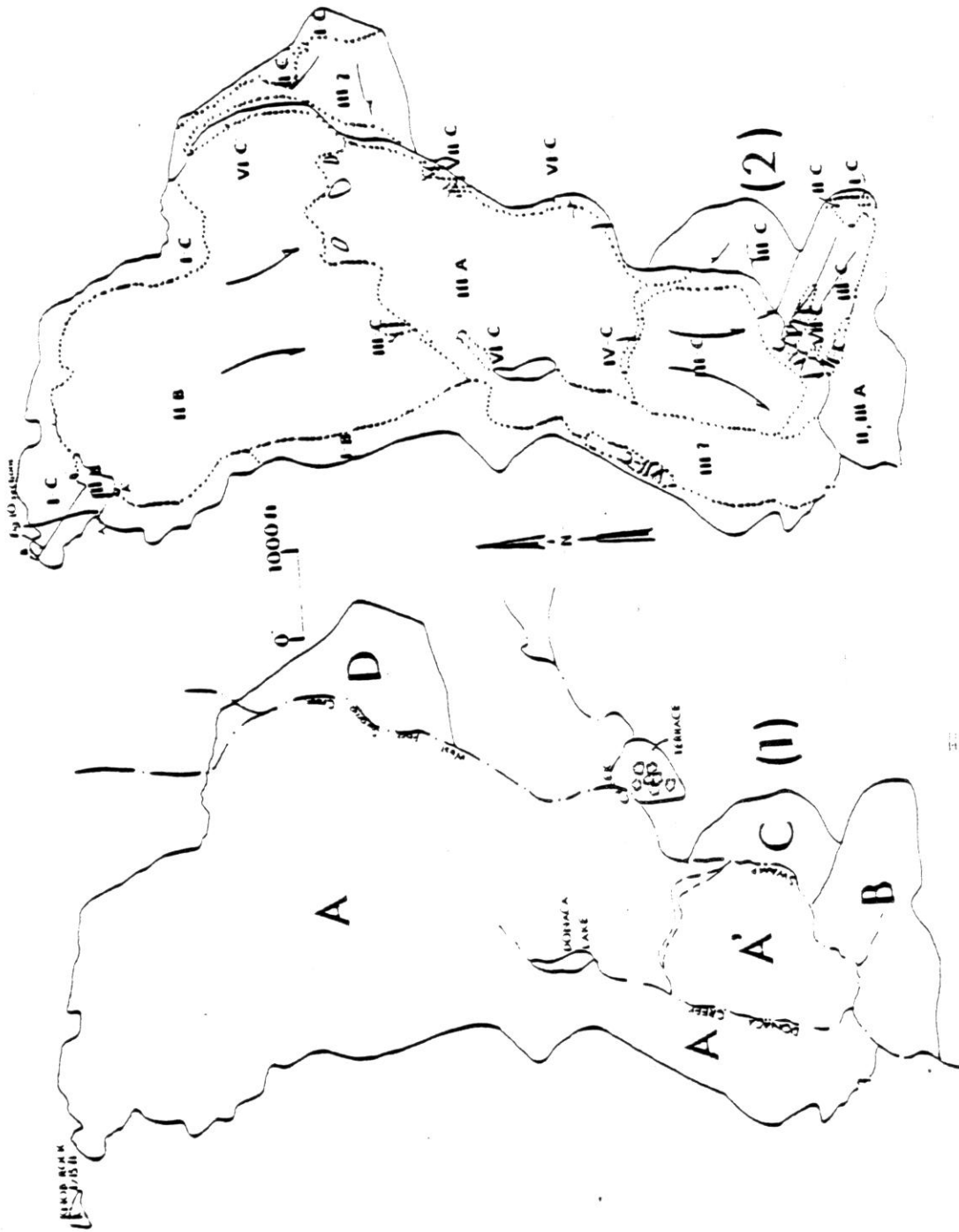


Figure 10. Donaca mass movement complex. Map of sites (1) and geomorphic unit map (2).

Site A is a huge active slump-earthflow covering 650 acres (approximately 1 mi²). It extends almost two miles from an elevation of about 4200 feet, below Knob Rock, to the junction of Donaca and Swamp Creeks, at approximately 2000 feet in elevation. Of all sites in the study area, it is the largest and was most intensively investigated in the field, so it is discussed in some detail.

Site B is mass movement terrain which covers 140 acres; it is divided into an active, variably wooded northern half and an inactive southern half. The active portion has a crown scarp exposing andesite or basaltic flow rock underlain by volcanoclastic rocks. Its steep upper portions are characterized by interior scarps and chaotic boulder piles on top of gravelly to sandy blocks and conical piles of eroded volcanoclastics. Lower portions are flatter and characterized by deep, mixed soils and earthflow debris, poorly-drained depressions and short, sediment-laden streams. The flow front consists of steep high banks of debris actively impacting on and being eroded by Swamp Creek. The southern inactive portion supports dense old-growth forest growing on bouldery terrain.

Site C is a 27 acre basin of unstable creeping slopes and poorly drained flats. Its dense forest cover shows effects of moderately active mass movement. There are no clearly defined crown or side boundary scarps.

Site D was not field checked. From examination of aerial photographs, the site appears to be a 50-acre slump-earthflow with a clearly defined bedrock crown scarp. The reach of Swamp Creek

flowing southeast past its toe is narrow and possibly impacted by active earthflow movements.

Geomorphic Units of Mass Movement Site A

In the following discussion, geomorphic units found on mass movement site A of the Donaca complex are described. Site A was chosen for detailed discussion because it is the largest and contains all geomorphic units described in Table 4.

Crown Scarp

The sparsely vegetated crown scarp of site A provides the largest, most continuous exposure of bedrock in the study area, about 250 feet of lava flows and volcanoclastic units (Figures 11, 12, and 13). Deep aprons of talus obscure any exposure of a slip plane or shear zone at the base of the scarp.

Fresh mudflows and debris avalanches originate from the crown scarp at the northeast contact of the lava flows and the intracanyon volcanoclastics. A perennial spring emerges at this contact. Springs emerge elsewhere on the scarp face, especially where lava flows overlie flow breccias.

Boulder Fields

Great, chaotic piles of boulders up to 15 feet across are spread over approximately 250 acres on the upper third of site A as an essentially continuous boulder field. The surface of the boulder field consists of a series of roughly north-south trending, steep-sided boulder ridges. These ridges are as much as 50 feet high, 250 feet wide at the base and 2000 feet long. Ridge morphology

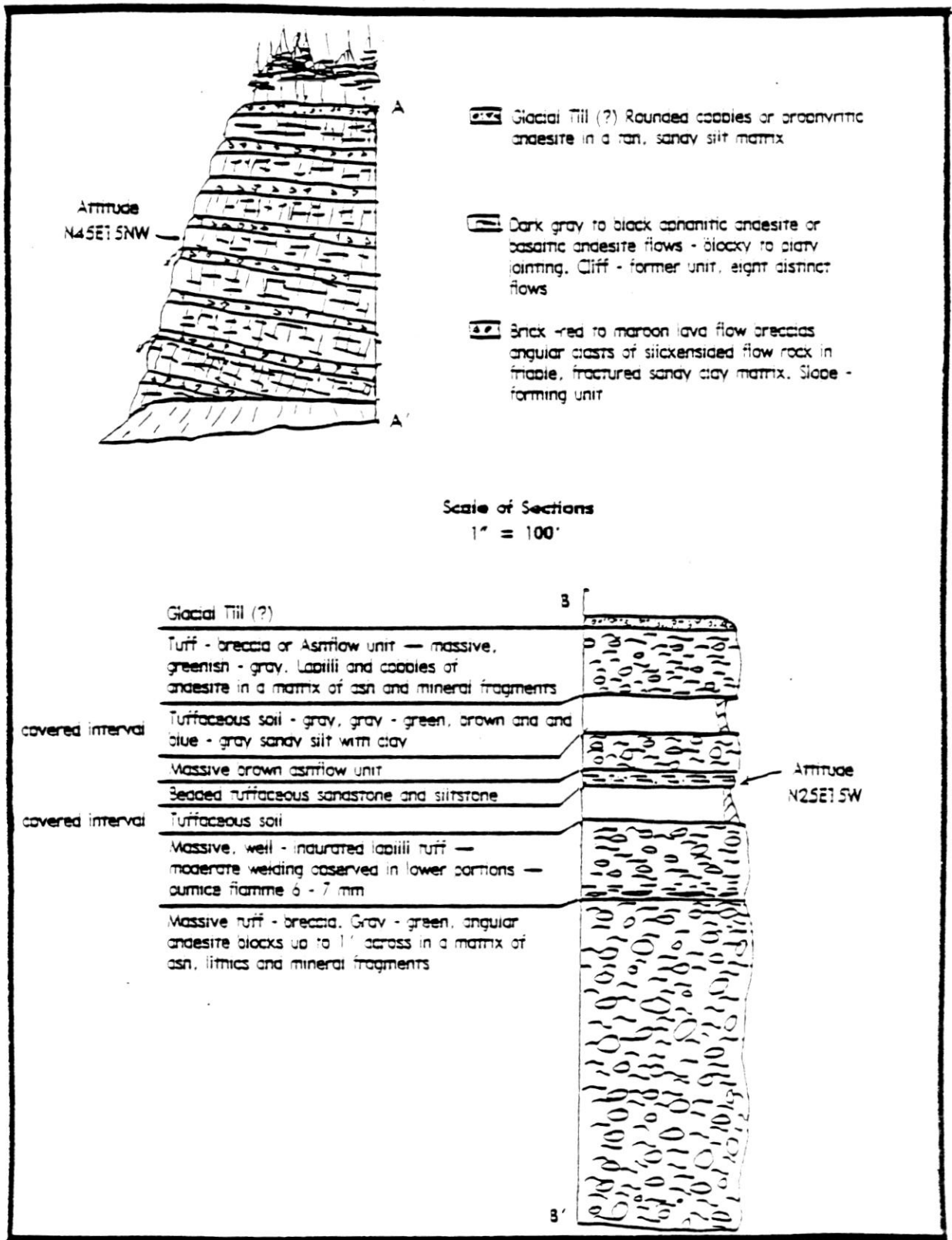


Figure 11. Rock types exposed on crown scarp of site A, Donaca mass movement complex. See Figure 10 for location of sections.

probably formed in response to stresses imposed by slumping of underlying materials.

The origins of this terrain type can possibly be traced to landforms which existed before the massive failure of site A. That is, some of the boulders that now lie within the mass movement site may have been talus deposits at the base of Knob Rock; slumping of the underlying terrain could have brought them to a much lower elevation. Subsequent rockfall from the crown scarp and settling and downslope movement of underlying materials resulted in the present morphology of the boulder fields.

Shifting of boulders within the boulder field is indicated by sparsely growing, curved and leaning conifers, scarred or downed trees, and slumping of boulders and colluvial soils from the ridge sides. Rock faces lacking or poor in lichen and moss cover indicate freshly fallen or moved boulders.

Drainage on these boulder fields is not well-defined. Precipitation probably filters through pockets of silty to sandy soil and voids between boulders. A fresh two-acre slump-earthflow with abundant active seepage lies below the snout of one boulder ridge, indicating saturation by water percolating through the boulder field, and loading of underlying materials by the boulder field mass.

Slump Benches

Slump benches on the site exhibit little evidence of active mass movement and appear to be internally stable landforms. The terrain shows no signs of active disturbance such as ground cracks, although subdued ridge and swale topography (each ridge and swale may be tens of feet in width) suggests that the terrain was formerly more

intensively disturbed. Ground cracks and soil slumps are now "healed". Generally, dense forest cover flourishes on this terrain type. Trees of young to moderate age (up to 100 years) do not appreciably lean or tilt, but some old growth (200+ years) trees do lean. Surface drainage on the benches is provided by a few 10-20 foot deep incised streams with gentle gradients, rectangular cross sections and gravelly beds. Poorly drained depressions (including Donaca Lake) scattered on the benches indicate local ponding in topographic depressions formed by slumping. A minimum age of slumping may be obtained by dating sediments deposited in these depressions. It is possible that these benches are undergoing translatory downslope movement. If so, their rate of movement may be very slow and they are moving as coherent units with little surface expression of deformation.

Bench A'

Most of the activity on mass movement site A of the Donaca complex appears to be concentrated on the lowermost block of terrain, designated A'. Bench A' is a slump bench that is separated from the rest of mass movement site A along a 60-foot high scarp. The scarp exposes patches of very weathered andesites and flow breccias, with springs emerging from some flow rock-breccia contacts. Several feet of bedded tuffs are exposed on the easternmost edge of the scarp.

Mass movement activity on bench A' is indicated by disturbed interior topography as well as by activity in the boundary stream erosion impact zone. Interior indicators include benches, abundant undrained depressions, small slumps, and jackstrawed trees.

The easternmost edge of bench A' is rimmed by a zone of tension cracks associated with slumping into Swamp Creek. High steep banks on both sides of the creek expose thick (15-20'), brown, gravelly colluvial soils overlying various volcanoclastic materials. These include multicolored breccias, bedded tuffs, ashfall units and bouldery lahars. These materials slump and flow into Swamp Creek, choking it with large organic debris and sediment ranging from sand to large boulders. The majority of the boulders are resistant andesites or basaltic andesites; the more erodible volcanoclastics contribute to the finer sediment fraction. From observation of their strength, plasticity, textural and mineralogic characteristics, it is likely that slip planes and shear zones underlying the Donaca complex consist of some of these volcanoclastic materials. The depth and shape of these planes or zones under site A are unknown. Primary basal shear may be along a single weak plane or zone, or along a complex of shear segments. Data on the Middle Santiam earthflow (this thesis) suggest one or more shear zones several feet in thickness. Seepage and spring lines were noted at several levels along the flow front and stream banks of bench A'. Peak flows in Swamp Creek and high groundwater levels combine to perpetuate bank instability in weak earthflow debris materials.

The Swamp Creek Watershed--Hydrology and Mass Movement

The Swamp Creek watershed covers 5.5 mi² (Figure 14). At the scale of Figure 14, the main and west forks of Swamp Creek are third order streams totaling 5.7 mi in length which flow into the Middle

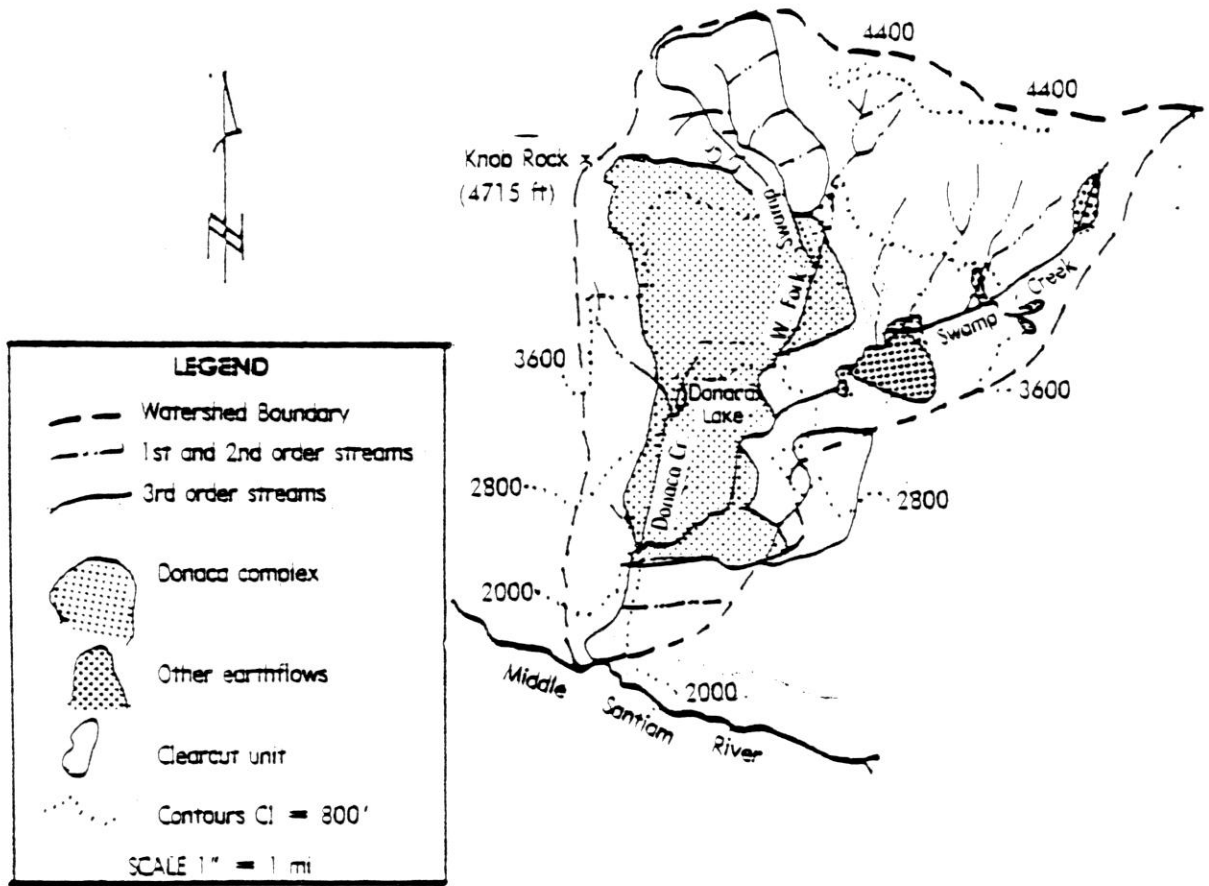


Figure 14. Swamp Creek watershed.

Santiam River. Approximately 8.1 mi of first and second order streams are tributary to Swamp Creek.

There are about 2.1 mi of streams within the four sites of the Donaca mass movement complex. The interior drainage density (total stream lengths/drainage area) of all four sites combined is only 1.5 compared to 5.6 for upper Swamp Creek watershed northeast of the complex. This contrast in drainage development can perhaps be partly explained in terms of the hydrology of slump-earthflow terrain.

Slump-Earthflow Hydrology and Impacts

Mass movement site A (including bench A') dominates the Donaca complex in terms of land surface area. Of its 650 acres of slump-earthflow terrain, approximately 38% is covered by boulder fields. Surface drainage is poorly developed on this terrain type because of the permeable nature of a jumbled boulder substrate. A few springs emerging from the lower portions of the boulder field give rise to short streams which feed Donaca Lake and some smaller ponds.

Although some seepage was observed along the face of the interior scarp above bench A', no continuous surface streams were noted in bench A'. Here mass movement activity is relatively high and the terrain is very disturbed, so that surface water tends to be intercepted by ground cracks, small slump basins and scarps. High groundwater seepage creates numerous bogs and poorly-drained depressions. The drainage density of site A is only 1.3.

The main form of Swamp Creek rises in a sub-basin which has some of the characteristics of an ancient inactive slump-earthflow complex. Based on aerial photographs, Forest Service geotechnical

reports and limited field reconnaissance, however, several active mass movement sites were identified along some stream reaches in this sub-basin (Figure 14, Plate 3). These mass movement sites impact adjacent reaches by earthflow, bank failure, channel constriction, sediment loading and upstream aggradation. Altogether, these sites affect 146 acres of terrain and impact 1.1 mi of first, second, and third-order streams. The largest mass movement site covers about 62 acres.

About 3.8 mi of stream are impacted by the earthflows of the Donaca complex. The reach between the main fork-west fork of the Swamp Creek junction, and the Donaca Creek-Swamp Creek junction is dramatically impacted by massive slumping of high, unvegetated stream banks, and by debris loading. Some aggradation above this reach is indicated by a 23 acre gravel terrace, now overgrown with alders. This reach is the most impacted in the watershed.

About 31% of the total stream length in Swamp Creek watershed is impacted by mass movement ; 24% of this impacted reach length lies within or adjacent to the four mass movement sites of the Donaca mass movement complex. About 29% of the terrain in the watershed is active mass movement terrain; the Donaca complex accounts for 25%.

Case Study II--Jude Creek Mass Movement Site

Jude Creek Watershed--Hydrology and Mass Movement

The Jude Creek watershed is approximately 3.8 mi² in area. Its drainage density is 3.0, with 11.4 mi of streams (at the scale of Figure 15, derived from 1:15840 Forest Service base maps) forming a dendritic drainage system.

Jude Creek has a total stream length of about four miles, including west and east upper forks, each about one mile long. First and second-order tributaries of Jude Creek comprise the rest of the mapped streams.

The watershed is underlain by the Sardine Formation and the Little Butte Volcanic Series (Peck et al. 1964). The Little Butte Series underlies 60% of the watershed.

The Jude Creek mass movement site is only one of eight identified active slump-earthflows in the watershed, affecting a total of 260 acres or about 11% of the watershed area.

The type of impact the Jude Creek earthflow has on Jude Creek's main channel (i.e., sediment and debris loading, channel constriction, and channel gradient alteration) is shared to differing extents by some of the other earthflows, most notably a large one just south of the Jude Creek site. About 2.5 mi, or 60%, of Jude Creek's main channel is impacted by earthflow activity.

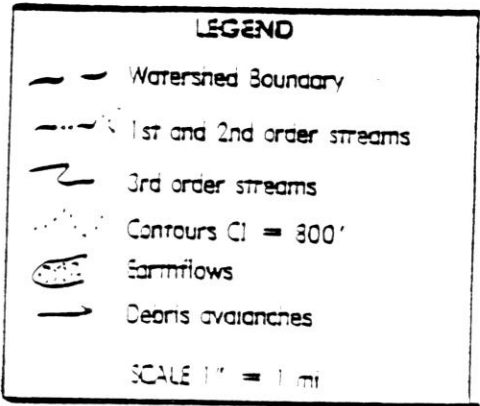
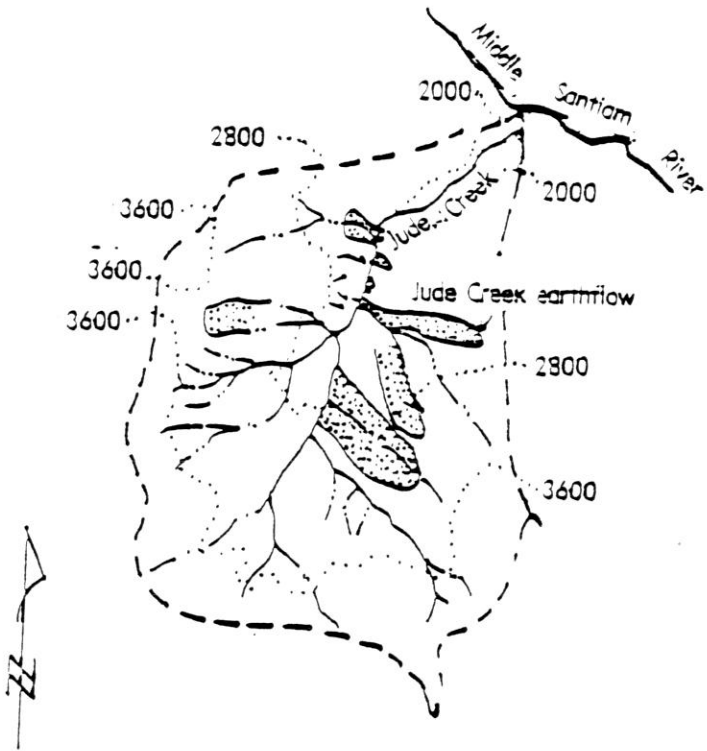


Figure 15. Jude Creek watershed.

Jude Creek Earthflow

The Jude Creek mass movement site is a 73 acre active slump-earthflow (Plate 1) located on west-facing slopes of Jude Creek watershed, about halfway between the head of Jude Creek and its junction with the Middle Santiam River. The site forms a discrete sub-basin bounded by bedrock and soil scarps, and by a stream which flows into Jude Creek. Jude Creek flows northeast past the toe of the earthflow.

A logging road crosses the site at midslope; salvage logging has been done just above and below the road, and several clearcut units harvested between 1958 and 1978 surround the site. A small quarry exists just off the logging road on the north boundary of the site. The rest of the site is in natural timber.

Geomorphic Units of the Jude Creek Earthflow

Boundary Scarps

Most of the site is bounded by three types of scarps (Plate 1, Geomorphic Unit map): vegetated crown scarps, unvegetated bedrock scarps and unvegetated soil scarps. The variations in form, height, and exposed materials of these scarps suggest differences in age, origin, and activity.

The vegetated crown scarp (I-A) is steep (60% +) and supports brush and conifer growth. This scarp was probably active in the past and subsequently stabilized.

Bedrock scarps (I-C) are fresh and active. One such scarp runs along the southeastern boundary for 900 feet, reaching 300 feet in maximum height. Fresh talus and scattered boulders at its base blending into boulder field terrain, and incipient separation along vertical joints within the scarp bedrock suggest recent and ongoing activity. Springs trickle down the joints and chip talus and sandy silt form deep aprons at the base of the scarp. Bedrock exposed on this scarp is massive and relatively smooth on outcrop. Vertical joints spaced 15 to 20 feet apart are evident on the face. The rock is pink to salmon colored tuff-breccia or crystal-lithic tuff, firmly indurated, with clasts of andesite up to one foot across in a sandy oxidized matrix. Bedrock of a different type is exposed on scarps along parts of the northern boundary just below the logging road. These scarps expose a weathered andesite flow or flows, grading upwards from a very decomposed, oxidized and zeolitized gray andesite to a fresher blocky to platy fractured unit. The base of the scarp is littered with some blocks of bedrock and gravelly soil. The freshness and unvegetated surfaces of portions of the site's boundary scarp indicate recent activity; fresh rockfall and slumping suggest current activity.

Soil scarps occur primarily in the lower portions of the site where slumping is not deep enough to expose bedrock.

Boulder Fields

Most of the boulders derived from recent rockfall are concentrated in the eastern and northeastern upper slopes of the site. A few boulders are scattered over slump bench terrain near the logging road. Only the most recent features are discussed below.

Recent boulder debris is largely derived from the southeastern boulder scarp. Many of the boulders are 15 feet or more across, due to the low density of jointing in the scarp bedrock. The morphology of the boulder field suggests that boulders have been rafted on top of a slumping substrate. The movement style has broken the underlying terrain into a downstepping series of narrow slump benches capped by large boulders or piles of shattered bedrock.

Conifers growing on and between these boulders lean mostly to the southeast, towards the scarp. Curves in their trunks indicate current moderate movement rates. Generally, timber cover is sparse on the boulder field.

Upper Interior Scarp

This 60-foot-high scarp is one of two interior scarps on the site. This scarp and the surrounding terrain mark a two-acre clearing in the natural timber canopy; recent and current episodes of rapid mass movements have not allowed vegetation to re-establish in the area.

The scarp is capped by cracking blocks and boulders of the pink tuffaceous unit. Underneath this bedrock, the scarp in places exposes a mixture of colluvial soils, large blocks of dark grey to black igneous rock (andesite or basalt) and volcanoclastic materials. The scarp profile generally is broken and covered with slope wash, rock fragments and organic debris; the average slope gradient is about 100%.

The igneous rock blocks are pervasively sheared and zeolitized and are imbedded in altered, thinly bedded volcanoclastics. Some of these volcanoclastics are saturated and flow from the scarp face

through a network of gullies, spreading out as a series of mudflow lobes onto the flatter terrain below.

Slump Benches

Most of the central portion of the mass movement site is dominated by slump bench terrain. Relative activity, according to observable vegetation and terrain stress indicators, varies on these benches. For a distance of about 600 feet downslope from the upper interior scarp (Plate 1, profile AA'), the terrain is quite disturbed and hummocky, scored by ground cracks and broken into blocks of colluvium and bedrock. Some hummocks consist of blocks of shattered or sheared bedrock. Vegetation in this area is also disturbed: downed and split conifers, roots in tension, and conifers with curved and twisted trunks are abundant (Figure 16).

Between this active area and the road, the terrain is characterized by mass movement landforms, such as low rounded hills (20-25 feet high) and hollows containing sag ponds and bogs supporting dense hydrophytic vegetation. Most of the conifers lean and twist at various angles and directions, suggesting moderate rates of current mass movement.

Terrain just below the road is similar to the moderately active terrain above it. In both these areas, no ground cracks were noted; current mass movement activity is indicated by vegetation.

Ground disturbance from scarps, tension and shear crack systems and accompanying stressed vegetation such as split trees and sheared and stretched roots, begins to appear again 400 feet below the road. The pattern of ground fracture is very complex. Some 800 feet below the road, a north-south trending ground fracture with a six-foot high

scarp curves to the west near the northern site boundary, forming a very distinct single shear crack traceable for about 500 feet. This shear crack splinters into two subparallel cracks just above the lower interior scarp. These cracks cannot be traced across this scarp. For much of its length, the shear crack is sharp and only a few inches wide and runs along the bottom of a wider trough-like feature. This system of tension and shear cracks marks the boundary between upper and lower blocks or benches which are rifting apart. A stake array (SA-1, plate 1), was established across this crack system to measure current rate of rifting.

Lower Interior Scarp

This scarp is similar to the interior scarp above bench A' of the Donaca mass movement complex in relative slope position and in its relationship to the terrain below it. The lower interior scarp of the Jude Creek site occurs about 3/4 of the way downslope from the eastern head of the site, or about 1000 feet from Jude Creek. It spans nearly the full width of the site at this location.

Two bedrock-soil units are exposed on the scarp : (1) two to three feet of tan to red-brown colluvial soil with fragments of andesite and basalt overlying (2) a purplish-gray decomposed pumiceous tuff-breccia unit. Clasts in the tuff unit are about 30% white to pale-green, somewhat flattened pumice fragments and 70% andesite and other lithic and crystal fragments. The entire scarp face is fresh and actively eroding. Springs and runoff carve rills and gullies in the soft volcanoclastic materials; mudflow deposits composed of these materials spread out over the flat portions of the slump bench below the scarp. Shallow ponds occupy depressions on the deposits. The

lower interior scarp divides moderately active terrain vegetated by dense coniferous forest upslope from very active earthflow slump bench and flow front terrain dominated by hydrophytic vegetation below it.

Lower Jude Creek Earthflow

Between the lower interior scarp and Jude Creek, the slump bench terrain (about 8.4 acres) is very disturbed, and movement is classified as very active. The mode of movement is classic earthflow, where a moist to saturated substrate moves downslope as a relatively fluid mass. The same general mode of movement applies to bench A' of the Donaca complex. Some of the surface features such as fresh ground cracks, scarplets, and poorly drained depressions are common to both sites.

In general morphology, this terrain resembles the lower portions of earthflows found in the San Francisco Bay Area (Keefer 1977). It is characterized by a sharply curving snout or flow front where part of it flows into Jude Creek, by straight or slightly curving lateral boundaries, and by ground surface broken into small blocks, separated by scarps, cracks, and hummocks.

Rapid earthflow movement below the lower interior scarp probably derives from relationships among slope, substrate and shear plane materials, interior drainage network and moisture conditions and erosion by Jude Creek.

The lateral boundary shear cracks are very distinctive and interesting features. Most of the northern boundary is marked by a soil scarp which developed from dip-slip movement along a shear crack. At its intersection with the lower interior scarp, the

northern boundary scarp is about 12 feet high, decreasing in height downslope. A well-defined, sharply incised shear crack cuts the substrate at the base of the scarp, and is clearly visible where it is not buried by scarp debris. At some points, current shear movement along this crack is indicated by slickensides cut into soft, moist clayey substrate (brown colluvial soils and purple-gray volcanoclastic soils) exposed on the walls of the crack.

Similar lateral shear surfaces defined by shear cracks are found near the southern boundary. This crack system extends continuously for about 450 feet, varying in form. At its upslope end, it is a narrow (10-15 inch) trough, pinching into a knife-edge crack downslope. The crack walls then develop into low scarplets that separate and become the walls of a twelve-foot wide trough at the lower end.

Earthflow-Jude Creek Interactions

The flow characteristics of Jude Creek strongly influence mass movement behavior, especially at or near the earthflow front. The flow front of the Jude Creek site is divided into northern and southern lobes which differ drastically in geomorphology and interaction with Jude Creek. The southern lobe (Figure 17) is a steep-sided and convex bulge of earthflow debris about 20 feet in height. This lobe consists of a one- to two-foot mantle of stony colluvium overlying soft volcanoclastic materials. Angular cobbles and boulders litter the surface and are piled at its base.

The northern lobe (Figure 18) is a very steep, 40-foot-high face of exposed soft, oozing blue-gray and purple volcanoclastic materials capped by a thin layer of brown stony colluvium and containing

cobbles and boulders, lumps of weathered volcanoclastic rock, and large organic debris. The face is intensively rilled and gullied.

The two reaches of Jude Creek which flow past these lobes contrast in gradient, channel form, bedform and velocity. From the west face of the southern lobe to some distance upstream, Jude Creek flows quiet and shallow over an aggraded channel bed and gravel and sand bars, some of which support thickets of alder. The streambed is mainly gravels and cobbles. The southern lobe contributes cobbles, boulders, and occasional organic debris which roll down its slopes or are deposited by creep and bank slumping.

A large organic debris and boulder jam effectively blocks the channel at a point where the southern lobe curves gradually eastward. The jam is built of debris eroded out of the earthflow and firmly wedged against a bedrock wall on the other side of the channel. The aggraded channel reach upstream is formed by the trapping of sediment and organic debris behind the jam. Water spills through the debris jam and tumbles 50 feet or so in a series of cascades down to a bedrock channel.

These features illustrate some of the changes an active earthflow can impose on a stream channel, and the concomitant impacts of streamflow on erodible earthflow debris. The cutting power of Jude Creek is greatly enhanced by its fall over and through the debris jam. The northern lobe is thus kept exposed and raw during most of the year, and the channel bed downstream is scoured to bedrock. Finer earthflow debris is flushed downstream, and large boulders eroded out of the flow front contribute to and buttress the debris

jam. Upstream of the jam, stream velocity is low and the southern lobe is able to advance debris into the channel.

The debris jam appears fairly stable, but in the event that high streamflow during an intense storm period occurs, parts of the jam may be shifted or dislodged, releasing some dammed sediment. A debris torrent would result, causing downstream scouring of the channel bed, bank erosion and deposition of a debris fan at the junction of Jude Creek and the Middle Santiam River. Comparison of aerial photographs taken in 1955 with photos of the same scale taken in 1967 indicate that such an event or series of events may have been caused by the intense storms during the winter of 1964-1965. Swanson and Swanston (1977) discuss this chain of events in relation to the Lookout Creek earthflow.

Movement Rates of the Jude Creek Earthflow

Earthflow Movement, 1979-1980

Stake arrays similar to those used by Swanson and Swanston (1977) were installed across ground crack systems on the Jude Creek site (Plate 1) to determine rates and styles of movement over the monitoring period 12/7/79 to 10/18/80. One stake array (SA-1) was installed across a tension crack scarp, another (SA-2) in a field of closely-spaced tension cracks developed from pressure ridges, and a third (SA-3) across a boundary shear crack system. Each array is quadrilateral, consisting of four stakes. Periodic measurement of distances separating these stakes disclosed direction and magnitude of tension or shear movement across these crack systems. For SA-3,

the diagonals of the rectangle were measured, with two endpoints located on stable ground and two on earthflow terrain.

Data indicate different movement rates on each of the arrays. Figure 19 is a time-displacement curve of translatory downslope movement on SA-3, plotted along with cumulative precipitation for the monitoring period. SA-1 and SA-2 were not tied to stable reference points, so data for these two arrays reflects only relative movement between internal blocks and not translatory downslope movements.

Total horizontal shear displacement indicated by translation of stakes in SA-3 was 229 inches, or an average rate of .71 inches per day and 21.6 ft/yr. These rates are much greater than rates obtained on the Lookout Creek earthflow just south of the study area by Swanson et al. (.08 to 5.6 in/yr) but are comparable to rates observed by Kelsey (1978) on the Halloween earthflow in northern California (22 ft/yr).

Ground extension, occurring as cracks widen and more cracks develop between stakes, was measured at SA-1 and SA-2 (Table 5). Differences in amounts of extension on two sides of the same array may indicate uneven crack formation or widening. Most of the extension at SA-2 occurred during May 1980, correlative with an acceleration of shear movement at SA-3 (Figure 19). Greater extension was measured at SA-2 over a shorter monitoring period than at SA-1, suggesting that local tensional forces are greater at SA-2.

Precipitation and Movement Rates

Figure 19 indicates large average rates of shear movement during the monitoring period, with maximum average rates occurring during winter and late spring. Interpretation of movement behavior from

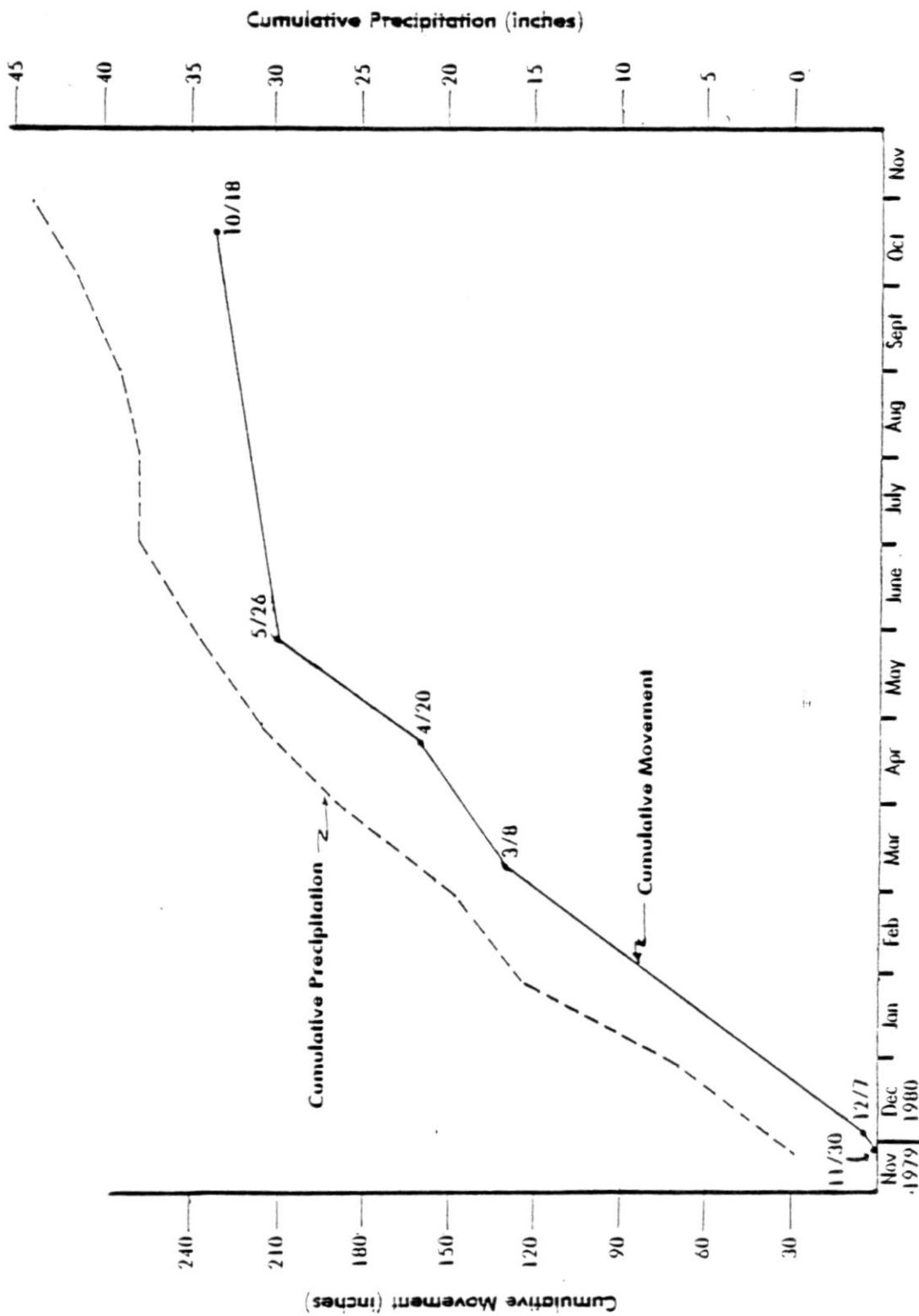


Figure 19. Cumulative movement along northern shear boundary, Jude Creek earthflow, at SA-3. Precipitation data is from Cascadia station, approximately 13 miles SW of the site at 860 feet elevation.

Array	Downslope measurement direction	Monitoring period	Total ground extension (inches)
SA-1	North side: S74W	11/30/79--5/26/80	9.8
	South side: S80W	11/30/79--5/26/80	4.8
SA-2	North side: S52W	11/30/79--10/18/80	4.1
	South side: S68W	11/30/79--10/18/80	2.8

Table 5. Ground extension across tension cracks, Jude Creek earthflow.

5/26/80 to 10/18/80 is difficult because only two data points are available; although the curve suggests continuous, somewhat slower movement rates during the summer months of 1980, it is also possible that movement could have stopped during the summer and started again in the fall. Recent data, developed by a crackmeter installed near SA-3 (Plate 1), indicate continuous movement during the summer of 1981. This crackmeter was installed on 6/22/81 as part of a continuing monitoring program by the Pacific Northwest Forest and Range Experiment Station in Corvallis.

Flattening of the movement rate curve during late winter and early spring was probably a response to overall precipitation decreasing through April. March precipitation was quite heavy, but the movement records are not sufficiently sensitive to show this. The record lacks the refinement to measure earthflow response to individual storms or series of storms. The acceleration of movement during late spring may be due to snowmelt, groundwater recharge, and higher pore pressures in the substrate (Harr 1981).

Sediment Input Rates

Rates of shear movement of the Jude Creek earthflow may be used to roughly calculate volumes of sediment movement into the Jude Creek channel at the flow front. Data for movement along only the northern shear boundary are available. Extrapolation of the same rates to the southern boundary is questionable, in view of the differences in geomorphology and channel influence on the southern lobe.

Assuming an average rate of .71 in/day, and estimating the dimension of the northern lobe or flow front at 80 ft wide and 40 ft high, about 2500 yd³ advance into Jude Creek annually. The

movement data indicate year-round advancement of debris into Jude Creek, but also suggest seasonally-related pulses of sediment input.

Case Study III--Middle Santiam Mass Movement Site

Introduction

Sections of Road 2041 built in 1965 to provide access from Oregon Hwy 20 to the Middle Santiam River began to experience stability problems that reached critical stages by the early 1970's. By then a section of the road through a clearcut unit about a half-mile from the Middle Santiam bridge crossing was showing signs of extensive subgrade and cutbank disturbance. Reconstruction and maintenance of the road subgrade and cutbank was attempted several times in efforts to keep the road open. Ultimately, these efforts proved to be ineffective, and the road was impassable by the fall of 1976.

Road 2041 was originally excavated in 1965 through the toe of a 13-acre earthflow approximately 780 feet long and 600 feet wide. Unlike many of the other mass movement sites in the study area, the Middle Santiam site is a mid-slope failure, with no evidence of erosion at the toe by stream activity.

About 42% (5.5 acres) of the Middle Santiam site was clearcut in 1965. Portions of the road prism and cutbanks failed as a debris avalanche and debris flow or a series of such events between 1967 and 1972. Roadfill, slash, and earthflow debris flowed down a 100% slope and spread out as a debris flow deposit into flat ground below. Subsequent debris avalanches and flows have followed the same track. The Middle Santiam mass movement site thus consists of a slump-earthflow and a debris avalanche--debris flow complex (Figure 20).

Current Forest Service plans to access the north side of the river preclude reconstruction of the road at its original location through the earthflow. This segment will be abandoned, and the route relocated onto river terraces north of the debris flow deposits.

Geomorphic Setting and Site Geomorphology

The Middle Santiam earthflow is a relatively small one within a landscape dominated by earthflow landforms. The entire north-facing slope rising from the Middle Santiam River southward to a ridge at 4000 feet in elevation, bounded to the east by a spur of this ridge, and to the west by a divide common to the Jude Creek watershed, comprises this landscape (Plate 3). Many of the earthflow landforms in the area appear to be older and inactive, covering tens of acres, and with boundaries not clearly defined on all sides.

Plate 2 is a detailed geomorphic map of the site showing features as they appeared in August and October of 1979. Since then, mass movement has shifted features and altered the mass balance of the terrain, but relationships of geomorphic units are still relatively unchanged. Features were mapped from aerial photographs and in the field, using surveyed site boundaries and surface points. Some of these points are included on the map to more easily identify and locate features discussed below.

Of the two main mass movement types on the site (earthflow and debris avalanche-debris flow complex) the earthflow is older. It is characterized by well-defined boundary scarps, slump benches, and a bulging flow front. The top of the crown scarp is at an elevation of

2400 feet and the lowest point of the earthflow is at approximately 2100 feet. The debris avalanche-debris flow complex consists of material derived from the earthflow front. The avalanche track slopes at about 100% to an elevation of 1900 feet, where the slope breaks sharply onto very gently sloping ground (12% gradient). The deposits are confined to approximately 2.5 acres by higher old slump terrain to the west and a stable ridge to the east.

Scope of Investigation

The Middle Santiam mass movement site was chosen for more detailed study than other sites because of its relatively easy access, its high level of current activity, and its management-related impacts. Field, laboratory, and analytic studies are described in the following sections.

Field studies were begun in July 1979, proceeding intermittently through May 1981. Points on the site were surveyed relative to stable ground in August and October 1979 and then resurveyed in September 1980 to determine magnitude and direction of surface movements. These points also were used as an aid to field mapping. Five stake arrays installed across shear boundaries and tension cracks were monitored from October of 1979 to May 1981, providing more data on surface mass movement rates.

Field mapping of most geomorphic features was accomplished in August and October of 1979, using compass, rangefinder, and tape. Field observations were supplemented by aerial photography.

On August 15 and 16, 1979, one hole was drilled on the site with Forest Service core drilling equipment. Core and core cuttings were logged (Table 6, Plate 2). Samples later excavated by hand provide data on classification, texture, plasticity, and strength of certain earthflow materials (Table 3, Figures 5 and 7).

Inclinometer casing was installed in the drill hole on August 16, 1979. An inclinometer probe was used to detect subsurface movements through September 1980.

Historic mass movement behavior was analyzed through aerial photography and a dendrochronologic technique.

Stratigraphy, Lithology, and Stability

General Statement

Roadcuts near the Middle Santiam mass movement site expose local lithologies and stratigraphic relationships that partly explain the development of the Middle Santiam earthflow. Examination of mass movement boundary scarps and drill cuttings and core (Table 6) indicate that the earthflow is underlain by the same rock types exposed on nearby roadcuts.

Roadcut Lithologies

Rock types exposed on the roadcuts include andesite flows, epiclastic breccias and tuffaceous sandstones and mudstones of the Little Butte Volcanic Series (Peck et al. 1964). All of these rock types are exposed along a 300 foot long, 20 to 60 foot high roadcut west of the flow front. A 34-foot thick section (Section MS-A)

exposed by the roadcut and by debris sliding was measured and logged (Figure 21, Plate 2).

Stability Relationships

All bedrock exposed in section MS-A is zeolitically altered. Zeolites in vugs and along narrow veins are abundant in the epiclastic volcanic breccias and can also be found as vesicle fillings in the andesite flows. Zeolitic alteration transforms original volcanic glass into green clays, or montmorillonite. Montmorillonite has been associated strongly with slope stability in a number of studies (Paeth et al., 1971; Borchardt, 1977; Taskey, 1978). Green, clayey material was found as fracture filling and as altered clasts in the breccias.

Besides being altered, other properties of tuffaceous mudstones make them suspect in terms of slope stability. They are extensively fractured, and tend to break out into small chips (1/2 to 2-inch) by random fracturing. These chips can be broken by hand. Many of the fracture surfaces in the mudstone are slickensided and thinly coated with clay. Their texture indicates that the mudstones are relatively impermeable; however, water is easily conducted along the fractures. Springs emerge from contacts between tuffaceous sandstones and mudstones in this and other sections at different locations in the study area.

Many of the clasts in the coarser epiclastic breccias are slickensided, indicating wetting of clast surfaces and slippage on a grain to grain or grain-matrix scale.

Additional sheared and slickensided materials occur between the lower andesite unit and an overlying epiclastic breccia unit in

section MS-A. These materials are yellowish, wet, soft, and have a clayey feel. The top few inches of the underlying andesite flow are bright bluish-gray in color, indicating prolonged wetting at the contact.

Weak, stratified volcanoclastic materials exist near the Middle Santiam mass movement site. There is evidence that slip planes could develop along bedding planes and fracture surfaces within the volcanoclastic strata, and also between volcanoclastics and andesite.

Similar volcanoclastic materials were excavated from the flow front and brought up as drill cuttings. Flow front materials may represent portions of a basal shear zone or zones (Figure 22). Shear vane strength tests show that they have low strength. Also, they slake rapidly when wetted, and montmorillonite is the dominant clay mineral as shown by x-ray diffraction determinations.

Local structure is also a significant factor affecting slope stability. Volcanoclastic strata exposed on the roadcuts dip as much as 30° northwest, or out of the slope.

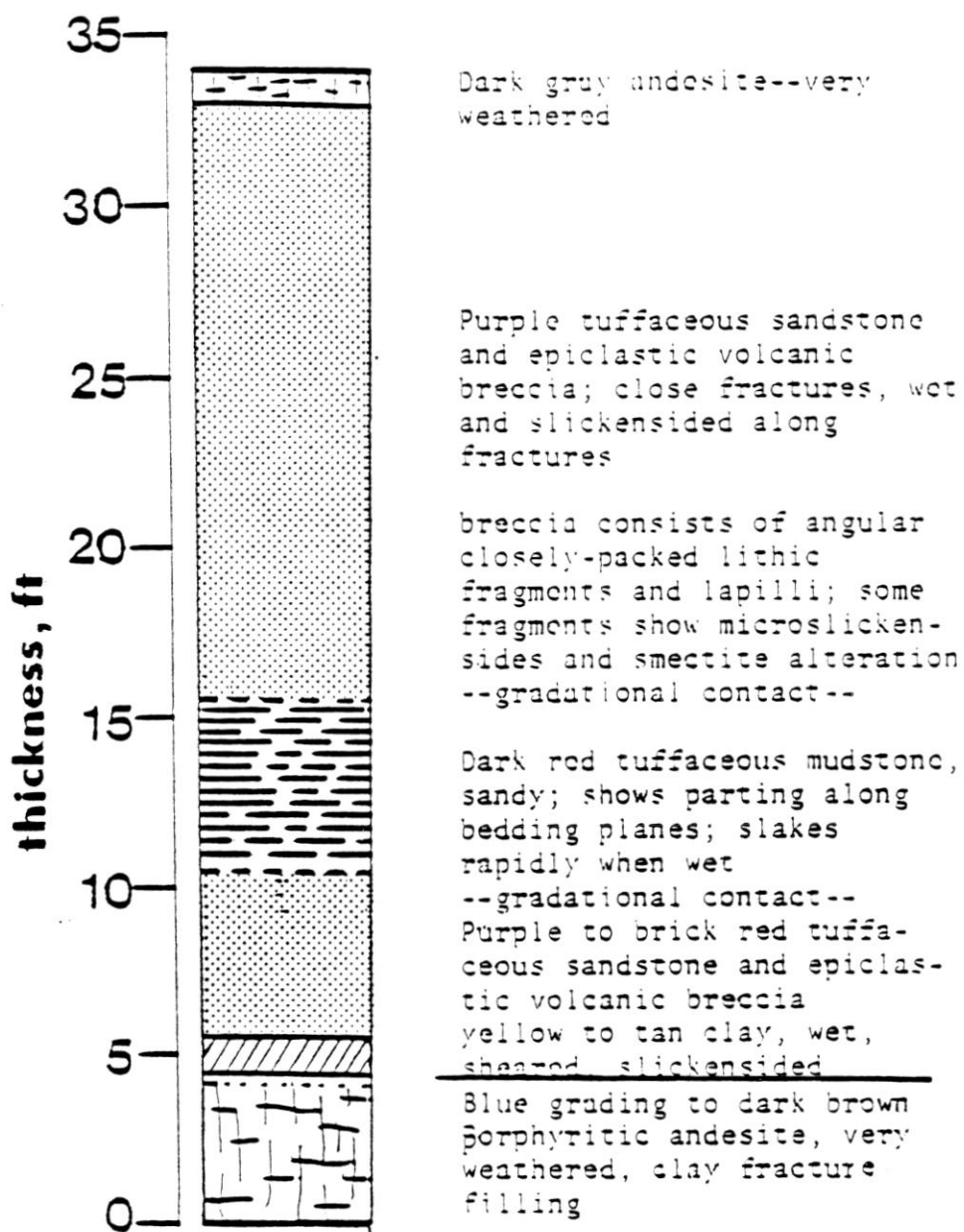
Geomorphic Units on the Earthflow

The Middle Santiam earthflow contains six terrain types (Plate 2). The entire earthflow is moving northward from the crown scarp. All geomorphic units are therefore moving downslope relative to stable ground. Additionally, extreme terrain disturbance indicates internal deformation and relative movement between slump benches.

Date	Depth Interval (ft)	Drilling Log	Condition of core and cutting core recovery percent	Description of recovered core
8/15/79	0.0-8.0	Reached HW casing Occasional woody debris		
8/15/79	8.0-16.5	20% H ₂ O return Hole caving, blasting 50% recovery of bit. Occasional voids	1/2-2 in rock fragments 50% recovery	Andesite, purple with red hematite streaks, also light gray to black. Porphyritic altered plagioclase, green pyroxene
8/16/79	16.5-26.0	20% H ₂ O return easier drilling	20% recovery, fragmented rock	Andesite, purple with red hematite streaks, also light gray to black. Porphyritic altered plagioclase, green pyroxene
	26.0-29.0	20% H ₂ O return	80% recovery, 4-6 in. core fragments Sandy clay fines adhere to rock	Porphyritic andesite, gray to grey-green, vesicular. Vesicles lined with zeolites and green clay
	29.0-29.3	"soft zone" 20% H ₂ O return	70% - 1/2 in. fragments of clay with imbedded sand	Plastic, laminated clays mixed with sand and decomposed rock. Clays are reddish-purple, blue-green, gray.
	29.3-30.8	Steady drilling	90% - rock	Andesite, brown-gray with red and orange hematite streaks
	30.8-35.0	20% H ₂ O return	50% - rock	Andesite, brown-gray with red and orange hematite streaks
	35.0-37.0	20% H ₂ O return	50% - 3-4 in. rock fragments	Andesite fragments with adhering clayey sand and silt
	37.0-39.3	20% H ₂ O return	50% - 3-4 in. rock fragments	Angular fragments of tuffaceous sandy sandstone mixed with sand, silt, and clay
	39.3-44.0	"soft zone" - very easy drilling	2 in. clay fragments	Pebbly clay: stiff, slickensided, green, red, and purple. Desiccated fragments are tough and platy. Slake rapidly when wet.
	44.0-44.5	20% H ₂ O return Attempted "push" sample-unsuccessful	30% - 3-4 in. decomposed rock fragments and clayey sand	Blue-gray tuffaceous sandstone and volcanic breccia with black lithics, red clinters (?) abundant slickensides on clasts. Low crushing strength
	44.5-47.0	20% H ₂ O return	Decomposed rock	Very decomposed, crushable blue tuffaceous sandstone and epiclastic breccias
	47.0-48.5	attempted "push" sample	Stiff clayey sand	Medium to coarse-grained with black lithic pebbles to bottom of hole.
	48.5-50.0	attempted "push" sample	Stiff clayey sand	
	50.0-51.5	attempted "push" sample	Stiff clayey sand	
	51.5-61.5	100% H ₂ retention	Decomposed rock	Bottom at 61.0 feet

Drill rig was Forest Service track mounted Acker (C0120)

Table 6. Borehole log and drilling record, Middle Santiam earthflow.



SECTION MS-A

Figure 21. Rock types exposed on roadcut west of Middle Santiam earthflow. See plate 2 for location of section.

Crown Scarp

The earthflow is bounded on the south side by an arcuate high crown scarp exposing soil and underlying andesite bedrock. The crown scarp connects smoothly with lateral boundary scarps to form an amphitheater enclosing the interior of the earthflow. The crown scarp is approximately 750 feet wide and 150 feet in height, forming an imposing nearly-vertical wall of bedrock (Figure 23).

Regular sets of joints appear to control the scale and likelihood of rockfall, rockslide, and toppling from the scarp face. Major joint sets are nearly vertical and spaced 10 to 15 feet apart along the width of the scarp. Attitudes of these joints are N50W75NE and N35E85NW. Minor sets of oblique to horizontal joints are spaced two to four feet apart. The major joint sets crosscut the minor, and may be tectonic in origin.

Rockfall has produced large talus cones and piles of rock blocks at the base of the scarp (Figure 23). Rectangular slabs of bedrock standing on end or leaning against the scarp at various angles attest to very recent block slide and toppling movements. These 15 to 30-foot-high slabs slide down the rock wall along joint surfaces and wedge themselves into talus and between previously fallen rock blocks, then topple or remain standing. Many of these blocks are unvegetated, bear fresh slickensides, and have knocked over trees near the base of the scarp. Occasionally, rockfall can be seen and heard during visits to the site.

More evidence for recent and current mass wasting can be observed on the scarp itself. Continuously across the face of the scarp, an upper limit of polish, or a lower limit of weathering, is represented

by a sharp contrast in bedrock color and vegetation cover above and below a near-horizontal line. Below this line, mass wasting is recent enough that polished surfaces created by block sliding and slickensided joint planes have not been weathered as much as rock surfaces above the line. Surfaces above the break are conspicuously duller and more uniformly covered with moss.

The role of water in scarp mass wasting is significant. Water infiltrates the mass from above, flows along joint surfaces, and is conducted into the slide mass below or emerges as ephemeral or perennial springs at points on the rock face. Often the bedrock is weakened by the water, and joint block failure occurs, creating re-entrants in the scarp face. One spring near the western end of the crown scarp flows perennially along one wall of a scarp re-entrant. The flow of water is rapidly weathering the bedrock into friable materials and further failure of joint blocks along intensively slickensided surfaces appears imminent. The persistence of flow over these weathered materials is shown by their texture and by their blue (indicating saturation) and brick-red (indicating oxidation) colors.

Slumping and pulling away of soil, rock, and organic debris from the crown scarp is indicated by deposits of these materials left adhering to sections of the scarp face; The tops of these deposits indicate a recent higher stand of debris which has since slumped away. Near the center of the scarp base, a slide breccia consisting of bedrock fragments imbedded in a soil matrix leaves a record of recent slumping. The deposit is about 15 feet high and 50 feet wide. The matrix is now a tough, hardened crust about an inch in

thickness; both matrix and imbedded clasts are slickensided (Figure 24). Deposits of fresh, grooved soil elsewhere along the scarp base indicate current subsidence of the debris mass.

Boundary Sidescarps

The boundary sidescarps represent a record of subsidence and downslope shearing movement of earthflow material relative to stable ground. On the Middle Santiam site, shear boundaries are marked by soil and bedrock scarps which pinch out downslope into systems of shear cracks showing little subsidence. Other side boundary structures include lateral ridges and complex shear zones.

The eastern shear boundary consists primarily of exposed bedrock and sandy silt colluvium scarps down to the elevation of the road subgrade, or about 2000 feet elevation. Below this elevation, a well-defined shear crack trends N20E for a distance of about 70 feet downslope. The crack abruptly terminates and below this point there are no traces of fresh ground disturbance. The boundary segment which slices through the old roadbed is defined by a lateral ridge. This feature is similar to lateral ridges defined by Keefer (1977). On the east side of this ridge, a lateral shear surface dips steeply westward under the earthflow. The ground on both sides of this shear surface has been buckled upward in response to mass movement. The lateral shear surface forms a portion of a thrust fault plane, in response to an eastward component of earthflow, and the upturned ground outside the earthflow probably formed by drag in response to this thrusting. Simultaneously, downslope (northward) boundary shear movement occurs.

The point at which scarps on the western boundary change to a defined surficial shear crack system occurs about 200 feet higher in elevation than on the eastern boundary. Evidence for current shear movement along the boundary is dramatic. Between survey points 11+46 and 9+75, the boundary zone consists of a band of terrain scored and chopped up by a complex of shear cracks. Stretched roots and downed vegetation are abundant in this zone. The earthflow deposits along portions of the outermost shear scarp are saturated and will not support a person's weight.

Boulder Fields

Boulder fields cover approximately 20% (2.6 acres) of the earthflow surface. Their source is the andesite lava flow unit exposed on the boundary scarps. Boulders are most concentrated at scarp bases in the upper slope portions of the earthflow. Two relative classes of boulder debris can be identified, very recent and older. Older boulder debris has vegetation growing on boulder surfaces or in pockets of soil between boulders. Trees and herbaceous ground cover are useful indicators of deposition recency. When observations were begun (July 1979), most of the boulder field could be classified as older. Trees exceeding 100 years in age were growing on the terrain (this area was not included in the clearcut unit), and topographic contours were generally smooth. Very recent boulder debris is sparsely vegetated, and forms chaotic piles of rock. One such pile perhaps 30-40 feet thick exists below a set of re-entrants on the eastern side of the crown scarp. Very recent boulder debris is actively encroaching on the upslope margins of the older boulder fields, indicated by a greater number of live trees

buried or knocked over by rockfall since first observations were made. Movement of debris down and away from the boundary scarps is indicated by open tension cracks and uprooted trees and probably increases scarp instability.

Slump Benches

Slump benches of the Middle Santiam earthflow consist of severely disturbed terrain, scored by a dense network of tension cracks, scarps, and grabens. Second-growth vegetation prevails on parts clearcut in 1965. A gully on the east side of the earthflow is in old-growth timber, but the gully sides and bottom are so broken into benches and scarps that most of the trees are down. No continuous surface streams now flow down the gully, but there may have been surface flow when the earthflow was not so active.

The main body of the earthflow is broken up into three main slump benches on the order of 100 feet or so along profile AA' (Plate 2) and generally extending across the width of the site. These three benches offer some contrasts in vegetation cover and apparent stability. Due to a rotational component of slumping, the benches tilt back slightly towards the crown scarp.

Flow Front

Aerial photographs taken in 1959 show that the flow front of the Middle Santiam earthflow was then a smoothly bulging landform, resembling the bulbous southern lobe of the Jude Creek earthflow, and snouts of earthflows described by Keefer (1977) and Zaruba and Mencl (1969).

When road 2041 was excavated through parts of the flow front, morphology and mass balance of the earthflow were altered, leading to

instability. Since then, earthflow debris has regularly slumped away and avalanched from the front.

Earthflow materials freshly exposed on the flow front by slope failures and trail excavations were observed during the course of this study. Slope failures and extensive exposure of these materials are associated with heavy precipitation and spring snow melt. Earthflow materials include multi-colored, interbedded plastic clays, silts, and sandy materials derived from stratified volcanoclastics (Figure 22). Although bedding is well-developed, exposed material is in blocks broken up and transported by earthflow. Individual strata could not be traced for more than several feet across the flow front. Possibly, these blocks are derived from stratified volcanoclastics within one or more basal shear zones.

Debris Avalanche-Debris Flow Complex

As earthflow debris fails from the west and west-central portions of the flow front, it is channeled into an incised trough or debris avalanche track some 120 feet wide and more than 10 feet deep at its head. Below the east-central portion (east of survey point 22+95), there is no well-defined avalanche track. The paths and style of debris movement downslope from the flow front appear to be controlled in part by the morphology of the slopes underlying the debris. Debris which does not move down the avalanche track creeps or moves as slump blocks over a slope with a benched profile. Some debris moves as a fluidized mass down a narrow channel which runs along the base of a stable north-trending ridge at the eastern boundary of the

clearcut. Debris moves down the avalanche track through a combination of avalanching, flowage and creep. Creep probably occurs year-round, but avalanching and debris flow seem to occur episodically, in response to storm events. Avalanches and debris flows are triggered at the head of the avalanche track by failures from the unstable flow front, or within the track as debris accumulates and becomes mobilized, or by a combination of these processes. Avalanches can mobilize into flows by dilatation and incorporation of additional water or through spontaneous liquefaction (Pierson, 1977). Avalanching then induces further instability of the flow front by deepening the head of the track and undermining the toe of the earthflow.

Debris Avalanche-Debris Flow Deposits

The debris which overlies gently sloping terrain below the earthflow has been deposited by events post-dating timber harvesting and road construction. Aerial photographs taken in July 1972 show a tongue-like deposit some 600 feet long and 250 feet wide covering approximately 2.5 acres. Deposits which have accumulated since then overlie the older debris.

Discussions with personnel at the Santiam Engineering Zone, Willamette National Forest, and a report ("Road Condition Survey, Mid-Santiam Slump, Rd. 1263", 9/73(?)) places the event in 1972. Intense storms on January 11 and 21, 1972, may have triggered debris avalanching.

Materials deposited by the 1972 event include about 25000 yd³ of unsorted to poorly sorted fragments of road fill, sands, gravels, cobbles of weathered andesite, fragments of volcanoclastic materials,

and organic debris. The deposit is sparsely vegetated, with most vegetation growing in and along a perennial stream following a sinuous northerly course through the deposit to the Middle Santiam River. The deposit varies in thickness. Over 10 feet of debris is exposed by the stream, but the deposit thins toward the east.

Observations of high mud marks on standing trees, run-up deposits, and other evidence indicate that the 1972 deposit was emplaced as a highly fluid debris flow. Large cedars near the distal end of the deposit bear mud marks four feet higher than the present level of the deposit's surface. These trees were in uncut forest beyond the clearcut unit timberline. Apparently the debris was sufficiently fluid and fast-moving to penetrate 150 feet or so into the uncut stand of timber, killing several trees by burying the basal portions of their trunks. Coarse debris stranded on top of partially buried stumps and pieces of slash also indicate a high flow crest. The flow had sufficient velocity to run up about 20 feet onto higher ground along the western edge.

The surface morphology of the debris deposit varies. Low hummocks underlying and surrounding large organic debris cover some areas. The surface is relatively smooth in areas where debris has been reworked by overland flow of water or deposition of sheets of finer sediments over the original coarse debris. Smooth areas along the boundaries of the deposit represent areas where flow velocity was lower and fine materials were deposited as the flow ebbed. Delicate plant stems were not disturbed by the debris flow in these areas.

Debris deposits which have accumulated since 1972 are lobate and hummocky in form and did not travel as far as the older deposit.

These newer debris lobes consist of mixed sandy colluvium, rock fragments, and large fragments of clayey volcanoclastic soils and entrained large organic debris. Fresh debris lobes were noted on December 27, 1979, after fall rains had begun. A total of 17.87 inches of rain had been recorded during September, October, November and December at Cascadia, 18 miles to the southwest. Cumulative precipitation at the site itself was approximately 29 inches¹ (Miller et al., 1973). Emplacement of the debris lobes cannot be associated with a specific storm. These lobate deposits represent storm-related debris flow pulses which are rather small compared to the 1972 event.

All the debris deposits are being reworked by surface streamflow. Fine sediments are eroded from the distal ends of debris lobes. In summer and late spring, mass movement slows enough to allow the stream which flows northward through the debris deposits to establish a gravelly bed. Debris from the flow front periodically blocks streamflow in its channel, forming ephemeral ponds, or aggrades the bed by flowing into the channel itself.

¹Precipitation amount corrections are based on 2-yr., 24 hr. isopluvial maps in Miller et al., 1973. Isopluvial contours show that the Cascadia Station receives about 40% less precipitation than parts of the Middle Santiam basin included in the study area.

Earthflow Movement Rates

Surface Movement, 1979-1981

Crackmeters, stake arrays, and surveying were used to monitor surface movement on the Middle Santiam site. Horizontal and vertical movement relative to stable points outside the earthflow can be analyzed with data from all three methods. Subsurface water level was monitored by taping the distance from ground surface to standing water in the borehole casing. Fluctuations in water level indicated changes in water input and drainage which may have influenced earthflow movements. Measured water levels represent seepage of water into the casing from points all along its length below ground surface. The bottom 12 feet of casing were perforated before installation, with no seals put in to limit seepage to certain depth intervals. Automatic water level recording equipment on the site suffered mechanical problems and vandalism, so data collected by this system was not used in the analysis.

A crackmeter was initially installed on 3/8/80 across the western shear boundary (Plate 2), and was operative through 7/19/80. The equipment has been used successfully on relatively slow-moving earthflows in the Andrews Forest (Swanson, Harr, Fredriksen, 1980). However, higher movement rates of the Middle Santiam earthflow overtaxed the crackmeter every two weeks or so. The equipment required resetting more often than site visits were made, leaving gaps in the record. The installation was finally dismantled in August 1980 after it had been vandalized. Personnel from the Pacific

Northwest Forest and Range Experiment Station in Corvallis installed a new crackmeter south of the old installation on 6/22/81.

Figure 25 presents movement data for the old crackmeter installation, plotted along with cumulative rainfall, and a borehole water level curve. The solid curve represents extension between the two endpoints of the crackmeter and is only a component of true shear movement along the boundary. The dashed curve is an approximate vector solution of the data, representing movement along the direction of boundary shear. Movement occurred at a fairly constant average rate of .48 in/day. A maximum rate of .57 in/day was reached during the month of April 1980; thereafter, rates declined to between .41 and .46 in/day. The water level in the borehole rose sharply by about two feet between April 20 and April 24, coinciding with the period of accelerated movement. Spring snowmelt from a late snowpack (snow was still on the ground at an elevation of 3000 feet in late April) in combination with rainfall may have caused this increase in water input and earthflow acceleration. The overall smoothness of the movement curve suggests that earthflow movement along the western shear boundary was not responsive to individual storms, or had a response lag time not covered by the duration of the record. Stake array 1 (SA-1) was installed across the shear boundary, with two points on stable ground and two on the earthflow, and provides a longer record of earthflow movement (Figure 26) from October 6, 1979 to July 17, 1981 (1.8 years). Total movement along the shear boundary was 550 inches (45.8 feet), representing an average rate of 25.5 ft/yr. During the 1979-1980 water year, the earthflow moved 174

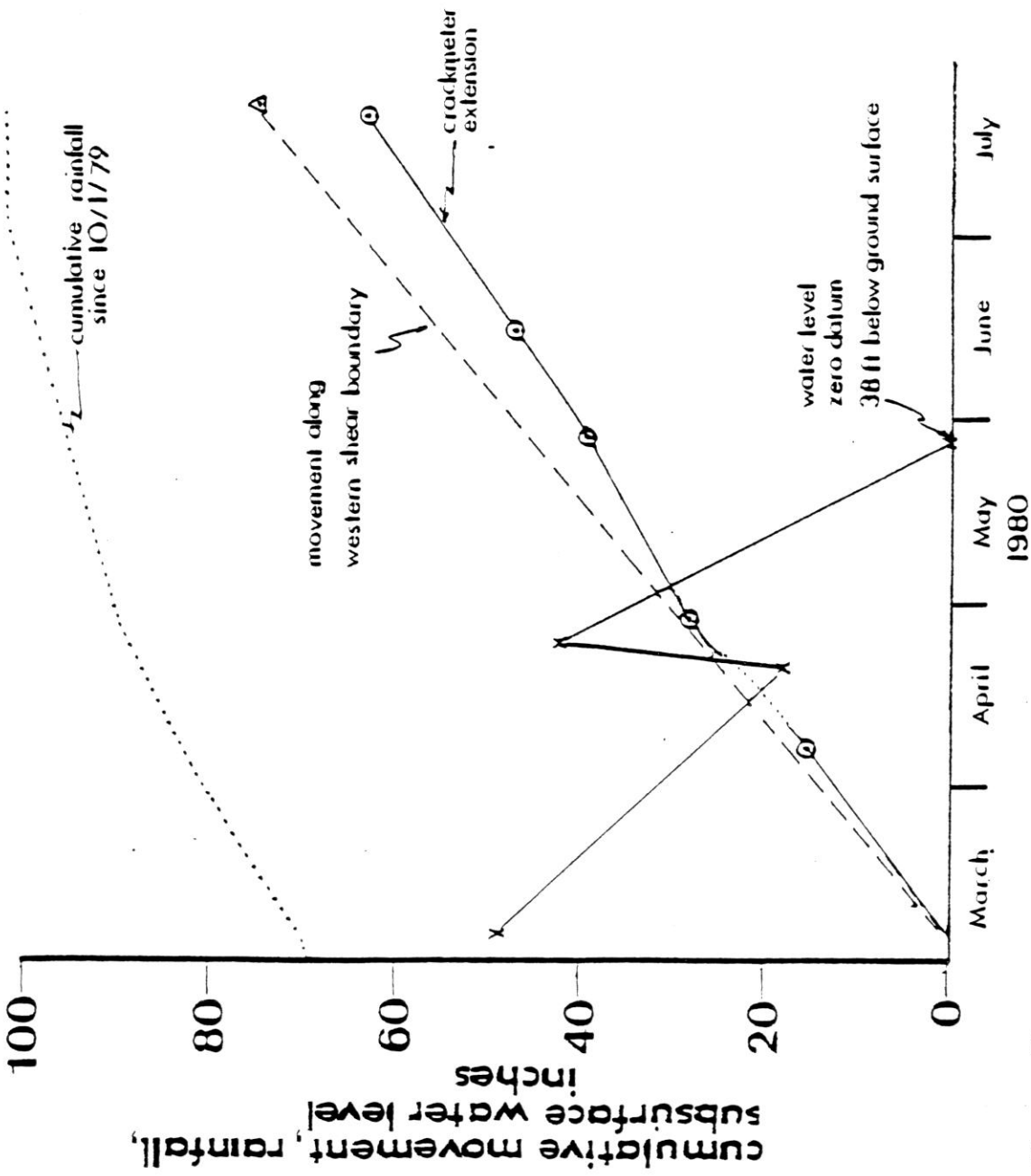


Figure 25. Shear movement along western shear boundary, Middle Santiam earthflow, measured by crackmeter, plotted along with rainfall and borehole water level data. Rainfall data from Cascadia station.

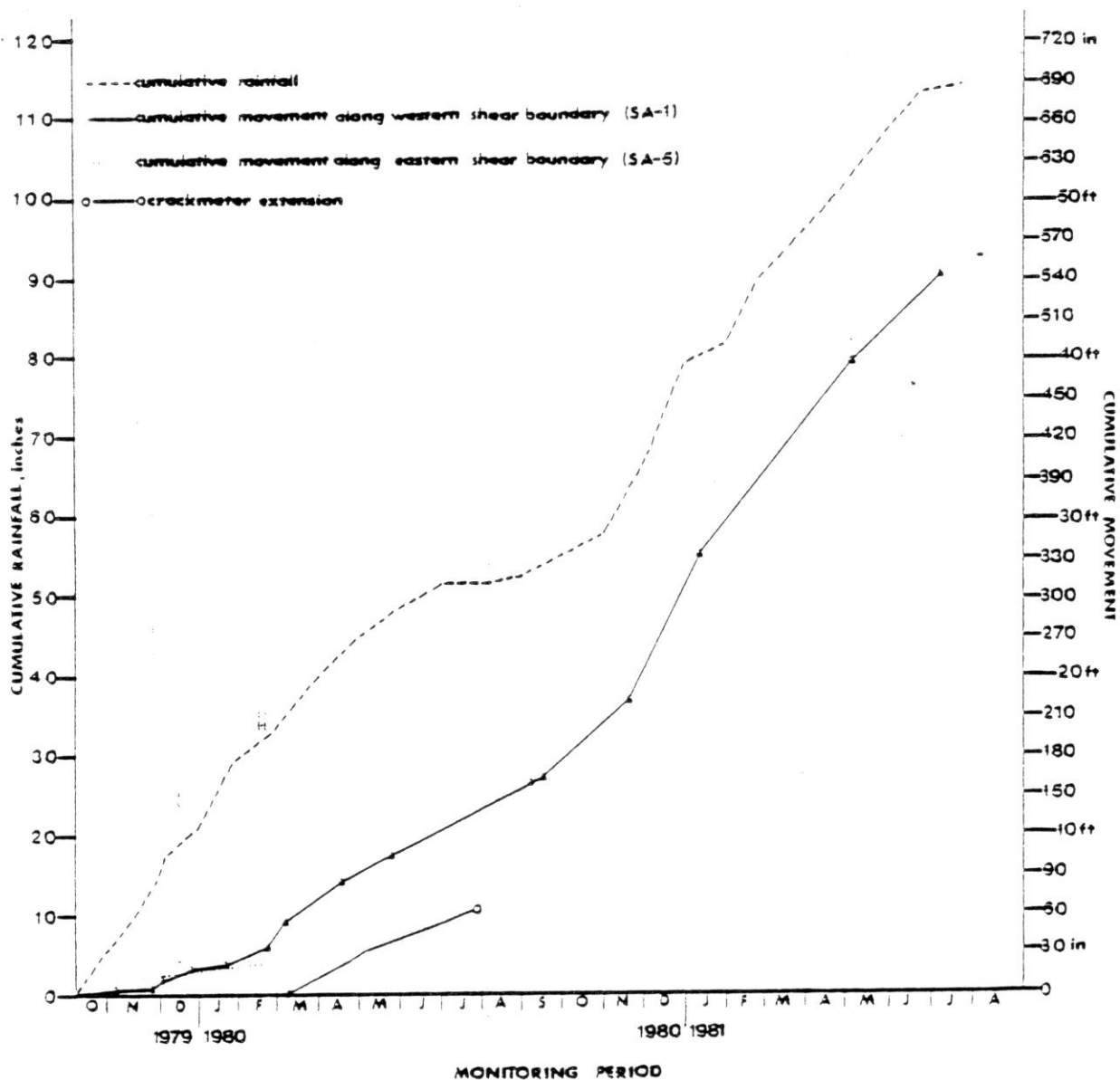


Figure 26. Crackmeter and stake array movement data for the Middle Santiam earthflow. Rainfall data from Cascadia station, approximately 20 miles SW of site at elevation 360.

inches or 14.5 feet, During nine and one-half months of the 1980-1981 water year, it moved 376 inches or 31.3 feet.

In general shape, the cumulative movement curve for SA-1 matches that of the cumulative rainfall curve fairly well. During the early part of the monitoring period (November 1979 to March 1980), the data show periods of acceleration which may correspond with peak rainfall periods. Earthflow movement accelerated dramatically in October and November 1980. From an average rate of .48 in/day for the 1979-1980 water year, the rate increased to .89 in/day through October and November 1980, and attained a maximum of 2.03 in/day through January 1981. Movement began to decline slightly through the summer of 1981, but rates were still higher than those measured during 1979 and 1980. Sixty percent of cumulative movement occurred from late November 1981 to July 17, 1981, only 36% of the monitoring period.

Factors contributing to this steady acceleration of movement include rainfall. The cumulative rainfall curve rises steeply at the end of October 1980. About 49% of the total measured rainfall fell from October 1980 to July 1981. The winter of 1980-1981 was somewhat wetter than that of 1979-1980, with 5.94 more inches of rain falling at Cascadia from November 1 1980 to January 31 1981 than during the same months in 1979-1980. The spring of 1981 was also wetter than the spring of 1980.

Other factors may be related to the mass balance of the earthflow. Massive failures from the flow front during late fall 1980 may have suddenly destabilized the earthflow and caused accelerated movement. Massive rockfall from the crown scarp may also have contributed. About 3000 yd³ of bedrock fell from the crown

scarp sometime between visits on November 21, 1980 and January 18, 1981, loading the head of the earthflow. Both types of failure events could have been triggered by heavy rains in November and December 1980.

Stake array 5 (SA-5) was installed across the eastern shear boundary of the earthflow on the same day as SA-1 (10/6/79). However, data from SA-5 is available only through February 24, 1980; thereafter, a lobe of earthflow debris buried one stake and the growing lateral pressure ridge along the shear crack made direct measurements of array diagonals impossible. The available data for this array indicate that movement rates were slightly different, perhaps due to the eastward thrusting component on the eastern side of the earthflow. Up to 12/7/79, average movement was slightly faster along this boundary than along the western boundary, .25 in/day to .19 in/day. From 12/7/79 to 2/24/80, rates averaged .10 in/day along the eastern shear boundary and .33 in/day along the western boundary.

Measurements at arrays SA-2, SA-3 and SA-4 indicate substantial changes across tension cracks (Table 7). Differences in amounts of extension on two sides of the same array may indicate widening of the cracks on one side. Most ground extension occurred at SA-2 and SA-3 and much less at SA-4, which is closer to the head of the earthflow.

Surface points on and around the Middle Santiam mass movement site were surveyed by Willamette National Forest crews on 7/30/79, 10/28/79, and 9/18/80. Transit, theodolite and tapes were used for the first two surveys, and an electronic distance meter (EDM) was used for the third. All points were marked by nails in wooden hubs;

Array	Downslope Measurement Direction		Total Extension (in.)
	Initial	Final	
SA-2	N20E	N30E	12.9
	N32E	N45E	72.6
SA-3	N17E	N26E	40.1
	N30E	N42E	—
SA-4	N6E	N7E	5.1
	N14E	N15E	1.3

Table 7. Ground extension across tension cracks, Middle Santiam earthflow, from 11/30/79 to 5/18/81.

accuracy is to hundredths of feet. Plate 2 shows some of these survey points at their locations as of 7/30/79 relative to a base point west of the earthflow.

Figure 27 is a vector map which shows how survey points were moved by the earthflow over the period of observation (7/30/79 to 9/18/80) (Table 8). Ground morphology was significantly changed by earthflow movement. The average horizontal translation for all survey points is 19.5 feet or approximately 19.7 ft/yr. This is within the range of rates of translation measured by Kelsey (1978) on the Halloween (22 ft/yr) and Cashlapooda Creek (15 ft/yr) earthflows in northern California.

Even though annual earthflow movement is continuous, large volumes of debris fall from the flow front only seasonally. This suggests that the toe area bulges as earthflow material builds up and the head of the earthflow thins, although scarp areas are recharged by rockfall. This is supported by the survey data, which shows relative subsidence near the crown scarp at points 12+81 and 17+04 and relative uplift at point 22+14, just above the toe of the earthflow. Bulging of parts of the flow front was indicated by vertical radial cracks through earthflow debris. These cracks were observed at the time of the third survey.

All points on the western parts of the earthflow moved downslope along bearings within a few degrees of north. The vector for point 22+14 has a strong eastward component. This seems to be expressed geomorphically by the formation of the eastern boundary lateral ridge, although more data points are needed to verify this.

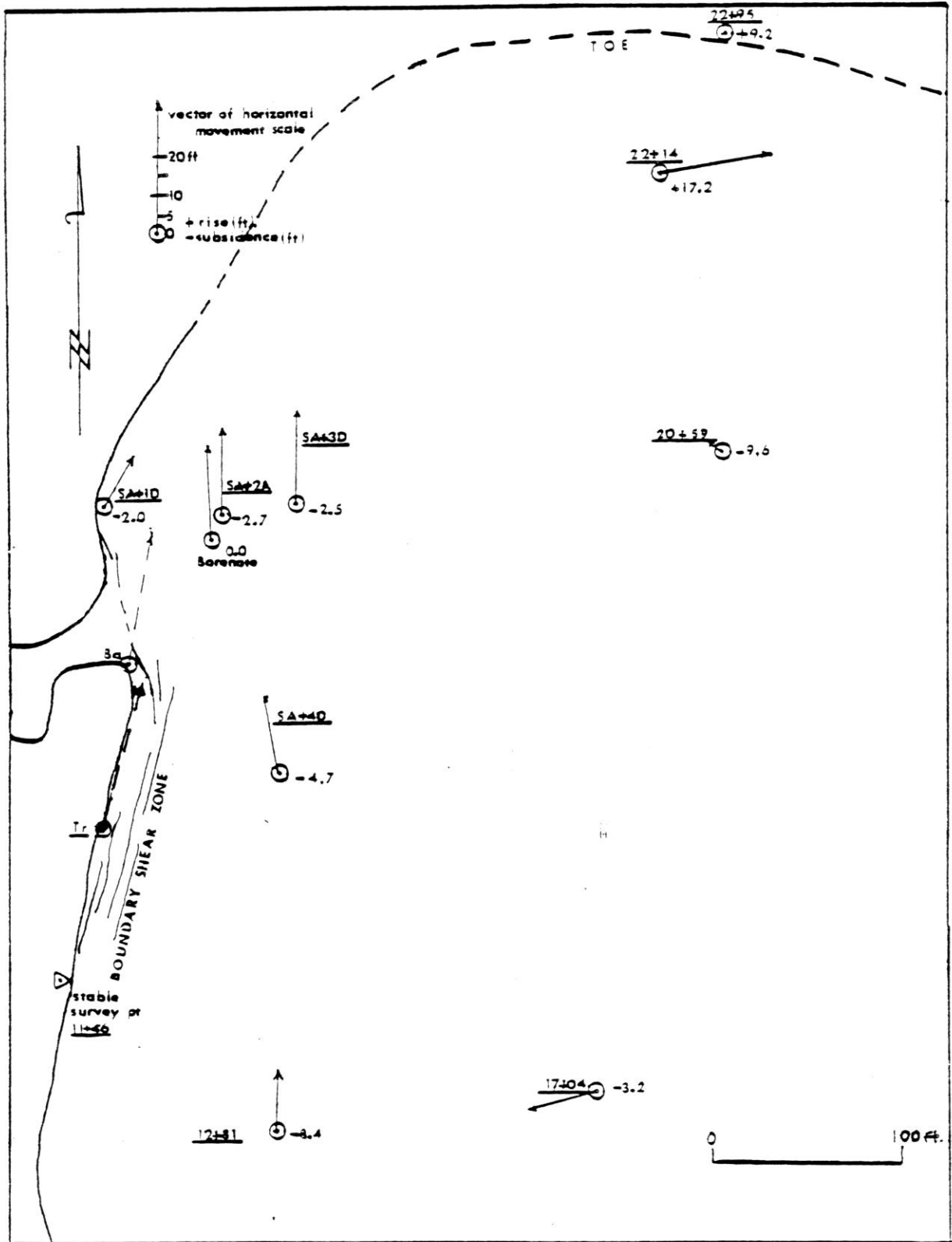


Figure 27. Surface movement vectors for the Middle Santiam earthflow, 7/30/79 and 10/28/79 to 9/12/80.

Survey Point	Period of Observation	Elevation		Horizontal Translation (ft)		Azimuth of Translation (degrees)		Average rate of translation	
		Change (ft)	Translation (ft)	Translation (ft)	Translation (degrees)	In./day	ft/yr		
Borehole ¹	10/28/19-9/18/80	0	25.0	357	0.92	20.0			
SA-1 D ²	"	-2.0	15.0	30	0.55	16.0			
SA-2 A	"	-2.7	22.5	0	0.83	25.2			
SA-3 D	"	-2.5	24.0	4	0.88	26.9			
SA-4 D	"	-4.7	21.0	349	0.77	23.5			
22195	7/30/19-9/18/80	19.2 ³	--	--	--	--			
22114	"	117.2	29.0	76	0.85	25.5			
20159	"	-9.6	5.0	294	0.15	4.4			
22114	"	-1.2	17.0	260	0.50	15.0			
20159	"	-8.4	18.0	5	0.53	15.0			

¹ Point is at top of borehole casing

² Points denote survey hubs located at base of one stake in each stake array

³ Approximate depth of burial of point by earthflow debris

Table 8. Movement of surveyed surface points on Middle Santiam earthflow.

The westward component of the vector for point 17+04 is problematic. This point is located on boulder terrain above and east of a broad swale, so that its displacement may be explained by creeping of the surface bouldery substrate toward this depression.

All points subsided except point 22+14. Relative subsidence decreasing northward from point 12+81 may indicate a shallowing basal shear zone, especially near the lateral shear boundaries. Significant subsidence at point 20+59 may reflect a deepening of the basal shear zone before it starts to shallow northward toward the flow front.

A number of other survey points were established on the earthflow during the first survey, but these were destroyed by burial, treefall, and ground crack expansion.

Subsurface movement, 1979-1980

After the borehole was drilled on the earthflow, riveted and glued ten-foot sections of plastic casing designed for use with an inclinometer were installed downhole. The casing extended from the bottom of the hole to about 18 inches above ground surface. The borehole was then backfilled with sand. The inclinometer system is electromechanical, consisting of a borehole probe connected by cable to a digital readout unit which displays sine of the angle of inclination of the casing. Figure 28 illustrates the principles of inclinometer operation.

Inclinometer equipment used in this study (Digitilt inclinometer, model types 50306 and 50309) is owned by the Forest Service and was manufactured by SINCO (Slope Indicator Company) of Seattle, Washington. Readout data were tabulated in the field and sent to

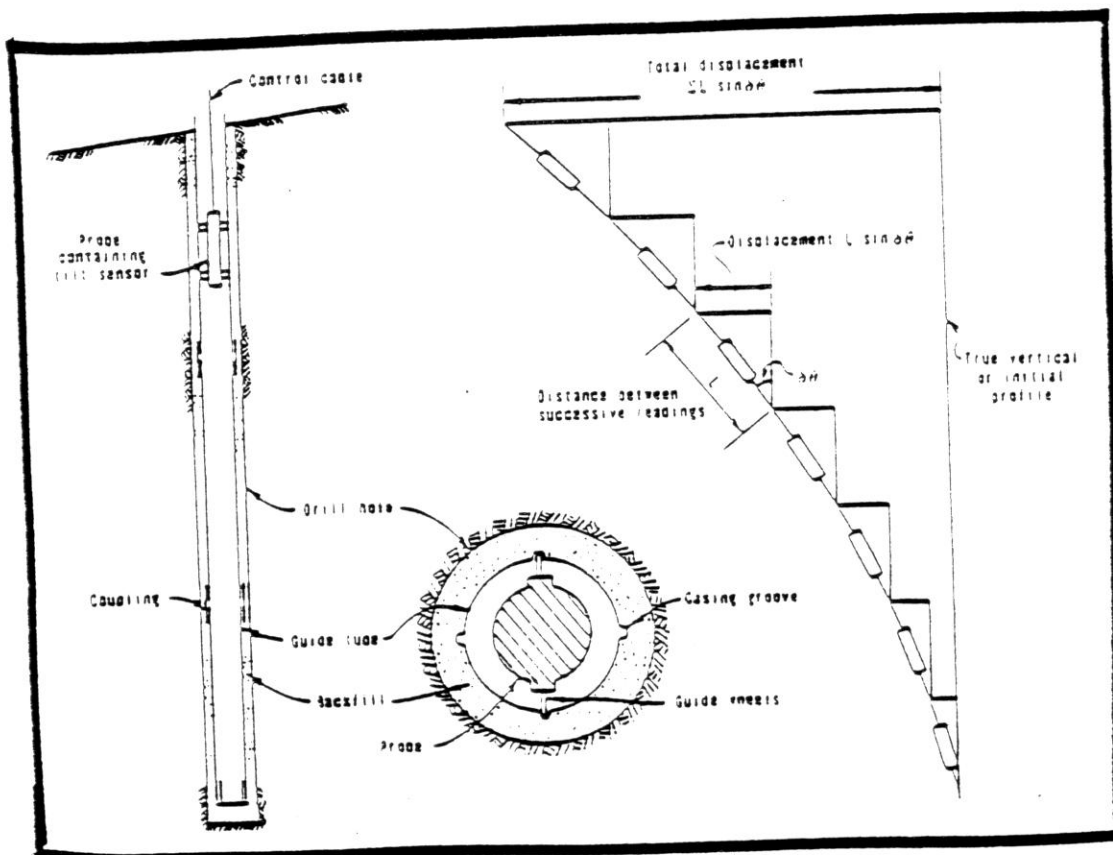


Figure 28. Principles of Inclinometer operation, from "Field Instrumentation", S. D. Wilson and P. E. Mikkelsen, in Landslides, Analysis and Control, 1978, National Academy of Sciences, p. 119.

Redwood Sciences Laboratory in Arcata, California for processing and plotting of deformation profiles.

Casing deformations were monitored on 9/5/79, 9/14/79, 10/13/79, 12/27/79, 1/24/80, 5/26/80, and 9/11/80. No monitoring was attempted after the last date because the probe could not be lowered farther than 46 feet down the hole. Shearing of the casing may have occurred at this depth.

Data interpretation problems became apparent when horizontal displacements of the top of the casing as determined by surveying and by plotting of the inclinometer data were compared. Survey data indicate a displacement of about 25 feet along a bearing of N3W between 10/28/79 and 9/18/80. The inclinometer profiles as originally plotted by Redwood Sciences Lab (Figure 29) indicate 9.2 feet of movement S50E for the top of the casing, while some subsurface points appear to have moved N50E. These profiles were plotted according to the assumption that the casing bottom was founded in stable materials.

In order to explain in part the discrepancies between survey and inclinometer data, it may be necessary to assume that the bottom of the casing was also moved. A depth of maximum earthflow displacement (at 43 feet) is indicated, as well as a southward component of displacement for the upper 43 feet of casing due to slump rotation.

It is difficult to reconcile the significantly different direction of translation for the top of the casing obtained by surveying. Wilson and Mikkelsen (1978) state that spiraling of casing grooves and deformation of the casing cross-section is a source of significant error for inclinometer movement direction.

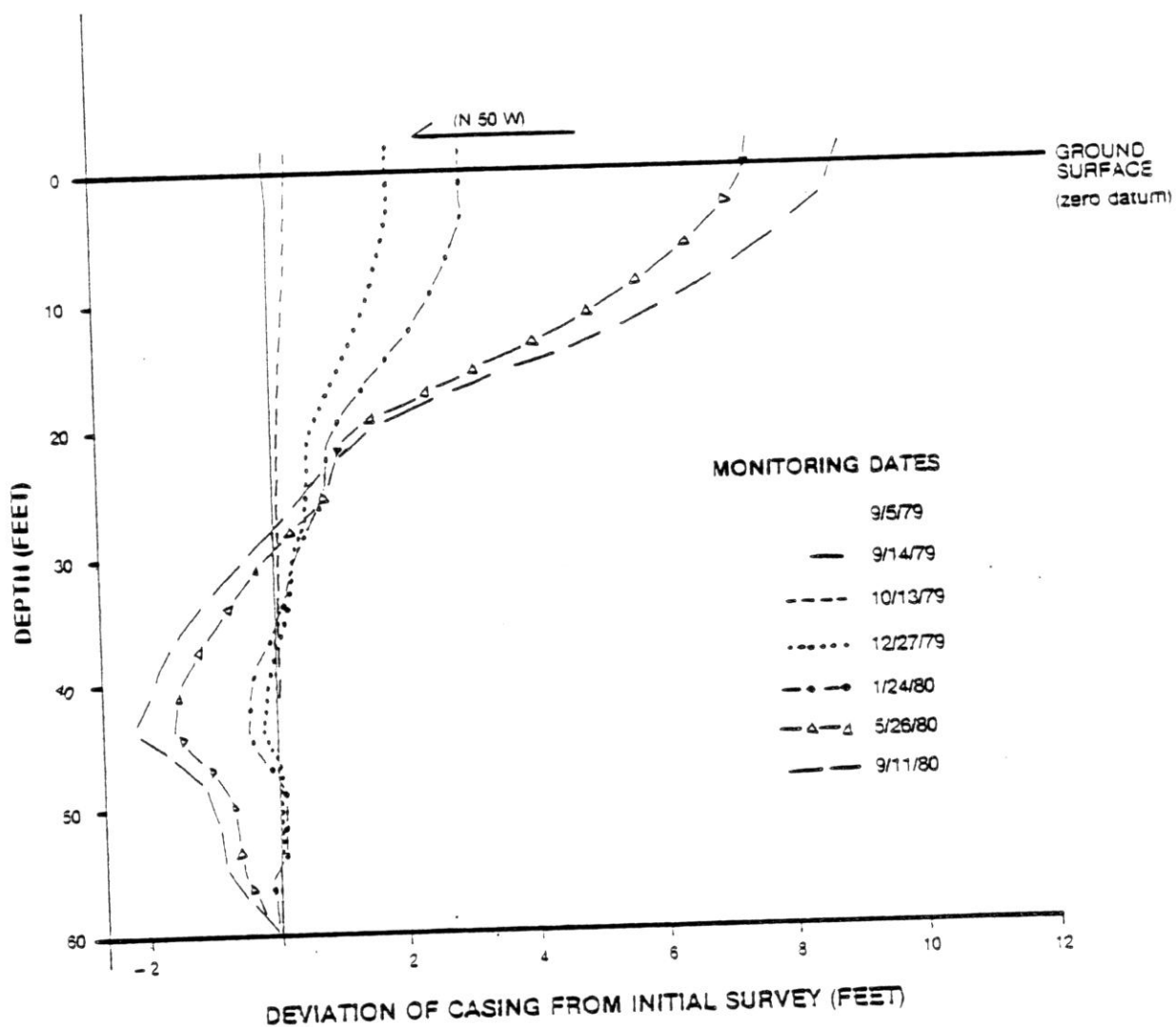


Figure 29. Profiles of borehole casing in Middle Santiam earthflow, assuming casing bottom was founded in stable materials. Modified from computer-plotted profiles by Redwood Sciences Lab, Arcata, California.

The inaccuracy of the instrument itself combined with the assumption that the casing bottom was not stable cast the plotted casing profiles (Figure 29) in a questionable light. However, the depth of greatest deflection is consistently shown by most of the profiles at about 44.5 feet from the top of the casing. Depths from ground surface (zero datum) are 18 inches less. Generally, Wilson and Mikkelsen (1978) feel that the inclinometer's most useful asset is its ability to measure deflections at specific depths rather than to survey an exact profile of the borehole casing. In this analysis, therefore, more weight is given to the location of planes of maximum deflection than to apparent magnitudes of subsurface displacement.

Correlation of Subsurface Movement with the Drilling Record

The borehole log (Table 6) shows that between depths of 39 and 44 feet below the ground surface, a zone of soft, deformable, plastic, slickensided clayey materials was encountered. Underlying this zone is decomposed granular bedrock. The inclinometer data indicate significant deformation at a depth of about 43 feet below ground surface, which correlates quite well with the location of the contact between the clayey materials and decomposed bedrock. Shear is probably distributed throughout the five-foot thick clayey zone. This depth of shear does not indicate the only shear plane location. Lesser shear between 21.5 and 22 feet below ground surface as shown by the inclinometer data may represent slippage of boulders or joint blocks along joint filling materials. Also, there should be deeper shear planes if the casing bottom was moving. Shear zones may be deeper within the interior of the earthflow, further from the shear boundaries. Additional borings would be required to verify this.

Correlation with Precipitation

Figure 29 shows that significant deformations began to occur by 12/27/79, after fall and early winter storms. Surface movement as recorded by SA-1 (Figure 25) also begins to accelerate slightly at this time. Between 1/24/80 and 5/26/80, more large deformations occurred, probably in response to winter rains, spring rains and snowmelt.

Recent Movement History

The lack of curved trunk growth of conifers 100 to 250 years old growing on unharvested sections of the earthflow imply no or very little movement within the lifetime of these trees before the current episode. The presence of leaning, straight-trunked conifers still rooted on the earthflow suggests a recent pulse of earthflow movement. Scar tissue growth rings on a sample taken from a tree split by an active tension crack (Plate 2) indicate initiation of this crack in 1971.

Road construction through the earthflow toe in 1965 may have contributed to reactivation of movement. In late January 1972, a storm large enough to produce the fourth-largest peak flow in a 150-acre watershed in the Andrews Forest in the last 26 years (Table 11, Harr, 1981) triggered debris avalanching from the front of the earthflow, setting up conditions of instability for the entire earthflow.

As part of timber harvesting operations in 1965, a fire trail and

a cat road were constructed onto the earthflow. Ground measurements on 5/8/81 indicated that both features had been displaced approximately 75 feet along the western shear boundary. Assuming that earthflow movement displacing these features began about 1971, average movement through the spring of 1981 was 7.5 feet per year. However, data from SA-1 (Figure 26) show an average movement rate of 25.5 feet per year from 10/6/79 to 5/8/81. Consequently, from 1971 to 1979 average movement was only 3.6 feet per year. Reasons for this drastic acceleration during the last two or so years are difficult to define with the data at hand. Storm history (Table 11) shows large peak flows (ranking fourth and fifth in the 26 year record) in January 1972 and 1976. The largest peak in 1979 ranked only 18th in this record. Rainfall data from Cascadia indicate that 57.24 inches of rain fell in 1979, 60.31 inches in 1980, and 35.42 through July 1981, all below the long term mean. Possibly, initial failures from the flow front set the stage for a period of instability; rockfall from the crown scarp aided continuous earthflow movement.

MASS MOVEMENT INVENTORIES

Earthflow Inventory

A total of 55 earthflows were identified and mapped in the study area (Plate 3; Table 9). Approximately 22% of the study area is underlain by active and inactive earthflow landforms. Inactive earthflows account for 7% of the total land area and 33% of the terrain underlain by earthflows.

Fifteen earthflows occur in the Sardine Formation, and only 4 of these have portions which are currently active. The rest occur in the Little Butte Volcanic Series, and none occur in Quaternary and Pliocene bedrock. About 29% of the land area underlain by the Little Butte Volcanic Series is earthflow terrain, in contrast to only 14% for the Sardine Formation.

Debris Avalanche Inventory

A total of 24 debris avalanches occurring since 1955 are inventoried in the study area (Table 9). Included in these is the large debris avalanche which initially failed from the flow front of the Middle Santiam earthflow in 1972. After this event, avalanches have periodically occurred at the same site. It is difficult to determine the total number of avalanches at this site, but it is likely that at least one occurred every winter following the 1972 event. These are all included under one inventory number in Table 9, but are treated as 10 separate events in erosion calculations below.

Table 9. Mass Movement Inventory. Abbreviations used in Table 9 for mass movement types are as follows: SE = slump-earth-flow, DA = debris avalanches, RR = rockfall-rockslide, DT = debris torrent. Geologic unit abbreviations are the same as those on the area geologic map (Figure 3). In the "remarks" column, "P" means sites identified by aerial photograph interpretation and not field-checked by the author. "R,P" indicates sites identified by geotechnical personnel from the Santiam Zone, Willamette National Forest, and discussed in geotechnical reports for the Middle Santiam unroaded area, 1977-1979. Land type designations for debris avalanches and debris torrents are as follows: F = forest, C = clearcut, Ro = road-related. All mass movements which occurred before 1955 (before period of aerial photo and field record) occurred in the forest land type.

Feature number	Type	Geologic unit	Area (acres)	Volume (cyl)	Aspect	Approximate year of initial occurrence or age	Remarks
1	SL	T ₂	19.0		SW	pre-1955	
2	SE	T ₂	35.0		S	pre-1955	
3	DA	T ₂	0.16	1100	E	1955-1972	
4	SE	T ₂	0.0		E	pre-1955	
5	DA	T ₂	0.21	700	E	1955-1972	
6	SE	T ₂	12.0		S	pre-1955	
7	SE	T ₂	-05.0		S, E	pre-1955	
8	SL	T ₂	126.0		M	pre-1955	F, currently active
9	SE	T ₂	16.0		M	pre-1955	
10	SE	T ₂	56.0		M	pre-1955	Currently active
11	SE	T ₂	35.0		S	pre-1955	
12	DA	T ₂	0.046	250	S	1978	Fresh streamside failure, not visible on aerial photos
13	DA	T ₂	0.057	150	S	1978	
14	SE	T ₂	9.0		S	pre-1955	
15	DA	T ₂	0.10	700	S	1955-1967	F, failure from northflow drain scarp postflow currently active, F
16	SE	T ₂	60.0		S	1955-1967	Site A, Bonaca complex
17	SE	T ₂	627.0		S	1955-1967	Site A, Bonaca complex
17A	SE	T ₂	110.0		SE, S, E	400, years	Site A, Bonaca complex
18	SE	T ₂	11.0		M	200, years	Site B, Bonaca complex
19	SE	T ₂	17.0		M	400, years	Site B, Bonaca complex
20	SE	T ₂	37.0		M	400, years	Site C, Bonaca complex
21	SE	T ₂	50.0		M	pre-1955	F, site D, Bonaca complex
22	SE	T ₂	0.7		SE	pre-1955	Streamside failure, Site A, Bonaca complex, F
23	SE	T ₂	0.3		SE	pre-1955	Streamside failure, Site A, Bonaca complex, F
24	SE	T ₂	4.0		S	pre-1955	Streamside failure, Site A, Bonaca complex, F
25	SE	T ₂	74.0		S	pre-1955	Streamside failure, Site A, Bonaca complex, F
26	SE	T ₂	5.0		S	pre-1955	Streamside failure, Site A, Bonaca complex, F
27	SE	T ₂	16.0		S	pre-1955	Streamside failure, Site A, Bonaca complex, F
28	SE	T ₂	9.6		S	pre-1955	Streamside failure, Site A, Bonaca complex, F
29	SE	T ₂	5.6		S	pre-1955	Streamside failure, Site A, Bonaca complex, F
30	SE	T ₂	5.0		S	pre-1955	Streamside failure, Site A, Bonaca complex, F
31	SE	T ₂	7.6		S	pre-1955	Streamside failure, Site A, Bonaca complex, F
32	SE	T ₂	62.0		M	pre-1955	Streamside failure, Site A, Bonaca complex, F
33	SE	T ₂	6.4		M	pre-1955	Streamside failure, Site A, Bonaca complex, F
34	SE	T ₂	8.0		M	pre-1955	Streamside failure, Site A, Bonaca complex, F
35	SE	T ₂	186.0		M	pre-1955	Streamside failure, Site A, Bonaca complex, F
36	DA	T ₂	0.21	2500	S	400, years	Active, pre-dates clearance
37	SE	T ₂	0.60	8100	S	1959-1972	Complex, slumpy basin
38	SE	T ₂	62.0		S	1959-1972	F, two failed avalanches
39	SE	T ₂	8.0		S	200, years	Active
40	SE	T ₂	3.0		SE	pre-1955	Active
41	SE	T ₂	3.0		E	pre-1955	Active
42	SE	T ₂	48.0		SE	pre-1955	
43	SE	T ₂	3.0		SE	pre-1955	
44	SE	T ₂	4.0		SE	pre-1955	
45	SE	T ₂	260.0		NE	pre-1955	
46	SE	T ₂	32.0		NE	pre-1955	
47	SE	T ₂	1.0		M	1973	
48	SE	T ₂	13.0	7,000,000	M	200, years	Middle Bonaca northflow
49	DA	T ₂	2.5	60,000	M	1972-1981	No, multiple debris avalanches, Middle Bonaca northflow
50	SE	T ₂	47.0		M	200, years	
51	SE	T ₂	4.0		E	1964, 1967	
52	DA	T ₂	0.41	5900	M	1967-1977	
53	SE	T ₂	300		M	1960	
54	SE	T ₂	28.0		M	200, years	
55	SE	T ₂	12.0	1400	M	pre-1955	Transitional with debris torrent, No
56	DA	T ₂	1300		M	1958-1967	Occurred between 11/21/80 and 1/18/81 in fresh
57	SE	T ₂	13.0		NE	pre-1955	clearcut
58	SE	T ₂	156.0		NE	200, years	

Table 9.

Feature number	Type	Geologic unit	Area (acres)	Value (yds)	Aspect	Approximate year of initiation	Remarks
37	SE	U1	24.0		W	200+ years	
38	DA	U1			M	1938 1967	Ro
39	DA	U1	0.25	2,000	M	1938 1967	C
40	DA	U1	0.39	4,500	M	1938 1967	Ro
41	DA	U1	0.14	1,000	M	1938 1967	Ro
42	SE	U2	0.5		W	200+ years	
43	SE	U2	0.5		W	200+ years	
44	SE	U1	7.2		M	pre-1935	
45	SE	U1	3.2		M	pre-1935	
46	SE	U1	73.0		M	200+ years	Inde Creek scarp/line
47	SE	U1	48.0		M	pre-1935	
48	SE	U1	40.0		W	pre-1935	
49	SE	U1	0.14	1100	NE	1938 1967	Ro
50	DF	U1			W	1938 1967	Ro
51	DA	U1	0.14	1100	E	1965 1967	Ro
52	DA	U1	0.18	1400	E	1965 1967	Ro
53	DA	U1	0.14	1100	E	1965 1967	Ro
54	DA	U1	0.41	3000	E	1965 1967	Ro
55	DA	U1	0.18	1600	E	1967 1972	Ro
56	DA	U1	0.18	1600	E	1967 1972	Ro
57	SE	U1	17.0		SE	200+ years	
58	SE	U1	208.0		M	pre-1935	
59	SE	U2	32.0		E	pre-1935	
60	SE	U2	224.0		M	pre-1935	
61	DA	U2	1.31	2,000	M	pre-1935	
62	DA	U2	0.65	800	M	pre-1935	From top of SE 400
63	SE	U2	3.7		M	1935 1967	From top of SE 400
64	DA	U1		4,500	M	1938 1967	Ro
65	DA	U1		1,500	M	1980	C
66	DF	U1			M	pre-1935	
67	DF	U1			M	pre-1935	
68	DF	U1			M	pre-1935	
69	DF	U1			W	pre-1935	
70	DF	U1			S	pre-1935	
71	DF	U2			S, SW	pre-1935	
72	DF	U2			SE	pre-1935	
73	DF	U2			SE	pre-1935	
74	DF	U2			SE	pre-1935	
75	DF	U2			S	pre-1935	
76	DF	U2			S	pre-1935	
77	DF	U2			S	pre-1935	

Table 9. (cont inued)

Seven other avalanches are associated with earthflows in forested terrain. Inventory numbers 5, 12, 13, and 36 are located near the margins and toes of earthflows. A fifth (inventory number 15) failed from steep slopes above the crown scarp of an active earthflow. Two other large avalanches which occurred before 1955 scarred nearly 2 acres of forested but very steep terrain at the head of a huge slump-earthflow. These scars are healing very slowly, and may still be eroding.

Earthflow movement advances debris into streams and streamside areas. Debris avalanches and slumps fail from unstable streambanks at the front and along the fringes of active earthflows. These events are not separately mapped but are collectively included in geomorphic unit VII (stream erosion impact zones). Only events with distinct boundaries, source areas and avalanche tracks are mapped and inventoried as debris avalanche events.

An inventory of debris avalanches in the study area provides data for assessing impacts of storms and forestry practices. Estimated rates of soil erosion by debris avalanching are based on (1) area of occurrence, (2) period of occurrence, and (3) volumes of displaced soil (Swanston et al., 1981). Debris avalanches were identified and soil volumes estimated primarily by interpretation of aerial photographs of varying scales. Age estimates or age brackets were obtained by comparing aerial photograph sets of varying scales taken in 1955, 1959, 1967, 1972, 1973, 1974, 1977, and 1978. Supplemental field observations were made in 1979 and 1980.

None of the photograph sets provides coverage of the entire study area. It is possible that not all debris avalanches and torrents in

the study area were identified, especially where dense forest cover limits the usefulness of aerial photograph interpretation.

Simonett (1967), in his study of earthquake-induced landslides in mountainous jungle areas of New Guinea, plotted field-measured areas against volumes of 201 mapped slides and derived a straight-line regression relationship which could be expressed by the equation:

$$\text{Log volume} = 1.386 \text{ Log surface area} - 0.6885$$

which is significant at the .1 percent confidence level, irrespective of other variables. Volumes of slides in Simonett's study had a broad range, from 1 yd³ to approximately 7 x 10⁷ yd³. Rice et al. (1969), derive a similar relationship for soil slips in southern California, but these slips had a narrow size range averaging 500 ft² in area. Simonett's (1967) equation therefore is probably more applicable.

Simonett's relationship was used to derive volumes of debris avalanches in the study area, once planimetric surface areas of their scars were measured. Areas were measured by overlaying traced outlines on a grid of evenly-spaced small dots and counting the number of enclosed dots (Rice, personal communication, 1981). All areas were plotted from aerial photographs. Simonett (1967) found a correlation coefficient of .92 between volumes plotted from aerial photographs and field-estimated volumes.

Seven debris avalanches were inventoried in forested areas in the study area (Table 10). These avalanches had an average volume of 2100 yd³, displacing nearly 15,000 yd³ of soil over a 26 year

Site	Area (mi ²)	Period of record	Number of events	Frequency (events mi ⁻² yr ⁻¹)	Average volume (yd ³)	Soil transfer rate (yd ³ mi ⁻² yr ⁻¹)
<u>Forested</u>						
Middle Santiam	18.20	1955-1981	7	0.015	2100	31.5
Blue River	19.00	1946-1980	19	0.026	4000	105.0
H.J. Andrews	3.30	1950-1974	32	0.065	1900	122.4
Alder Creek	4.72	1950-1975	7	0.060	2600	153.0
Bull Run	—	1938-1978	—	0.008	1100	8.5
<u>Clearcut</u>						
Middle Santiam	4.30	1958-1981	6	0.054 (3.6)	2000 (0.95)	108.0 (3.4)
Blue River	3.90	1958-1980	30	0.622 (24)	3500 (0.36)	2200.0 (21)
H.J. Andrews	3.04	1950-1974	36	0.252 (3.9)	1700 (0.90)	448.0 (3.7)
Alder Creek	1.74	1960-1975	18	0.694 (12)	340 (0.2)	398.0 (2.6)
<u>Road right of way</u>						
Middle Santiam	0.35	1958-1981	10	1.24 (83)	2400 (1.1)	3000 (95)
	0.35*	1958-1980*	20*	2.48 (166)*	3200* (1.5)	3000 (260)
Blue River	0.77	1955-1980	69	6.56 (253)	1700 (0.41)	11000 (105)
H.J. Andrews	0.58	1950-1974	73	3.60 (55)	1800 (0.95)	6000 (49)
Alder Creek	0.23	1960-1975	75	21.7 (360)	2400 (0.94)	53000 (350)

* Includes debris avalanches from flow front of Middle Santiam earthflow, assuming at least one event every winter from 1972-1981

Table 10. Frequency, average volume, and soil transfer rate of debris avalanches under forested, clearcut and road rights-of-way conditions in the Middle Santiam study area and in H. J. Andrews Experimental Forest (Swanson and Dyrness, 1975); Alder Creek (Morrison, 1975), Willamette National Forest, Oregon, and in the Blue River Drainage (Marion 1981). Data for forested conditions only are available for the Bull Run Watershed (Schulz, 1980). Shown in parentheses is the factor by which each value exceeds the comparable value for forest conditions. Forest and clearcut areas were measured planimeter; road right-of-way area equals road mileage \times assumed width of hydrologic influence, (about 66 feet).

period (1955-1981). Only 12,000 yd³ of soil were displaced by avalanches in clearcut areas, but since the area of land in clearcut is smaller, the soil transfer rate is greater, 108 yd³ mi⁻² yr⁻¹ for clearcuts compared to only 31.5 yd³ mi⁻² yr⁻¹ for forested areas. The rate for road rights-of-way was about 95 times greater than the forest rate, if the 1972 debris avalanches at the Middle Santiam mass movement site are excluded. If they are included, the rate is almost 260 times greater. The amount of material eroded from the flow front in 1972 roughly equals the combined amounts of material deposited by ten road-related avalanches at other locations.

Data from other studies (Table 10) yield points of comparison. The soil transfer rate from forested areas in the Bull Run watershed west of Mt. Hood, (Schulz, 1980) is significantly lower than rates in the Willamette Forest at the Middle Santiam, H. J. Andrews Forest (Swanson and Dyrness 1975) and Alder Creek (Morrison, 1975). Rates in forested areas at Alder Creek and the Andrews Forest are 4 to 5 times higher than at the Middle Santiam. In each of these three areas, rates of soil transfer in clearcut are greater by a factor of about 4 than rates for forested conditions. In all cases, debris avalanches from roads rights-of-way were most abundant and had the highest rates of soil transfer. The highest rate of soil transfer occurred from road rights-of-way in Alder Creek, seven times higher than Middle Santiam rates, even if debris avalanches from the Middle Santiam earthflow are included.

Erosion data from this study support the general conclusion reached by many workers that road construction is a more important

factor than deforestation by clearcutting in accelerating erosion (Dyrness, 1967; Fredriksen, 1970; O'Loughlin, 1972; Swanson and Dyrness, 1975 and others). These authors found that the maximum impact of roads probably occurs during the first few severe storms after disturbance.

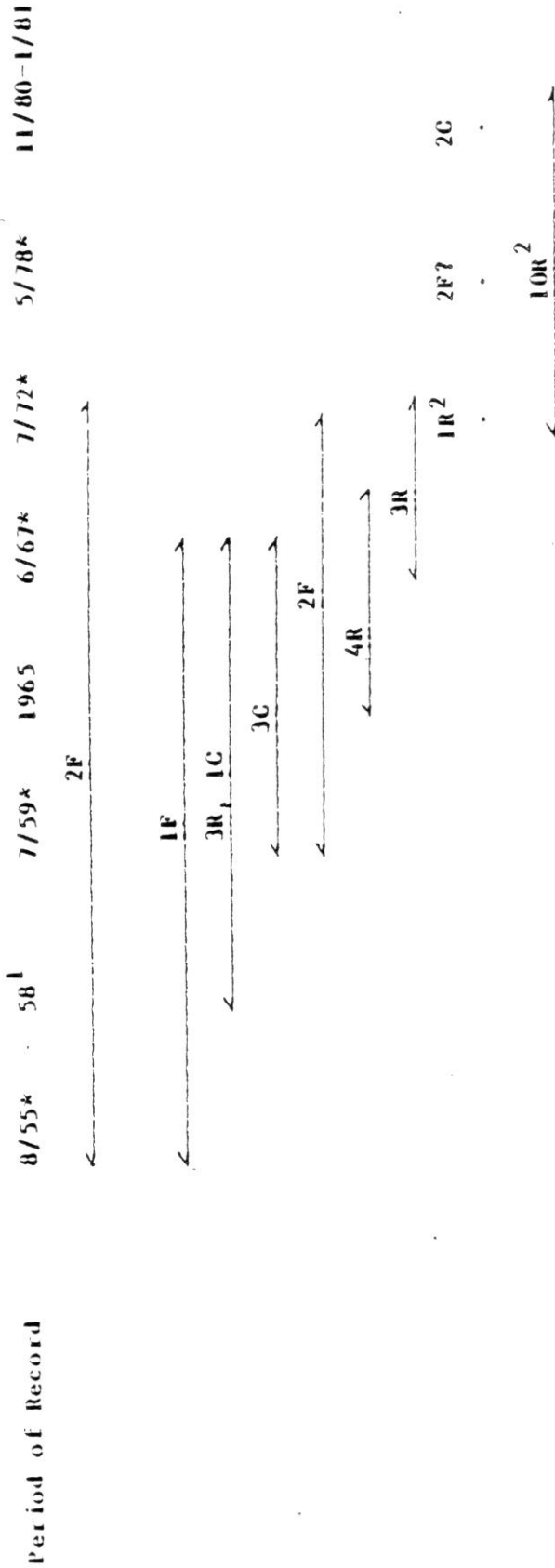
Calculated soil transfer rates for forested and clearcut areas in the Middle Santiam study area, however, are lower than those in other areas of the Willamette Forest. This may reflect the fact that debris avalanches were mainly mapped from aerial photos, whereas in the other studies, extensive field work was conducted in support of aerial photo interpretation. Also, much of the Middle Santiam area is underlain by earthflow terrain, with slope gradients which are generally less steep than those where debris avalanches occur, about 27-42° (Marion, 1981).

Mass Movement and Recent Storm History

Compilations of data on peak flows can be combined with age data for mass movement events to match mass movement occurrence with periods of high water input (Tables 11 and 12). Peak flow data for a small watershed are better than only rainfall data because the streamflow records reflect antecedent soil moisture conditions as well as precipitation. Management practices may affect rates of water input to soil. Clearcutting influences runoff and infiltration of precipitation and rates of evapotranspiration. Roads may alter drainage patterns. Storm sequence is important also. A large storm may cause all sufficiently unstable slopes to fail; a succeeding

Date	Magnitude (cfs/mi ²)	Rank
Dec. 21, 1955	79.23	14
Jan. 15, 1956	82.53	12
Dec. 11, 1956	98.08	6
Dec. 20, 1957	113.48	3
Feb. 15, 1958	69.62	19
Nov. 24, 1960	67.52	21
Dec. 19, 1961	89.75	8
Feb. 10, 1961	93.69	7
Dec. 22, 1964	150.41	1
Jan. 27, 1965	122.69	2
Nov. 9, 1968	64.04	23
Dec. 4, 1968	82.62	11
Jan. 18, 1970	64.14	22
Jan. 17, 1971	77.77	15
Jan. 18, 1971	83.35	9
Dec. 5, 1971	72.28	17
Jan. 21, 1972	115.55	4
Mar. 2, 1972	81.98	13
Dec. 20, 1973	63.59	24
Jan. 15, 1974	61.02	25
Dec. 1, 1975	68.62	20
Jan. 8, 1976	108.60	5
Nov. 25, 1977	77.27	16
Dec. 13, 1977	83.32	10
Jan. 13, 1980	70.49	18

Table 11. Ranking of 25 highest peak flows measured at Watershed 2, H. J. Andrews Experimental Forest, 1955-1980. Modified from Harr, 1981, p. 291.



F = Forest, C = Clearcut, R = Road-related

* = Dates of air photo sets

1/year road construction and timber harvesting began in study area

2/debris avalanche from flow front, Middle Santiam earthquake

Table 12. Distribution of debris avalanches and combined debris avalanche-debris torrent events over period of record in different land types.

water input event may then produce few if any slope failures. On the other hand, slopes may only be weakened by a large storm, setting up conditions of marginal stability so that failures occur during a subsequent storm of equal or less magnitude.

The December 22, 1964, and January 27, 1965 storms probably caused a number of slope failures in the study area. The 1964 event was one of the most destructive storms in 104 years in western Oregon. It ranks second in peak flow magnitude to a storm which occurred in December 1861. The succeeding storm in late January of 1965 was of slightly lesser but still formidable magnitude. In the spring and summer of 1965, Dyrness (1967) mapped 47 soil mass movements triggered by previous winter storms in the Andrews Forest. Subsequently, Swanson and James (1975) mapped more events that had been caused by the 1964-1965 storms. At least 30% of the debris avalanches in the Andrews occurred as a result of these storms. A similar pattern probably occurred in the Middle Santiam study area. Sixteen debris avalanches in all land types may have been caused by the 1964-1965 storms, as shown by their bracketed period of occurrence (Table 12). This comprises two-thirds of the inventoried debris avalanches, excluding the avalanches from the Middle Santiam earthflow. With the available data, it is difficult to pinpoint the year of occurrence, and other large storms may have been responsible for some of the events. For example, on December 20, 1957, the third largest peak flow was recorded and on January 21, 1972, the fourth largest occurred.

Although Table 11 presents the 20 largest peak flows since 1955, some mass movement events may have occurred during relatively minor

storms. Two of the six debris avalanches (inventory numbers 50 and 85) in clearcut units occurred between November 1980 and January 1981 in a unit harvested in the summer of 1980. Peak flows during this period do not rank in the 45 largest since 1955 and have return periods of only two years.

Mass Movement Impacts on the Middle Santiam River

Mass movements directly impact the Middle Santiam River by advancing debris into its channel (Table 13). Rates of advancement vary according to mass movement type. Impacted reaches are littered with large boulders and piles of large organic debris, while finer sediment is carried downstream by the river.

Ten active earthflows currently advance debris into the Middle Santiam River (Table 13), impacting about 22% of its total channel length within the study area. Two impact points are marked by high, steep and intensively gullied fronts of earthflows exposing boulders and organic debris imbedded in soft, clayey volcanoclastic colluvium. Springs emerge at numerous points on these unstable, unvegetated flow fronts, and debris perennially slumps and flows into the main channel.

Massive earthflows advancing huge amounts of debris into a river channel over a short period of time may significantly alter channel morphology. Earthflow debris may constrict or even block the channel at the point of impact, temporarily damming the river and causing upstream aggradation and the construction of a broad flood plain or channel bars and islands. Such events are described by Swanson and

James (1975) on Lookout Creek in the H.J. Andrews Experimental Forest. Adams (1981) describes lakes formed by the damming of rivers by rapid earthquake-induced landslides in New Zealand. The lakes formed over a short period of time (less than a decade), whereas earthflows may continuously impact a channel, and aggradation may be a long-term process.

On the Middle Santiam River, large, currently inactive earthflows altered channel morphology between Jude Creek and the western boundary of the study area. This reach was constricted, and bars and islands were built upstream to the Pyramid Creek junction.

Mass movement inventory number (see Table 9)	Type	Approximate length of impacted reach (feet)
2	SE-(A)	660
11	SE-(A)	660
16	SE-(A)	1,300
34	SE-(A)	900
37	SE-(A)	2,500
38	SE-(A)	150
39	SE-(A)	250
40	SE-(A)	800
44	SE-(A)	600
47	SE-(A)	150
		<u>7,970 (1.51 mi)</u>
<hr/>		
47	SE-(I)	1,830
56	SE-(I)	3,300
57	SE-(I)	1,056
78	SE-(I)	4,000
80	SE-(I)	2,900
		<u>13,086 (2.48 mi)</u>
<hr/>		
13	DA	100
35	DA	270
36	DA	270
		<u>640</u>

Table 13. Mass movement impact on the Middle Santiam River.
(A) = active, (I) = inactive. Total channel length in the
study area is 6.75 miles.

SUMMARY

1. The Middle Santiam study area is underlain by basalt and andesite flows and flow breccias, lapilli tuffs, lahars, ashflows, and water-laid tuffs of the Little Butte Volcanic Series of Oligocene and early Miocene age; andesite flows, massive lapilli tuffs, tuff-breccias and water-laid tuffs of the Sardine Formation of middle and late Miocene age; and andesite flows of Pliocene and Quaternary age. Basaltic and andesitic dikes and plugs of late Eocene to late Miocene age also are present.

All rocks in the study area are altered to some extent. Zeolitic alteration dominates, but some Sardine rocks in the southwestern corner of the area show argillic alteration.

2. Quaternary to Recent surficial deposits include talus, scattered small glacial deposits, colluvial soils, mass movement debris and alluvium.

3. Some local folding of bedrock is indicated by dipping bedded tuffs at some locations and a northeast-trending anticline through the study area (Peck et al., 1964). A high-angle normal fault cutting Little Butte rocks was noted in the field.

4. The most critical materials in mass movement processes are soils or extremely weathered bedrock with the strength properties of soils. Shallow debris avalanches occur on steep slopes in

noncohesive soils with generally low plasticity, while slump earthflow are associated with cohesive materials.

Soils samples collected in the study area can be assigned to four main groups from a stability-lithologic standpoint: (1) residual soils overlying volcanoclastic bedrock; (2) non-volcanoclastic soils from slump scarps and debris avalanches; (3) soils derived from volcanoclastics from (a) unstable sites and (b) stable sites; and (4) lava flow breccia soils. Most of these soils are silty sands or poorly graded sand-silt mixtures. Some samples from mass movement sites are clayey, with high plasticity indices and low strength. The weakest materials tested by a shear vane device were samples from the flow front of the Middle Santiam earthflow derived from tuffaceous mudstones.

The average clay content of soils from unstable slopes is slightly higher than soils from other sites. X-ray determinations on two samples of volcanoclastic soils from the flow front of the Middle Santiam earthflow indicated that the dominant clay mineral is montmorillonite, a high expandible clay associated with mass movement.

5. Structural discontinuities such as joints, faults, and shear zones, lithologic contacts and bedding planes influence mass movement by acting as slip surfaces and by serving as avenues for, or barriers to, groundwater flow. In the study area, slump-earthflow were common where fairly permeable lava flows and less permeable volcanoclastic breccias and bedded epiclastics are interbedded.

6. The occurrence of mass movements in the study area may have been related in part to climatic, hydrologic, vegetative, and terrain conditions which prevailed during late Pleistocene time, although these relationships are largely speculative. On the strength of age determinations on earthflows in the Andrews Forest, earthflows in the study area may date back to the Pleistocene. Evidence for glaciation in the study area is not conclusive; however, the study area may have been in a periglacial environment. Effects of glacial climates and glaciation favorable for mass movement include timberline suppression and concomitant reduced evapotranspiration and root strength. Warm interglacial periods also may have been favorable, due to increased water input to soil from glacial melt water and higher pore water pressures.

7. Geomorphology of three slump-earthflow case studies (Donaca, Jude Creek, and Middle Santiam) and rates of current movement on the Jude Creek earthflow and current and historic movement on the Middle Santiam earthflow are treated in detail.

Geomorphology of mass movement sites in the study area is described in terms of mappable geomorphic units; each unit consists of a terrain type based on landforms, and an activity class which reflects recency and rates of movement as indicated by terrain and vegetation. Seven terrain types (boundary scarps, boulder fields, slump benches, interior scarps, flow fronts, boundary stream erosion impact zones, and debris avalanche-mudflow areas) and three activity levels (inactive, moderately active, and very active) are used.

(a) Donaca mass movement complex. The Donaca complex consists of four active sites (A,B,C,D) dominated by slump-earthflow processes. Site A is the largest, covering 760 acres; the lower portions of this site (slump bench A') are very active, dumping large amounts of sediment and debris yearly into Swamp Creek from high steep banks.

(b) Jude Creek earthflow. The Jude Creek earthflow is a 70-acre, mostly forested earthflow, with a very active lower portion characterized by ground cracks, downed vegetation and poor drainage. At Jude Creek, two earthflow lobes advance into the channel. The southern lobe moves into an aggraded reach upstream of a log jam, but the northern lobe is being actively eroded by high streamflow. Surface movement along a shear boundary as measured by a stake array was 19.1 feet from 12/7/79 to 10/18/80 with maximum movement recorded during winter and late spring.

(c) Middle Santiam mass movement site. In 1965, a road was excavated through the toe of the Middle Santiam earthflow, setting up unstable conditions which may have contributed to reactivation of earthflow movement. A large storm in January 1972 triggered debris avalanching from the flow front. Movement data indicate cumulative surface movement northward along the western shear boundary of 45.8 feet from 10/6/79 to 7/17/81, with periods of acceleration coincident with increased water input periods. Since 1965, displacement along the boundary was 75 feet. Rapid earthflow movement has resulted in extreme disturbance over the entire earthflow.

8. A total of 96 mass movement sites were identified in the study area: 55 earthflows, 24 debris avalanches, 12 debris torrents,

3 combined debris avalanche-debris torrents, and two rockfall-rockslides.

A debris avalanche inventory provides data for assessing impacts of storms and forestry management practices in the study area. Debris avalanches associated with road construction, excluding the Middle Santiam mass movement site, had a soil transfer rate of $3000 \text{ yd}^3 \text{ mi}^{-2} \text{ yr}^{-1}$ from 1958 to 1981, or 28 times that of events in clearcut areas for the same period and 95 times that of events in forested areas for the period 1955-1981.

9. Recent storm history indicated by peak flow data can in some cases be generally correlated with mass movement occurrence.

10. Earthflows impact the Middle Santiam River by advancing debris into its channel. In the past, large earthflows have constricted the River and caused upstream aggradation.

BIBLIOGRAPHY

- Adams, John, 1981, Earthquake-dammed lakes in New Zealand: *Geology*, V. 9, p. 215-219.
- Agard, S. S., 1979, Investigation of recent mass movements near Telluride, Colorado, using the growth and form of trees: unpubl. Master's Thesis, Univ. of Colorado, 157 p.
- Beeson, M. H., Moran, M. R., Anderson, J. L., Timm, S., and Vogt, B. F., 1979, Stratigraphy and structure of the Columbia River Basalt Group in the Cascade Range, Oregon: Portland, Oreg., unpublished report to Oreg. Dep. of Geol. and Mineral Ind., 87 p.
- Bjerrum, L., 1973, Problems of soil mechanics and construction on soft clays and structurally unstable soils: Proc., 8th Int. Conf. on Soil Mechanics and Foundation Eng., Moscow, V. 3, p. 111-159.
- Blong, R. J., 1973, A numerical classification of selected landslides of the debris slide-avalanche-flow type: *Eng. Geol.* V. 7, p. 99-114.
- Borchardt, Glenn A., 1977, Clay mineralogy and slope stability: special report 133, Calif. Div. of Mines and Geology.

- Bouyoucos, G. J., 1962, Hydrometer method improved for making particle size analysis of soils: *Agronomy J.*, V 54, p. 464-468.
- Broms, B. B., 1975, Landslides: In Winterkorn, H. F., and Fang, H. Y., eds., *Foundation Eng. Handbook*, Van Nostrand-Reinhold, New York, p. 373-401.
- Burroughs, E. R., Chalfant, G. R., and Townsend, M. A., 1976, Slope stability in road construction: *USDA Bureau of Land Management*, Portland, Oreg., 102 p.
- Cadling, L., and Odenstad, S., 1950, The vane borer: an apparatus for determining the shear strength of clay soils in the ground: *Proc., Royal Swedish Geotechnical Inst.*, No. 2, 88 p.
- Callaghan, Eugene, 1934, Some aspects of the geology of the Cascade Range in Oregon (abstr.): *Washington Acad. Sci. J.*, V. 24, No. 4, p. 190-191.
- Callaghan, Eugene, and Buddington, A. F., 1938, Metalliferous mineral deposits of the Cascade Range in Oregon: *U.S. Geol. Survey Bull.* 893, 141 p.
- Claridge, G. G. C., 1960, Clay minerals, accelerated erosion, and sedimentation in the Waipaoa River catchments: *New Zealand J. Geology and Geophysics*, 3:184-191.

Crandell, D. R., 1965, The glacial history of western Washington and Oregon, in: Wright H. E. and Frey, D. G., eds., The Quaternary of the United States, p. 341-353.

Durr, D. L., 1974, An embankment saved by instrumentation: Transportation Research Board, Transportation Research Record 482, p. 43-50.

Dyrness, C. T., 1967, Mass soil movement in the H. J. Andrews Experimental Forest: USDA For. Serv. Res. Paper PNW-42, 12 p.

Fredriksen, R. L., 1965, Christmas storm damage on the H. J. Andrews Experimental Forest: USDA For. Serv. Res. Note PNW-29, 11 p.

Gage, M., and Black, R. D., 1979, Slope stability and geological investigations at Mangatu state forest: For. Res. Inst., New Zealand For. Serv., Technical Paper No. 66.

Gottesfeld, A. S., Swanson, F. J., and Gottesfeld, L. M., 1981, A Pleistocene low-elevation sub-alpine forest in the western Cascades, Oregon: Northwest Sci., Vol. 55, No. 3.

Harden, D. R., Janda, R. J., and Nolan, K. M., 1978, Mass movement and storms in the drainage basin of Redwood Creek, Humboldt County, California: U.S. Geological Survey open-file Report 78-486.

- Harr, R. D., 1981, Some characteristics and consequences of snowmelt during rainfall in western Oregon: J. Hydrology, V. 53, p. 277-304.
- Heusser, C. J., 1956, Postglacial environments in the Canadian Rocky Mountains: Ecological Monographs 26:263-302.
- Hodge, E. T., 1933, Age of Columbia River and lower Canyon (abs.): Geo. Soc. Am. Bull., V. 44, P. 156-157.
- Janda, R. J. Nolan, K. M., Harden, D. R., and Colman, S. M., 1975, Watershed conditions in the drainage basin of Redwood Creek, Humboldt County, California, as of 1973: U.S. Geol. Survey open-file report 75-568, 266 p.
- Keefer, D.K., 1977, Earthflow: unpubl. Ph.D. thesis, Stanford Univ., Palo Alto, California.
- Kelsey, H.M., 1977, Landsliding, channel changes, sediment yield and land use in the Van Duzen River basin, North Coastal California, 1941-1975: PhD thesis, University of California, Santa Cruz, 370 p.
- Loughnan, F. C., 1969, Chemical weathering of the silicate minerals: New York, Elsevier, 154 p.

Marion, D. A., 1981, Landslide occurrence in the Blue River Drainage, Oregon: M.S. thesis, Oreg. State Univ, 114 p.

McBirney, A. R., Sutter, J. F., Naslund, H. R., Sutton, K. G., and White, C. M., 1974, Episodic volcanism in the central Oregon Cascade Range: Geol., V. 2, No. 12, p. 585-589

Merriam, R., 1960, Portuguese Bend Landslide, Palos Verdes Hills, California, J. Geol., V. 68, No. 2, p. 140-153.

Miller, J. F., Frederick, R. H., and Tracey, R. J., 1973, Precipitation-frequency atlas of the western United States, Vol. X-Oregon: U.S. Dept. of Commerce NOAA Atlas 2.

Mitchell, J. K., 1976, Fundamentals of soil behavior: John Wiley and Sons, Inc., New York, 422 p.

Morrison, P. H., 1975, Ecological and geomorphological consequences of mass movements in the Alder Creek watershed and implications for forest land management: B. A. thesis, Univ. of Oreg., Eugene, 83 p.

Nemcok, A., and Rybar, J., 1968, Landslide investigation in Czechoslovakia: Proc. 1st session of the IAEG, Prague, p. 183-198.

- O'Loughlin, C. L., and Gage, M., 1975, A report on the status of slope erosion on selected steep areas, West Coast Beech project Area: New Zealand Forest Service (FRI) report.
- Paeth, R. C., Harward, M. E., Knox, E. G., and Dyrness, C. T., 1971, Factors affecting mass movement of four soils in the Western Cascades of Oregon: Soil Sci. Soc. Am. Proc., Vol. 35, No. 6, p. 943-947
- Peck, D. L., Griggs, A. B., Schlicker, H. G., Wells, F. G., and Dole, H. M., 1964, Geology of the central and northern parts of the western Cascade Range in Oregon: Geol. Survey Professional Paper 449, 56 p.
- Pierson, T. C., 1977, Factors controlling debris flow initiation on forested hillslopes in the Oregon Coast Range, Ph.D. dissertation, Univ. Wash., Seattle, 166 p.
- Piteau, D. R., and Peckover, F. L., 1978, Engineering of rock slopes: In Schuster, R.L., and Krizek, R.J., eds., Landslides: Analysis and Control, Special Report 176, Trans. Res. Board, Nat. Acad. of Sci., p. 193.
- Pope, R. S., and Anderson, M. W., 1960, Strength properties of clays derived from volcanic rocks: Res. Conf. on Shear Strength of Cohesive Soils, Proc., Boulder, Colo., p. 315-340.

- Prior, D. B., and Stephens, N., 1972, Some movement patterns of temperate mudflows: Examples from Northeastern Ireland: Geol. Soc. Am. Bull., V. 83, p. 2533-2544.
- Rice, R. M., Corbett, E. S., Bailey, R. G., 1969, Soil slips related to vegetation, topography, and soil in southern California: Water Resources Res., 5(3):647-659.
- Rice, R. M., Corbett, E. S., and Bailey, R. G., 1969, Soil slips related to vegetation, topography, and soil in southern California: Water Resources Res. 5(3):647-659.
- Rybar, J., 1973, Representation of landslides in engineering geological maps: Landslide, Vol. 1, No. 1, p. 15-21.
- Santiam Engineering Zone, 1973, Road condition survey, Mid-Santiam slump: unpublished report, on file at Santiam Engineering Zone, Willamette Nat. For., Sweet Home, Oreg., and RWU 1653, PNW For. and Range Exp. Stn., Corvallis, Oreg.
- Savarenski, F. P., 1935, Experimental construction of a landslide classification: Geolog. Razvedochnyi Instit. (TSNICTRI), p. 29-37, in Russian—cited in Varnes, D. J., 1978, Landslide Analysis and control: Nat. Acad. Sci., Trans. Res. Board, Special Report 176.

- Schulz, M. G., 1980, The quantification of soil mass movements and their relationship to bedrock geology in the Bull Run Watershed, Multnomah and Clackamas Counties, Oregon: unpublished M.S. thesis, Oreg. State Univ., 170 p.
- Scott, W. E., 1977, Quaternary glaciation and volcanism, Metolius River area, Oregon: Geol. Soc. Am. Bull. 88, p. 113-124.
- Shannon and Wilson Inc., 1964, Report on geology and engineering feasibility of increased storage at Bull Run Lake, Oregon: Portland, Oregon, unpubl. report to City of Portland, 22 p.
- Sharpe, C. F. S., 1938, Landslides and related phenomena: Pageant, New Jersey, 125 p.
- Shroder, 1980, Dendrogeomorphology: review and new techniques of tree-ring dating: Progress in physical geography, 4(2):161-188.
- Simonett, D. S., 1967, Landslide distribution and earthquakes in the Bewani and Torricelli Mountains, New Guinea: in Jennings, J. N. and Mabbatt, J. A., eds., Landform studies from Australia and New Guinea, Australian Nat. Univ. Press, Canberra, p. 64-84.
- Skempton, A. W., 1953, Soil mechanics in relation to geology: Proc. Yorks. Geol. Soc., v. 28, p. 33-62.

Skempton, A. W., and Bishop, A. W., 1954, Soils: in Reiner, M., ed.,
Building materials: their elasticity and inelasticity,
North-Holland Pub. Co.

Sowers, G. F., and Royster, D. L., Field investigation: Chapt. 4: in
Schuster, R. L., and Krizek, R. J. eds., Landslides: Analysis and
Control, Special Report 176, Transportation Res. Board, Nat.
Acad. Sci., p. 81-111.

Stout, Martin L., 1977, Radiocarbon dating of landslides in southern
California: Calif. Geol., Vol. 30, No. 5, p. 99-105.

Swanson, F. J. and Dyrness, C. T., 1975, Impact of clearcutting and
road construction on soil erosion by landslides in the western
Cascade Range, Oregon: Geol. 3(7):393-396.

Swanson, F. J., Harr, R. D., and Fredriksen, R. L., 1980, Field trip
guide: Geomorphology and hydrology in the H. J. Andrews
Experimental Forest, western Cascades: in Oles, K.F., Johnson,
J.G., Niem, A., and Niem, W.A., eds.: Geologic field trips in
western Oregon and southwestern Washington, Oregon Dept. Geol.
and Mineral Ind., Bull. 101, p. 217-232.

Swanson, F. J., and James, M. E., 1975, Geology and geomorphology of
the H. J. Andrews Experimental Forest, western Cascades, Oregon:
USDA For. Serv. Res. Paper PNW-188, 14 p.

Swanson, Frederick J., and Lienkaemper, George W., 1978, Physical consequences of large organic debris in Pacific Northwest streams. USDA For. Serv. Gen. Tech. Rep. PNW 69, 12 p.

Swanson, F.J., Lienkaemper, G.W., and Sedell, J.R., 1976, History, physical effects, and management implications of large organic debris in western Oregon streams. USDA For. Serv. Gen. Tech. Rep. PNW 56, 15 p.

Swanson, F. J., Swanson, M. M., and Woods, C., 1977, Inventory of mass erosion in the Mapleton Ranger District, Siuslaw National Forest: Final Report on file, Forestry Sciences Lab., Corvallis, Oreg., USA.

Swanson, F. J., Swanson, M. M., and Woods, C., 1981, Analysis of debris-avalanche erosion in steep forest lands: an example from Mapleton Oregon, USA: in Erosion and sediment transport in Pacific Rim steeplands, LAHS, Publ. No. 132, Christchurch, N.Z., p. 67-75.

Swanson, F. J. and Swanston, D. N., 1977, Complex mass-movement terrains in the western Cascade Range, Oregon: in Reviews in Engineering Geology, Geol. Soc. Am., v.3, p. 113-124.

Swanston, D. N., 1971, Principal soil mass movement processes influenced by logging, roadbuilding, and fire: in Proceeding of a symposium on forest land uses and stream environment, October 19-21, 1970, Oreg. State Univ., Corvallis, p. 29-40.

Swanston, D. N., 1974, Slope stability problems associated with timber harvesting in mountainous regions of the western United States: USDA For. Serv. Gen. Tech. Rep. PNW-21, 14 p.

Swanston, D. N., 1980, Influence of Forest and Rangeland Management on Anadromous Fish Habitat in western North America: Impacts of natural events, USDA For. Serv. Gen. Tech. Rep. PNW-104.

Swanston, D. N., and Swanson, F. J., 1976, Timber harvesting, mass erosion, and steepland forest geomorphology in the Pacific Northwest: in Donald R. Coates, ed., Geomorphology and engineering, Dowden, Hutchinson & Ross, Inc., Stroudsburg, Penn, p. 199-221.

Taskey, R.D., 1977, Relationships of clay mineralogy to landscape stability in western Oregon: Ph.D. thesis, Oreg. State Univ., Corvallis, Oreg., 122 p.

Taylor, E., 1980, Volcanic and volcanoclastic rocks on the east flank of the central Cascade range to the Deschutes River, Oregon, in Oles, K. F., Johnson, J. G., Niem, A., and Niem, W. A., eds.: Geologic field trips in western Oregon and southwestern Washington, Oreg. Dep. Geol. and Mineral Ind., Bull. 101, p.1-7.

Terzaghi, K., 1958, Design and performance of the Sasamua Dam: in Proc. Inst. of Civil Eng., Vol. 9, p. 369-393.

Terzaghi, K., and Peck, R. B., 1967, Soil mechanics in engineering practices: John Wiley and Sons, New York, 2nd Edition, 729 p.

Thayer, T. P., 1936, Structure of the North Santiam River section of the Cascade Mountains in Oregon: J. Geol., V. 44, p. 712-716.

Thayer, T. P., 1937, Petrology of later Tertiary and Quaternary rocks of the North-central Cascade Mountains in Oregon, with notes on similar rocks in western Nevada: Bull. Geol. Soc. Am., V. 48, p.1611-1652.

Thayer, T. P., 1939, Geology of the Salem Hills and the North Santiam River Basin, Oregon: Oreg. Dept. of Geol. and Mineral Industries Bull. 15., 40 p.

Theisen, A. A., and Harward, M. E., 1962, A paste method for preparation of slides for clay mineral identification by X-ray diffraction: Soil Sci. Soc. Am. Proc. 26:90-91.

- Thrall, F. G., 1981, Geotechnical significance of poorly crystalline soils derived from volcanic ash: unpubl. Ph.D. thesis, Oregon State Univ., Corvallis, Oregon
- Treasher, R. C., 1942, Geologic history of the Portland area: Oregon Dept. of Geol. and Mineral Industries, Short Paper 7, 17 p.
- Varnes, D. J., 1978, Slope movement types and processes: in Schuster, R. L. and Krizek, R. J., eds., Landslides, Analysis and Control, Special Report 176, Trans. Res. Board, Nat. Acad. of Sci., p. 12-33.
- Wilson, S. D., 1974, Landslide instrumentation for the Minneapolis freeway: Transportation Res. Board, Transportation Res. Record 482, p. 30-42.
- Wilson, S. D., and Mikkelsen, P. E., 1978, Field instrumentation: in Schuster, R. L. and Krizek, R. J., eds., Landslides, analysis and control, special report 176, Transportation Res. Board, Nat. Acad. Sci., Wash., D.C., p. 112-137.
- Wu, T. H., and Sangrey, D. A., 1978, Strength properties and their measurement, Chap. 6: in: Schuster, R. L. and Krizek, R. J., eds., Landslides, analysis and control, special report 176, Transportation Res. Board, Nat. Acad. Sci., Wash., D.C., p. 139-152.

Zaruba, Q., and Mencl, V., 1969, Landslides and their control:

Elsevier-Academia, New York, 205 p.